

ALMA MATER STUDIORUM · UNIVERSITÀ DI BOLOGNA

SCUOLA DI SCIENZE
Corso di Laurea Magistrale in Fisica

Large N expansion for scattering amplitudes in QCD

Relatore:
Prof. Fabio Maltoni

Presentata da:
Alessio De Santis

Sessione III
Anno Accademico 2018/2019

Sommario

La Cromodinamica Quantistica (QCD) è la teoria di campo che descrive le interazioni forti nel contesto del Modello Standard (SM). La QCD è una teoria di gauge non abeliana basata sul gruppo di simmetria $SU(N)$ con $N = 3$, caratterizzata da un'unica costante di accoppiamento g_S che varia con la scala di energia. Le ampiezze di scattering nel regime perturbativo a grandi scale possono essere ottenute via una espansione in potenze di g_S . A basse scale di energia, dove la teoria perturbativa non è utilizzabile, si rivela utile cercare un parametro di espansione alternativo. Una possibilità suggerita da 't Hooft negli anni 80 e risultata poi estremamente potente, è di considerare il limite della teoria a grandi N , ossia espandere rispetto l'inverso del numero di colori della teoria. L'obiettivo principale di questo lavoro è quello di esplorare l'efficacia dell'espansione a grandi N anche nel regime perturbativo, in concomitanza con l'usuale espansione in g_S , per semplificare il calcolo di ampiezze di scattering gluoniche con molte particelle esterne. Utilizzando tecniche moderne, come diverse decomposizioni di colore e approcci ricorsivi, calcoliamo e classifichiamo prima la complessità poi l'accuratezza della espansione fino a 10 gluoni esterni a tree-level, e fino ad 8 al loop-level. I risultati numerici per ampiezze al tree-level mostrano come l'espansione nel numero di colori all'ordine più basso sia sempre meno efficace per un alto numero di gluoni esterni, mentre all'ordine successivo sia estremamente accurata (rispetto all'espansione in g_S). Inoltre, la classificazione dei fattori di colore fino a dieci gluoni permette di fare ipotesi sulla loro struttura e sul valore numerico massimo dei vari ordini per un numero di gluoni più alto. Infine, dimostriamo che il numero di fattori di colore di ordine più basso per la decomposizione di colore nota come color-flow è dato da un opportuno coefficiente binomiale che cresce molto lentamente all'aumentare dei gluoni esterni. In conclusione, i risultati ottenuti aprono la strada ad un approccio più efficiente per il calcolo di ampiezze di scattering in QCD.

Abstract

Quantum Chromodynamics (QCD) is the quantum theory describing strong interactions in the framework of the Standard Model (SM). It is a non-abelian gauge theory based upon the symmetry group $SU(N)$, with $N = 3$, characterized by a single coupling constant g_S running with respect to the energy scale. In the perturbative regime and high energy scales, scattering amplitudes are expanded perturbatively in powers of g_S . However, at low energy scales, where perturbation theory breaks down, it is useful to find another expansion parameter. A possibility suggested by 't Hooft that turned out to be very powerful consisted in considering the large N limit of the theory, expanding with respect to the inverse of the number of colors of the theory itself. The main goal of this thesis is to explore the efficacy of the large N expansion even in the perturbative regime, in conjunction with the usual expansion in g_S , in order to simplify the computation of gluon scattering amplitudes with many external particles. Using modern techniques, like different color decompositions and recursive approaches, we compute and classify first the complexity then the accuracy of the expansion up to 10 external gluons at tree-level, and up to 8 at loop-level. Numerical results for tree-level amplitudes show how the expansion at lowest order in the number of colors becomes less and less accurate increasing the number of external gluons, while at the next order it is extremely accurate (compared to the expansion in g_S). In addition, the classification of color factors up to 10 gluons allows us to make guesses about their structure and their maximum values for each order for an higher number of external gluons. Finally, we prove that the number of lowest order color factors for another color decomposition known as color-flow is given by a suitable binomial coefficient growing very slowly for an increasing the number of external gluons. In conclusion, the results we obtained pave the way to a more efficient approach to the computation of scattering amplitudes in QCD.

Acknowledgements

First of all, I would like to thank Professor Fabio Maltoni, for the contributions, the suggestions and the help he gave to me in writing this thesis.

Then, I would like to thank all my relatives and friends, for their patience. A special thought goes to my little brother, hoping that one day he will understand that what I did was all for his greater good. Finally, the most important thanks goes to my dear Maura, for her love, support and patience. I perfectly know I can never be thankful enough for all of this.

*Alla mia amata Maura
e a mio fratello,
nonostante i miei tanti errori.
Possa il Fato proteggerci
dall'arrivo della tempesta.*

*To my beloved Maura
and to my brother,
despite my many errors.
May the Fates hold off
the coming of the storm.*

A premise

One morning, the Commander of a ship found the First Mate completely drunk during his guard duty; he immediately reported on what he had found on the log book (it was not properly difficult to find, as matter of fact he stank like a distillery). Once the hangover was ended, the First Mate, realizing himself being caught red handed, rushed to the Commander begging him to remove the note. Unfortunately, the Commander was uncorruptible and strongly devoted to duty, so he categorically refused to remove the note reprimanding harshly his subordinate. Longing for revenge, the next day the First Mate wrote the following note on the log book:

Today the Commander is not drunk.

This note was certainly true but, being written in a context in which one always finds news or reports of exceptional events, the reader can easily misunderstand that the Commander was drunk everytime but that day.¹

The context can turn black to white and viceversa.
It must be taken into account, always.

¹Partially reworked version of an anecdote told by Dr. Piercamillo Davigo, italian magistrate and member of the CSM.

Contents

1	Quantum chromodynamics	5
1.1	Generalities on the $SU(N)$ group	5
1.2	Construction of the theory	9
1.3	QCD lagrangian and Feynman rules	12
1.4	Asymptotic freedom	14
2	The large N limit	18
2.1	Introduction: the large N expansion	18
2.2	The Gross-Neveu model in the large N limit	19
2.3	Quantum chromodynamics in the large N limit	26
2.3.1	N counting and surface topology	28
2.4	The 't Hooft model	32
2.4.1	Dressed propagator	36
2.4.2	Bethe-Salpeter equation and mesons	38
3	Color decomposition of gluon amplitudes at tree-level	42
3.1	Preliminary calculations	42
3.2	Gluon scattering amplitudes at tree-level	44
3.2.1	Trace decomposition	44
3.2.2	Reducing the complexity	49
3.2.3	The adjoint color decomposition	50
3.2.4	Calculating the cross-section	54
3.2.5	BCJ relations and color-kinematics duality at tree-level	55
3.2.6	Proof of the fundamental BCJ relations	58
4	Large N expansion at work	63
4.1	Tree-level partial amplitudes up to $n = 7$	63
4.2	Color coefficients classification	64
4.2.1	Six gluons	65
4.2.2	Seven gluons	65
4.2.3	Eight gluons	66

4.2.4	Nine gluons	67
4.2.5	Ten gluons	69
4.2.6	An additional comment on numerators	70
4.3	Expansion efficacy for MHV amplitudes up to eight external gluons in the adjoint basis	73
4.3.1	Six gluons	73
4.3.2	Seven gluons	76
4.3.3	Eight gluons	77
5	NLO corrections and large N expansion	78
5.1	Definition	78
5.2	Six gluons	79
5.3	Seven gluons	81
5.4	Eight gluons	82
6	Color-flow decomposition	85
6.1	Definition	85
6.2	Number of NLC contributions	85
6.2.1	Proof	86
7	Summary and conclusions	88
A	Color factors computations	90
B	Spinor-helicity formalism	96
B.1	Momenta	96
B.1.1	Helicity spinors and light-like momenta	98
B.2	Polarizations	99
B.3	Dirac spinors	101
B.4	Examples of calculation	103
B.4.1	Example from QED	103
B.4.2	Pure gluon tree-level amplitudes	104
B.5	Little-group scaling	105
B.6	Complex momenta	106
B.6.1	Three-point amplitude	106
B.6.2	BCFW recursion relations	107

Chapter 1

Quantum chromodynamics

Quantum Chromodynamics (QCD from now on) is a non-abelian gauge theory with symmetry group $SU(3)$ that describes strong interactions and nuclear forces in terms of elementary particles called quarks and gluons. There are six different flavors of quarks with different masses: up (u), down (d), strange (s), charm (c), beauty (b) and top (t), interacting with each other through the exchange of gluons, corresponding to the gauge boson mediators of the strong interaction. All hadrons are made up of five flavors of quarks, since the top quark is not a constituent of any hadron. Quarks carry a non-abelian charge quantum number called color, taking three possible hues conventionally chosen to be green, red and blue, while gluons carry a pair of anti-color-color charges. Thus, color turns out to be the charge of the strong interactions.

By definition, QCD is a particular theory belonging to a larger set of theories called $SU(N)$ non-abelian gauge theories. As a matter of fact, these theories are the natural generalization of Quantum Electrodynamics (QED) to systems describing the dynamics of N different fields. Therefore, to keep the discussion more general, in the following we will describe these theories leaving $N \geq 2$ unspecified.

1.1 Generalities on the $SU(N)$ group

To start with, it is mandatory to briefly discuss some of the most important features of the underlying symmetry group of these theories. $SU(N)$ is the Lie group of generic $N \times N$ unitary matrices U with unit determinant:

$$U^\dagger = U^{-1}, \quad \det U = +1. \quad (1.1)$$

Any element of the group can be written in an exponential form in the following way:

$$U = e^{i\omega_a T^a}, \quad a = 1, 2, \dots, N^2 - 1, \quad (1.2)$$

where ω_a are real numbers parametrizing a specific element of the group and T^a are called group generators. It is easy to see that these generators are hermitian since, from the first equation in (1.1), we find:

$$U^\dagger = e^{-i\omega_a(T^a)^\dagger} = e^{-i\omega_a T^a} = U^{-1}, \iff (T^a)^\dagger = T^a. \quad (1.3)$$

In addition they are traceless. To prove it, we consider a group element infinitely close to the identity, namely:

$$U = \mathbb{I} + i\epsilon_a T^a + O(\epsilon^2), \quad (1.4)$$

where $\epsilon_a \ll 1$. Since the determinant of an arbitrary $SU(N)$ element must be equal to one, we obtain:

$$\det(\mathbb{I} + i\epsilon_a T^a + O(\epsilon^2)) = 1 + i\epsilon_a \text{Tr}(T^a) + O(\epsilon^2) = 1. \quad (1.5)$$

Hence, for $\epsilon_a \rightarrow 0$, we get:

$$\text{Tr}(T^a) = 0, \quad \forall a = 1, 2, \dots, N^2 - 1. \quad (1.6)$$

The generators also form a Lie algebra defined by the following commutation relations:

$$[T^a, T^b] = i f^{abc} T^c, \quad (1.7)$$

where the f^{abc} are called structure constants of the algebra and the mapping $[,]$ is called Lie bracket. Obviously, the structure constants do not identically vanish, hence the group is non-abelian. The Lie brackets satisfy the Jacobi identity, given by:

$$[A, [B, C]] + [B, [C, A]] + [C, [A, B]] = 0. \quad (1.8)$$

This identity can be rewritten in terms of the structure constants as follows:

$$f^{abd} f^{dce} + f^{bcd} f^{dae} + f^{cad} f^{dbe} = 0. \quad (1.9)$$

Until now, we have given a definition of the $SU(N)$ group in terms of matrices, but one should always keep in mind that a group is always defined as a purely abstract mathematical object. Hence, when we think about it in terms of matrices, we are implicitly

selecting a specific representation of this group.

In a nutshell, a representation R of a group \mathcal{G} is a map that associates every element g of the group itself with a linear operator

$$g \in \mathcal{G} \longrightarrow \mathcal{R}(g) \in \text{GL}(V) \quad (1.10)$$

that acts on a certain vector (or linear) space V and preserves the group structure¹. The dimension of a representation is defined as the dimension of the vector space on which the linear operators act; if we identify an element of $SU(N)$ with an $N \times N$ unitary matrix with unit determinant, we are dealing with the so called **fundamental representation** of the group. It acts on N -dimensional column vectors and is the non-trivial representation with the minimum dimension. Therefore, the generators T^a mentioned above are in fact the generators of the fundamental representation of the group T_{fund}^a (we will omit the subscript to lighten the notation). For the group $SU(3)$ the fundamental representation is indicated as **3** and the generators are given in terms of the **Gell-Mann matrices** λ^a defined as:

$$\begin{aligned} \lambda^1 &= \begin{pmatrix} 0 & 1 & 0 \\ 1 & 0 & 0 \\ 0 & 0 & 0 \end{pmatrix}, & \lambda^2 &= \begin{pmatrix} 0 & -i & 0 \\ i & 0 & 0 \\ 0 & 0 & 0 \end{pmatrix}, & \lambda^3 &= \begin{pmatrix} 1 & 0 & 0 \\ 0 & -1 & 0 \\ 0 & 0 & 0 \end{pmatrix}, & \lambda^4 &= \begin{pmatrix} 0 & 0 & 1 \\ 0 & 0 & 0 \\ 1 & 0 & 0 \end{pmatrix}, \\ \lambda^5 &= \begin{pmatrix} 0 & 0 & -i \\ 0 & 0 & 0 \\ i & 0 & 0 \end{pmatrix}, & \lambda^6 &= \begin{pmatrix} 0 & 0 & 0 \\ 0 & 0 & 1 \\ 0 & 1 & 0 \end{pmatrix}, & \lambda^7 &= \begin{pmatrix} 0 & 0 & 0 \\ 0 & 0 & -i \\ 0 & i & 0 \end{pmatrix}, & \lambda^8 &= \frac{1}{\sqrt{3}} \begin{pmatrix} 1 & 0 & 0 \\ 0 & 1 & 0 \\ 1 & 0 & -2 \end{pmatrix}. \end{aligned}$$

and then normalized as $T^a = \frac{1}{2}\lambda^a$. Their normalization for unspecified N is given by:

$$\text{Tr}(T^a T^b) = T_F \delta^{ab} = \frac{1}{2} \delta^{ab}. \quad (1.11)$$

In addition, there is another important representation acting on a vector space of dimension N , that is called **antifundamental representation** and indicated as $\bar{\mathbf{3}}$. Its generators are defined as $\bar{T}^a = -(T^a)^T = -(T^a)^*$ in order to make them satisfy the same Lie algebra the fundamental generators do. Indeed:

$$[\bar{T}^a, \bar{T}^b] = [-(T^a)^T, -(T^b)^T] = -([T^a, T^b])^T = -if^{abc}(T^c)^T = if^{abc}\bar{T}^c, \quad (1.12)$$

thus the Lie algebra is perfectly satisfied. As a matter of fact, every representation has

¹In mathematical words, \mathcal{R} is a group homomorphism.

its peculiar set of generators T_R^a , where the subscript R labels the representation itself. To construct a generic element of a representation, all we have to do is to take its generators and exponentiate them as it is done in (1.23) for the fundamental representation. We incidentally remark that the normalization given in (3.6) can be generalized to the generators of any representation:

$$\text{Tr}(T_R^a T_R^b) = T(R) \delta^{ab}, \quad (1.13)$$

where $T(R)$ is defined as the index of the representation.

Another physically relevant representation of $SU(N)$ is the **adjoint representation**. Its generators are given by the structure constants:

$$(T_{\text{adj}}^a)_{bc} = i(f^a)_{bc}, \quad (1.14)$$

and it acts on a vector space of dimension $N^2 - 1$ equal to the number of generators. The structure constants are real numbers, hence the adjoint representation is real by definition.

If we now take the following composition of generators of a generic representation:

$$C(R) = T_R^a T_R^a = \sum_{a=1}^{N^2-1} T_R^a T_R^a, \quad (1.15)$$

it can be easily demonstrated that it commutes with all the generators themselves. Indeed:

$$[T_R^a T_R^a, T_R^b] = i f^{abc} \{T_R^c, T_R^a\} = 0, \quad (1.16)$$

because of the antisymmetry of f^{abc} . Hence, by definition, $C(R)$ is a **Casimir operator** of the group. Moreover, **Schur's lemma** forces this operator to be proportional to the identity:

$$C(R) = T_R^a T_R^a = C_2(R) I. \quad (1.17)$$

Combining equations (1.17) and (1.13) we obtain:

$$T(R) d(G) = d(R) C_2(R). \quad (1.18)$$

Here $d(G)$ is the dimension of the $SU(N)$ group and $d(R)$ is the dimensionality of the

representation R . It is now straightforward to calculate $C_2(R)$ for the fundamental and the adjoint representation:

$$\begin{aligned} C_F = C_2(\text{fund}) &= \frac{N^2 - 1}{2N}, \\ C_A = C_2(\text{adj}) &= N. \end{aligned}$$

Furthermore, manipulating equation (3.1) in a suitable way, one can obtain another useful relation for the structure constants, namely:

$$f^{abc} = -\frac{i}{T_F} \text{Tr} \{ [T^a, T^b], T^c \}. \quad (1.19)$$

Finally, another important relation is given by the **Fierz identity**:

$$\sum_a T_{ij}^a T_{kl}^a = \frac{1}{2} \left(\delta_{il} \delta_{kj} - \frac{1}{N} \delta_{ij} \delta_{kl} \right). \quad (1.20)$$

All the relations we have listed above for $SU(N)$ are used in almost every cross section calculation in QCD, where obviously $N = 3$. We can also contextually underline that the second term on the right hand side of equation (1.20) is suppressed by a factor $1/N$. This feature will turn out to be very useful in the following.

1.2 Construction of the theory

In order to construct QCD as a non-abelian gauge theory with $SU(3)$ color symmetry, the right path is to generalize the abelian $U(1)$ gauge field theory of electromagnetic interaction, known as QED, to the non-abelian framework. For the sake of clarity, we focus on a single flavor quark, which can assume 3 different color charges. This generalization proceeds as follows:

- First, we require that the fermion fields transform under the fundamental representation of $SU(3)$, namely:

$$\psi(x) \rightarrow \psi(x)' = U_\omega(x) \psi(x), \quad (1.21)$$

where $U_\omega(x) = e^{i\omega_a(x)T^a}$ and T^a is a generic generator of the fundamental representation. In other words, the fermionic matter fields live in the fundamental representation of the gauge group and their indices transform under this specific

N -dimensional representation. Expressing the color indices and performing infinitesimal transformations, we have:

$$\psi_i(x)' = [\delta_{ij} + i\omega_a(x)T_{ij}^a + O(\omega_a^2)]\psi_j(x), \quad (1.22)$$

or alternatively at first order:

$$\delta\psi_i(x) = i\omega_a(x)T_{ij}^a\psi_j(x). \quad (1.23)$$

Furthermore, the Dirac-adjoint spinor field transforms as:

$$\bar{\psi}(x) \rightarrow \bar{\psi}(x)' = \bar{\psi}(x)U_\omega(x)^\dagger, \quad (1.24)$$

where $U_\omega(x)^\dagger = e^{-i\omega_a(x)T^a}$. Expressing again the color indices and neglecting spinor degrees of freedom, we obtain:

$$\begin{aligned} \psi_i^*(x)' &= \psi_j^*(x)[\delta_{ji} - i\omega_a(x)T_{ji}^a + O(\omega_a^2)] \\ &= [\delta_{ij} + i\omega_a(x)\bar{T}_{ij}^a + O(\omega_a^2)]\psi_j^*(x), \end{aligned}$$

where in the last step we used the definition of the complex generators $\bar{T}_{ij}^a = -T_{ji}^a$. Hence infinitesimally we get:

$$\delta\psi_i(x)^* = i\omega_a(x)\bar{T}_{ij}^a\psi_j^*(x). \quad (1.25)$$

As a consequence, the complex conjugate field transforms under the antifundamental representation $\bar{\mathbf{3}}$, that is **not** equivalent to the fundamental one $\mathbf{3}$. It is worthwhile to stress that the transformations we listed act only on the color indices of the quark fields and not on spinor indices.

- Then we impose that the non-abelian strength tensor $F_{\mu\nu}(x)$ transforms **homogeneously** under the gauge group, exactly as its abelian electromagnetic counterpart does in QED. To this end, we define the covariant derivative generalizing it to non-abelian gauge fields as:

$$D_\mu = \partial_\mu - igA_\mu(x) = \partial_\mu - igA_\mu^a(x)T^a. \quad (1.26)$$

Now we require that under the gauge group the covariant derivative $D_\mu\psi$ of a fermion field transforms as follows:

$$D'_\mu\psi'(x) = D'_\mu U_\omega(x)\psi(x) = U_\omega(x)D_\mu\psi(x), \quad (1.27)$$

so that it can be easily demonstrated that:

$$D'_\mu = U_\omega(x)D_\mu U_\omega^\dagger(x). \quad (1.28)$$

Therefore, it is straightforward to see that, if we define the strength tensor in the same way we do in QED, namely:

$$F_{\mu\nu}(x) = \frac{i}{g} [D_\mu, D_\nu] = \partial_\mu A_\nu - \partial_\nu A_\mu - ig [A_\mu, A_\nu], \quad (1.29)$$

it will transform in an homogeneous way under the gauge group, as required:

$$F'_{\mu\nu}(x) = \frac{i}{g} [D'_\mu, D'_\nu] = U_\omega(x)F_{\mu\nu}(x)U_\omega^\dagger(x), \quad (1.30)$$

To fulfill all these conditions, the non-abelian gauge fields necessarily transform in a non-homogeneous way as:

$$A'_\mu(x) = U_\omega(x)A_\mu(x)U_\omega^\dagger(x) - \frac{i}{g} [\partial_\mu U_\omega(x)] U_\omega^\dagger(x), \quad (1.31)$$

where $A_\mu(x) = A_\mu^a(x)T^a$.

At this point it is not so difficult to obtain the infinitesimal transformation laws of matter and gauge fields, in order to see what is the representation under which they transform:

$$\begin{aligned} \delta\psi(x) &= ig\omega^a(x)T^a\psi(x), \\ \delta A_\mu^a(x) &= \partial_\mu\omega^a(x) - gf^{abc}A_\mu^c(x)\omega^b(x), \\ \delta F_{\mu\nu}^a(x) &= gf^{abc}F_{\mu\nu}^b(x)\omega^c(x). \end{aligned} \quad (1.32)$$

Hence, it is evident by direct inspection that the strength tensor $F_{\mu\nu}^a$ transforms according to the adjoint representation of $SU(N)$ gauge group.

As a final remark, we stress that from its definition (1.29) this tensor is not linear in the gauge fields $A_\mu(x)$, because of the presence of the commutator $[A_\mu, A_\nu]$.

1.3 QCD lagrangian and Feynman rules

The $SU(3)$ invariant lagrangian for QCD is then given by:

$$\begin{aligned} \mathcal{L}_{\text{QCD}} = & -\frac{1}{4}(F_{\mu\nu}^a)^2 - \frac{1}{2\xi}(\partial_\mu A_\mu^a)^2 + \sum_k^{N_F} \bar{\psi}_i^{(k)} (i\not{D}_{ij} + \delta_{ij}m^{(k)})\psi_j^{(k)} + \\ & + (\partial_\mu \bar{c}^a)(\delta^{ac}\partial_\mu + gf^{abc}A_\mu^b)c^c, \end{aligned} \quad (1.33)$$

where:

$$F_{\mu\nu} = \partial_\mu A_\nu^a - \partial_\nu A_\mu^a + gf^{abc}A_\mu^b A_\nu^c, \quad (1.34)$$

(k) labels the flavor of quarks and c^a and \bar{c}^a are the Faddeev-Popov ghost and anti-ghost fields. We only expressed the sum over the flavor indices and used the first letters of latin alphabet to label adjoint indices and mid-alphabet latin letters to label the fundamental ones. As already mentioned, it describes the interactions between matter spinor fields called quarks and the non-abelian gauge fields called gluons. As a matter of fact, the lagrangian (1.34) can be split into a free quadratic and a higher order interaction part. The free part reads:

$$\mathcal{L}_0 = -\frac{1}{4}(\partial_\mu A_\nu^a - \partial_\nu A_\mu^a)^2 - \frac{1}{2\xi}(\partial_\mu A_\mu^a)^2 + \sum_k^{N_F} \bar{\psi}_i^{(k)} (i\not{\partial} - m^{(k)})\psi_i^{(k)} - \bar{c}^a \square c^a, \quad (1.35)$$

while the interaction part reads:

$$\begin{aligned} \mathcal{L}_{\text{int}} = & -gf^{abc}(\partial_\mu A_\nu^a)A_\mu^b A_\nu^c - \frac{g^2}{4}(f^{eab}A_\mu^a A_\nu^b)(f^{ecd}A_\mu^c A_\nu^d) + \\ & + gf^{abc}(\partial_\mu \bar{c}^a)A_\mu^b c^c + gA_\mu^a \sum_k^{N_F} \bar{\psi}_i^{(k)} \gamma^\mu T_{ij}^a \psi_j^{(k)}. \end{aligned} \quad (1.36)$$

Therefore, deriving the Feynman rules for the theory is now straightforward and we can focus only on color indices without loss of generality. Inverting the free quadratic part of (1.35) we can derive the expressions for the propagators of quarks, gluons and ghosts.

- The quark propagator is given by:

$$j \longrightarrow \begin{array}{c} \xrightarrow{\quad} \\ \xrightarrow{p} \end{array} i = \frac{i\delta_{ij}}{\not{p} - m + i\epsilon}. \quad (1.37)$$

- The gluon propagator is instead:

$$a; \mu \text{ \scriptsize \textcircled{w}} \xrightarrow{p} b; \nu = -\frac{i\delta^{ab}}{p^2 + i\epsilon} \left[\eta_{\mu\nu} + (\xi - 1) \frac{p_\mu p_\nu}{p^2} \right]. \quad (1.38)$$

- Finally, the ghost propagator is given by:

$$b \text{ \scriptsize \textcircled{d}} \xrightarrow{p} a = \frac{i\delta^{ab}}{p^2 + i\epsilon}. \quad (1.39)$$

The presence of factors δ_{ij} and δ^{ab} clearly encodes the conservation of color charge along the lines. We remark again that (i, j) are indices transforming under the fundamental representation of $SU(3)$, while (a, b) transform under the adjoint representation. In other words, they are both color indices but living in different representations of the same gauge group. Similarly, from the higher order term (1.36), we can easily derive the interaction vertices.

- The quark-gluon interaction term reads:

$$\mu; a \text{ \scriptsize \textcircled{w}} \text{ \scriptsize \textcircled{v}} \begin{array}{l} \nearrow j \\ \searrow i \end{array} = ig\gamma^\mu T_{ij}^a. \quad (1.40)$$

- We also have a ghost-antighost-gluon vertex:

$$\mu; b \text{ \scriptsize \textcircled{w}} \begin{array}{l} \nearrow c^c \\ \searrow \bar{c}^a \end{array} = -gf^{abc} p^\mu. \quad (1.41)$$

- For the three gluon vertex we have:

$$\begin{array}{l} \nu; b \\ \nearrow p \\ \mu; a \text{ \scriptsize \textcircled{w}} \xrightarrow{k} \text{ \scriptsize \textcircled{w}} \xrightarrow{q} \searrow \rho; c \\ \nearrow q \end{array} = gf^{abc} [\eta^{\mu\nu}(k-p)^\rho + \eta^{\nu\rho}(p-q)^\mu + \eta^{\rho\mu}(q-k)^\nu]. \quad (1.42)$$

- Finally, the four gluon vertex gives:

$$\begin{array}{c}
 \mu; a \\
 \text{|||||} \\
 \rho; c \text{ } \text{|||||} \text{ } \nu; b \\
 \text{|||||} \\
 \sigma; d
 \end{array}
 = -ig^2 \left[f^{abe} f^{cde} (\eta^{\mu\rho} \eta^{\nu\sigma} - \eta^{\mu\sigma} \eta^{\nu\rho}) + \text{non cyclic perm.} \right].$$

(1.43)

From the last two interaction vertices, it is evident that the gluon gauge fields interact with each other. This feature of non-abelian gauge theories is completely in contrast to the behaviour of QED, in which photons do not interfere. This is due to the non-linearity of the non-abelian equations of motion caused by the presence of the commutators $[A_\mu, A_\nu]$ in the definition of the strength tensor (1.29). Thus gluons carry a non-abelian color charge and do not interact only with quarks but also self-interact.

1.4 Asymptotic freedom

To proceed further, we discuss one of the most astonishing features provided by QCD: asymptotic freedom. This property displayed by strong interactions was independently discovered in 1973 by D. J. Gross and F. A. Wilczek in [1] and by H. D. Politzer in [2]. The detailed discussion of this topic is beyond the scope of this work, nevertheless we can sketch the most important points. Because of the self-interaction between gluons, if we want to compute loop corrections to the quark propagator in QCD, we have to consider not only quark loops, like in QED, but also gluon loops, as shown in figure 1.1:

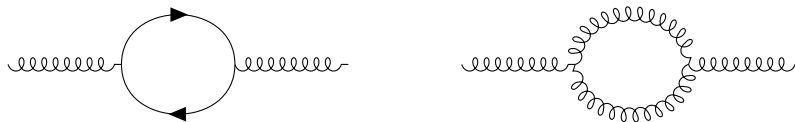


Figure 1.1: Two examples of one loop corrections to the quark propagator in QCD.

Unfortunately, these two diagrams and almost all the other possible Feynman diagrams give rise to divergent integrals that must be suitably regularized. It is very well known that this renormalization procedure makes the coupling constant of the theory to run

with respect to the energy scale of a given process. For example, in QED the presence of fermion loops screens the electron charge, making the fine structure constant α to become larger as the energy of the process² grows up. As a matter of fact, in QCD things are not so easy. It can be shown by direct calculations that the first diagram in 1.1 screens the color charge of the quark, while the second anti-screens it. Suppose we can experimentally measure the value of the coupling constant at an arbitrary renormalization scale μ^2 and define Q^2 as the the energy scale at which we run a certain process. As a result, it turns out that at leading order the strong coupling constant runs in the following way:

$$g(Q^2) = \frac{g(\mu^2)}{1 + \beta_0 g(\mu^2) \ln\left(\frac{Q^2}{\mu^2}\right)}. \quad (1.44)$$

The β_0 coefficient is nothing but the leading order term in the expansion of the **β -function** of the theory, defined as the rate of variation of the strong coupling constant as a function of the logarithm of Q^2 :

$$\beta(g) = \frac{dg(Q^2)}{d\ln(Q^2)} = - [\beta_0 g^2(Q^2) + \beta_1 g^3(Q^2) + \dots], \quad (1.45)$$

and its value is given by:

$$\beta_0 = \frac{1}{4\pi} \left(\frac{11}{3} C_A - \frac{4}{3} T_F N_f \right) = \frac{7}{4\pi}, \quad (1.46)$$

where $N_f = 6$ is number of quark flavors. This coefficient encodes the contributions of loop diagrams of the form depicted in figure 1.1 sewed together side by side and to all orders in perturbation theory. We give two examples of such diagrams in figure 1.2.



Figure 1.2: Two examples of two-loop corrections contributing to the β_0 coefficient.

As we anticipated, the equation (1.44) for the running coupling constant is obtained by solving the differential equation for the β -function truncated at leading order, indeed:

$$\frac{dg(Q^2)}{d\ln(Q^2)} = -\beta_0 g^2(Q^2). \quad (1.47)$$

²For example the momentum transfer, or the energy in the center of mass frame $E_{\text{cm}} = \sqrt{s}$.

We may wonder when we can trust the solution of this equation. To answer this question, first we note that the truncated equation (1.47) makes sense only if the coupling constant $g(Q^2)$ is sufficiently small, allowing us to neglect all the higher order terms. Then it is sufficient to notice that β_0 is **positive**; as a consequence, from (1.47) we see that increasing the energy scale of the process, the coupling constant gets smaller and smaller, thus enforcing the efficacy of the approximation. In more detail, if we truncate the expansion of the β -function up to a certain order, we are including in the correction a certain set of many-loop Feynman diagrams that produces the screening or anti-screening of the bare strong charge of quarks. If we stop the expansion at leading order retaining only the β_0 -term, as the energy scale gets higher, the contribution given by the diagrams we neglected becomes smaller compared to the leading order diagrams, like those shown in figure 1.2. Therefore all the discarded diagrams give only tiny subleading corrections in the high energy range, making the approximated solution satisfying. This property of the QCD coupling constant is called asymptotic freedom: the higher is the energy scale of our probe of hadronic matter, the lower is the strength of interaction between quarks. Hence, quarks behave like free particles in high energy processes.

If at the contrary the energy scale gets lower, the coupling gets larger, the leading order approximation we made breaks down and we must include higher order terms (accounting for more complicated diagrams like multi-gluon exchange between loops, see figure 1.3) until the coupling becomes approximately equal to one. At this point, perturbation theory cannot be employed anymore. This mechanism is called **confinement** or infrared slavery and its mathematical proof is not yet known, since we cannot rely on the perturbative approach. However, it is very well described in lattice QCD simulations.

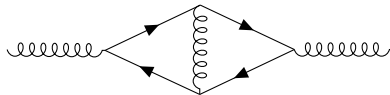


Figure 1.3: An example of two-loop diagram to be included at next-to-leading order for the calculation of the β -function.

The discovery of asymptotic freedom allows us to employ perturbative calculations for processes involving strong interactions, at least at high energy. Furthermore it successfully explained the results of an experiment performed in 1968 at SLAC on deep-inelastic scattering between electrons and nucleons indicating that the strong interaction becomes weaker at high energy. In fact the diffusion of the electron was not compatible with a pointlike structure of the nucleon: the electron interacts only with a single quark and not with the entire nucleon. Thus the other two quarks do **not** participate to the interaction and are called **spectators**. In other words, the three quarks weakly interact with each other and this is perfectly explained by asymptotic freedom. Another important

fundamental process in QCD is given by the annihilation of an electron and a positron into a quark-antiquark pair through the emission of a virtual photon, namely:

$$e^+e^- \rightarrow \gamma^* \rightarrow q\bar{q}. \quad (1.48)$$

Since the effects of strong interaction in quark-antiquark pair production can be neglected at high energy, asymptotically we expect the process to be almost entirely electromagnetic, so that it can be efficiently described by QED. We can compare this total cross section with the one of a well known QED process, the annihilation into muon-antimuon pair. Hence we expect the ratio of these two cross sections to give:

$$\lim_{\beta \rightarrow 1} \left[\frac{\sigma(e^+e^- \rightarrow q\bar{q})}{\sigma(e^+e^- \rightarrow \mu^+\mu^-)} \right] \sim 3 \cdot \left(\sum_{\text{flav}} Q_{\text{flav}}^2 \right), \quad (1.49)$$

at a given high energy scale $E_{\text{cm}} = \sqrt{s}$. Here Q_{flav} is the electric charge of the quark and the overall factor 3 encodes the existence of color: every pair can be produced in three different configurations, red-antired, blue-antiblue and green-antigreen. For example, if the energy scale is fixed to be 45GeV, the effective number of flavors is $N_f = 5$ (the **top** quark cannot be produced since the energy scale is not high enough), hence:

$$\lim_{\beta \rightarrow 1} \left[\frac{\sigma(e^+e^- \rightarrow q\bar{q})}{\sigma(e^+e^- \rightarrow \mu^+\mu^-)} \right] \sim 3 \cdot \left[2 \left(\frac{2}{3} \right)^2 + 3 \left(-\frac{1}{3} \right)^2 \right] = \frac{11}{3}. \quad (1.50)$$

This theoretical result is in good agreement with experimental measurements between 2.5GeV and 45GeV, see figure 1.4 and [10] for details and an up-to-date review.

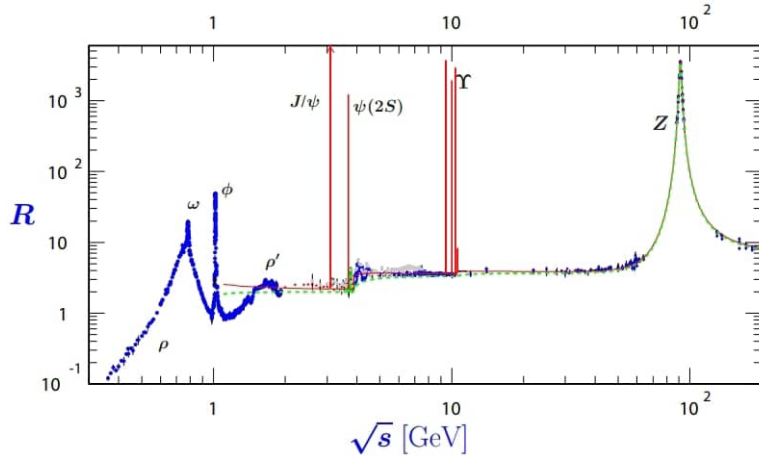


Figure 1.4: The ratio R of $\sigma(e^+e^- \rightarrow q\bar{q})$ and $\sigma(e^+e^- \rightarrow \mu^+\mu^-)$ as a function of $E_{\text{cm}} = \sqrt{s}$ [10]. Large deviations from (1.49) are due to resonances like J/ψ ($c\bar{c}$).

Chapter 2

The large N limit

2.1 Introduction: the large N expansion

When dealing with interacting quantum field theories in $(1 + 3)$ -dimensional Minkowski space-time, no exact solutions of the equations of motion are known, even in the simplest case. To circumvent this problem, it is then necessary to develop a perturbative approach to calculate probability amplitudes:

- First we define the generating functional for the **free theory** and solve it (whenever possible) using the functional integral approach.
- Then we define the generating functional for the **interacting theory** in terms of generating functional of the free theory, writing the probability amplitudes as perturbative series in the coupling constant, treated as a small parameter.

However, this perturbative technique cannot be applied at energy scales in which the coupling constant of the theory is not sufficiently small. Unfortunately, as we exposed in the previous chapter, QCD is **not perturbative** at low energy scales, when the coupling constant runs becoming larger and larger. As a consequence, we should try to find a different way to perform the perturbative expansion for QCD in order to avoid this problem. For this purpose, the large N expansion can be useful to us. This particular perturbative method is used to study quantum field theories endowed with gauge symmetries like $SU(N)$ or $SO(N)$ that otherwise would not be studied using standard perturbative techniques. It consists in expanding the probability amplitudes in powers of $1/N$, in the limit in which $N \rightarrow +\infty$. We also define the **large N limit** as the description of a theory carried up at leading order in the $1/N$ expansion. One could think that enlarging the number of colors of the theory (and correspondingly the number of degrees of freedom of the fields) would make the theory much more complicated. However, if the expansion is performed in a suitable way, it turns out that this procedure vastly simplifies

our task and allows us to catch some key features of the theory at an energy scale that could otherwise be inaccessible. In particular, retaining only the leading order terms in the expansion, computations become surprisingly simple and powerful. The idea of letting the dimensionality of a gauge symmetry group become large was first developed in statistical mechanics by Stanley [3]. A few years later, Wilson applied this method to quantum field theory, noticing the occurring simplification of the ϕ^4 theory to leading order in the expansion. Finally, the first who applied this method to QCD was 't Hooft in [5] and [6].

The procedure runs as follows: we first solve the theory to leading order in the large N expansion and to all orders in the coupling constant, then we include subleading orders to improve our predictions, even if this last step is usually not straightforward and requires much more efforts.

In this chapter we illustrate how the large N limit works applying it to the Gross-Neveu model and to QCD. Furthermore, we will solve the so called 't Hooft model, that is nothing but $(1 + 1)$ -dimensional QCD studied to leading order in the $1/N$ expansion.

2.2 The Gross-Neveu model in the large N limit

The Gross-Neveu model [9] is a **$(1 + 1)$ -dimensional** field theory that shares some features with QCD. In fact we can anticipate that this theory is asymptotically free and manifests a spontaneous chiral symmetry breaking. As a consequence, it can be considered a good toy-model for QCD. We will follow the developments of the topic given in [7] and [8].

The Gross-Neveu lagrangian is given by:

$$\mathcal{L} = \bar{\psi}^a i\gamma^\mu \partial_\mu \psi^a + \frac{\lambda}{2} (\bar{\psi}^a \psi^a)^2. \quad (2.1)$$

The ψ^a , $a = 1, \dots, N$, are N Dirac fields and the Einstein summation convention is understood. In $(1 + 1)$ dimensions, the lagrangian has mass dimension $[M]^2$, then the Dirac fields have mass dimension $[M]^{1/2}$. As a consequence, the coupling constant λ is **dimensionless**. The lagrangian of the model is invariant under the internal global symmetry group $U(N)$ acting on the fermion fields:

$$\psi^a(x) \rightarrow U_b^a \psi^b(x). \quad (2.2)$$

Furthermore, it is also manifestly invariant under the discrete chiral symmetry given by:

$$\psi \rightarrow \gamma_5 \psi, \quad \bar{\psi} \rightarrow -\bar{\psi} \gamma_5, \quad \bar{\psi} \psi \rightarrow -\bar{\psi} \psi. \quad (2.3)$$

The minus sign appearing in (2.3) for the transformation of the fermion bilinear $\bar{\psi} \psi$ is responsible for the absence of a mass term in the lagrangian, thus all fermions are massless. Therefore, it turns out that (2.1) is the most general lagrangian describing a $(1+1)$ -dimensional **renormalizable** field theory of N interacting fermion fields endowed with the symmetries mentioned above.

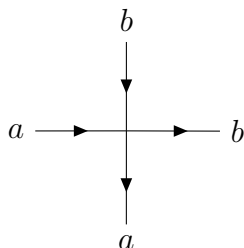


Figure 2.1: The four-fermion vertex of the Gross-Neveu model. Here a and b are flavor indices.

To start with, we study the process $a + \bar{a} \rightarrow b + \bar{b}$ ($a \neq b$) in which a fermion-antifermion pair annihilates into another pair of different flavors. The low-order diagrams contributing to this process in ordinary perturbation theory are shown in figure 2.2. The first diagram is the **Born contact term**, that is of order λ . The other two diagrams are both one-loop corrections to the amplitude; in the first one the internal indices are fixed, so it is of order λ^2 , while in the second one the color index c is arbitrary and we must sum over all its possible values, producing a factor N . Hence this last diagram is of order $N\lambda^2$. Therefore it is evident from the above analysis that the radiative corrections to the process grow with powers of N and do not possess a well-defined large N limit. In order to circumvent this problem, we rescale the coupling constant λ as

$$\lambda = \frac{g^2}{N} \quad (2.4)$$

and perform the limit $N \rightarrow +\infty$ keeping g^2 fixed. This procedure is known as the **'t Hooft limit** and allows us to obtain a well defined $1/N$ expansion.

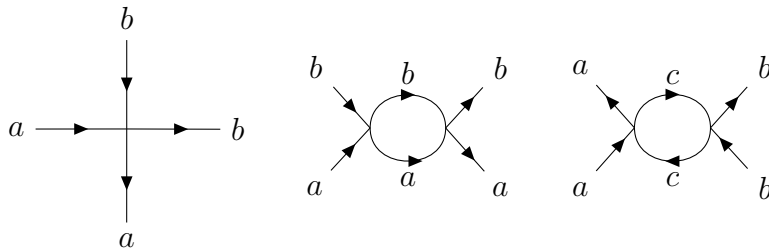


Figure 2.2: Low-order diagrams for the process $a + \bar{a} \rightarrow b + \bar{b}$. In the third graph the c flavor index is summed over producing a factor N .

The Gross-Neveu lagrangian written in terms of g^2 then becomes:

$$\mathcal{L} = \bar{\psi}^a i \gamma^\mu \partial_\mu \psi^a + \frac{g^2}{2N} (\bar{\psi}^a \psi^a)^2. \quad (2.5)$$

After this rescaling, the diagrams in figure 2.2 become of order g^2/N , g^4/N^2 and g^4/N respectively. Only vertices and flavor-index loops contribute to the power counting. However, we still have a problem: if we look at the last two diagrams from a topological point of view, we easily see that they have the same number of vertices, momentum loops, internal and external lines. Nonetheless, they have different behaviours at large N . The underlying reason for this is that in the first diagram the momentum loop in the middle carries two uncontracted flavor indices, while in the second one the contracted index c produces a factor of N . This difference can be easily checked following the arrows associated to each fermion line. As a consequence, from the point of view of the $1/N$ expansion, these two diagrams are completely **different** and we should find a way to make this difference manifest without keeping track of flavor indices at all. For this purpose, we introduce an auxiliary flavor-singlet field σ , modifying the lagrangian as follows:

$$\mathcal{L} \rightarrow \mathcal{L} + \frac{N}{2g} \left(\sigma - \frac{g}{2N} \bar{\psi}^a \psi^a \right)^2. \quad (2.6)$$

The auxiliary field does not affect the dynamics, since using the approach of functional integration the term we added is gaussian and therefore can be easily integrated. The integration produces an irrelevant overall constant that multiplies the generating functional of the theory. Through a little bit of algebra we find that:

$$\mathcal{L}_\sigma = \bar{\psi}^a i \gamma^\mu \partial_\mu \psi^a + \sigma \bar{\psi}^a \psi^a - \frac{N}{2g^2} \sigma^2. \quad (2.7)$$

Although the dynamics is the same, the Feynman rules are different and listed below:

$$\longrightarrow = \frac{i}{\not{p} + i\epsilon} \quad (2.8)$$

$$\text{-----} = -\frac{ig^2}{N} \quad (2.9)$$

$$\begin{array}{c} a \\ \nearrow \\ \text{-----} \\ \searrow \\ a \end{array} = 1 \quad (2.10)$$

Counting powers of $1/N$ is now easier than before, since the only vertex is now given by $\sigma\bar{\psi}\psi$, where one of the fermions is incoming and the other is outgoing. Factors of $1/N$ come only from the internal σ lines. Furthermore, by the inspection of the new Feynman rules given above, it is evident that every closed fermion line carries the same flavor index¹, and this index must be summed over producing a factor of N . Hence, the N -dependence from fermions is only included in their loops (see figure 2.3).

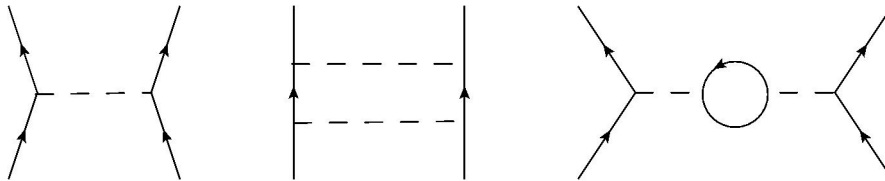


Figure 2.3: The three diagrams in figure 2.2 drawn in terms of the new lagrangian 2.7. Closed fermion loops like the one in the third diagram are now clearly distinguished from loops like the one in the second diagram, that involves both fermion and auxiliary fields and thus does not carry the same flavor index.

However, we can further simplify the counting: as we just mentioned, the only powers of N are carried by σ -propagators and fermion loops. As a consequence, we choose to describe the theory using an **effective action**² $S_{\text{eff}}(\sigma, N)$ obtained integrating out the fermion fields. In fact, the theory encoded by the lagrangian (2.7) is described in terms of a generating functional given by:

$$Z = \int \mathcal{D}\sigma \mathcal{D}\bar{\psi} \mathcal{D}\psi e^{iS[\sigma, \bar{\psi}, \psi]}. \quad (2.11)$$

¹It is evident by inspecting the flow of the arrows.

²A short review of its definition is given in appendix D.

Hence, we integrate over all the configurations of the fields defining the theory, and each of them is weighted by the complex exponential of the **classical action**. The key feature of the effective action is that it includes quantum corrections to the classical solutions of the equations of motion. It is computed integrating over all the configurations of the fermion fields only:

$$e^{iS_{\text{eff}}(N,\sigma)} = \int \mathcal{D}\bar{\psi}\mathcal{D}\psi e^{iS[\sigma,\bar{\psi},\psi]}. \quad (2.12)$$

The functional integral can be performed exactly, since the lagrangian (2.7) is quadratic in the fermion fields: the effective action we are computing is **exact**, thus no information encoded in the original lagrangian has been thrown out, we are only describing the same theory in terms of the auxiliary field and new vertices. These new vertices are given by the sum of all 1PI³ diagrams given by the lagrangian (2.7) connected to an arbitrary number of external σ lines. Since we are mainly interested in the leading order diagrams in powers of $1/N$, we realize that these new vertices collapse into the sum of only those 1PI diagrams shown in figure 2.4. We can prove this performing the integral. We actually find that:

$$S_{\text{eff}}(\sigma, N) = N\tilde{S}_{\text{eff}}(\sigma), \quad (2.13)$$

so the effective action is proportional to N and the power counting becomes trivial. It is not important to give an explicit expression for $\tilde{S}_{\text{eff}}(\sigma)$, it is only sufficient to notice that it does not depend on N anymore.

³A Feynman diagram is one particle irreducible when we cannot disconnect it cutting a single internal line.

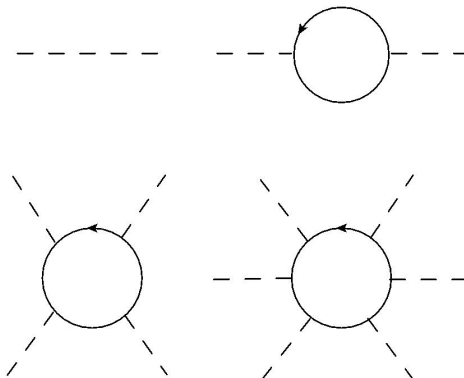


Figure 2.4: Diagrammatic expansion of the effective action $S_{\text{eff}}(\sigma, N)$ at large N . The first diagram represents the σ propagator, while the others represent the possible interaction vertices surviving at large N .

Inspecting (2.13), it is evident that the interaction vertices for this effective action carry a factor of N each, no matter what their explicit mathematical expression is. As a consequence, they can be regarded as single fermion loops, since for each of them we sum over flavors, obtaining the desired factor of N . Furthermore, each σ propagator has a factor of $1/N$, since it is given by the inverse of the quadratic term in $\tilde{S}_{\text{eff}}(\sigma)$, thus everything goes as expected. Consider a connected Feynman diagram in our effective theory with E external lines, I internal lines, V vertices and L σ -loops⁴. It is very well known that these numbers are not independent, but satisfy the following relation:

$$L = I - V + 1. \quad (2.14)$$

The power of N of this diagram can be easily expressed in terms of this quantities: every σ propagator, external or internal, gives a factor $1/N$ and every vertex gives a factor N . Thus, using the relation 2.14, we have:

$$N^{V-I-E} = N^{1-L-E}. \quad (2.15)$$

As a consequence, if we fix the number of external σ lines, every σ -loop reduces the power of N by a unit. Therefore the leading order diagrams are those without loops (**tree diagrams**) and the least possible number of external σ lines required to connect the (true) external fermion lines appearing in the original diagram⁵. The more loops we have, the more we are subleading in N (see figure 2.5).

⁴We remark that every line in this effective diagram is given by σ lines. The external lines in this case must not be confused with the external lines for the diagram in our original theory (2.7), that are trivially given by incoming or outgoing fermions.

⁵For the $a + \bar{a} \rightarrow b + \bar{b}$ amplitude we have $E = 2$.

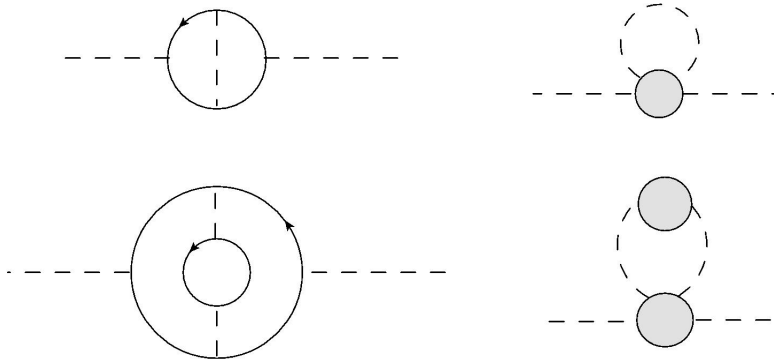


Figure 2.5: To the left: two 1PI loop diagrams in the original theory. To the right: their effective counterparts, described in terms of new vertices and σ propagators closed to form σ loops. In the large N limit both these effective diagrams are suppressed.

In order to prove that this theory is asymptotically free, we need to compute the **Coleman-Weinberg potential**, given by the effective action evaluated for incoming σ lines carrying zero momenta⁶, namely:

$$-iV(\sigma) = -i\frac{N}{2g^2}\sigma^2 - N \sum_{n=1}^{+\infty} \frac{1}{2n} \text{Tr} \left[\int \frac{d^2p}{(2\pi)^2} \left(\frac{-\not{p}\sigma}{p^2 + i\epsilon} \right)^{2n} \right]. \quad (2.17)$$

The main simplification provided by the large N limit is the fact that the diagrams of the effective theory reduced to a subset of all 1PI ones shown in figure 2.4, allowing us to sum them exactly to obtain the second term in (2.17). Thus we neglected two (or more) loops corrections to the effective potential (see figure 2.5) We obviously only have even powers of the quantity inside the trace because a trace of an odd number of gamma matrices identically vanishes. Performing the trace and suitably regulating the momentum integrals using the \overline{MS} scheme, we obtain:

$$V(\sigma) = N \left[\frac{\sigma^2}{2g^2} + \frac{\sigma^2}{4\pi} \left(\ln \frac{\sigma^2}{\mu^2} - 1 \right) \right]. \quad (2.18)$$

Since more-loop corrections are suppressed at large N , this effective potential is exact and satisfies the renormalization group equation, given by:

⁶This condition corresponds to a space-time constant auxiliary field, indeed:

$$\sigma(x) = \sigma = \int \delta(p) e^{ipx} dp, \quad (2.16)$$

thus $p = 0$.

$$\left[\mu \frac{\partial}{\partial \mu} + \beta(g) \frac{\partial}{\partial g} - \gamma_\sigma(g) \frac{\partial}{\partial \sigma} \right] V(\sigma) = 0, \quad (2.19)$$

where μ is the renormalization scale. Thus we have:

$$\beta(g) = -\frac{g^3}{2\pi}. \quad (2.20)$$

The theory is then asymptotically free to all orders in g^2 in the large N limit. Furthermore, the Gross-Neveu model also exhibits spontaneous chiral symmetry breaking. From (2.18) we can find the extrema of the effective potential:

$$\sigma_{\max} = 0, \quad \sigma_{\min} = \pm \sigma_0 = \pm \mu e^{-\pi/g^2}, \quad (2.21)$$

at which V takes the values:

$$V(0) = 0, \quad V(\pm \sigma_0) = -\frac{N\sigma_0^2}{4\pi}. \quad (2.22)$$

Therefore chiral symmetry is spontaneously broken, since:

$$\langle \sigma \rangle = \frac{g^2}{N} \langle \bar{\psi} \psi \rangle. \quad (2.23)$$

The fermions then acquire a mass $m = \sigma_0$. As a final remark, we notice that for the theory described by the effective lagrangian $S_{\text{eff}}(\sigma)$ the large N limit is equivalent to the semiclassical approximation, as it is evident by the following equality:

$$\int \mathcal{D}\sigma e^{\frac{i}{\hbar} S_{\text{eff}}(\sigma, N)} = \int \mathcal{D}\sigma e^{\frac{iN}{\hbar} \tilde{S}_{\text{eff}}(\sigma)}. \quad (2.24)$$

Thus, the expansion in \hbar is equivalent to an expansion in $1/N$. This is an alternative way to see why we only considered tree-level (**classical**) diagrams and neglected all σ -loop corrections in our analysis at large N . To sum up, the large N limit of the Gross-Neveu model is equivalent to a semiclassical limit of an effective action $S_{\text{eff}}(\sigma, N)$ describing the dynamics of a flavor-singlet field σ defined through a quark-bilinear (**mesons**).

2.3 Quantum chromodynamics in the large N limit

At this point we want to apply the large N limit to quantum chromodynamics. Developing this subject we mainly follow [8] and [22]. The idea of applying the large N limit to

QCD was first developed by G. 't Hooft in [5]. The main difficulty we are going to face is just that now we are dealing with fields transforming according to the **adjoint representation** of the $SU(N)$ gauge group, namely the gauge fields $A_\mu^a(x)$. In addition we have the quark fields $\psi_i(x)$ with the index $i = 1, \dots, N$ living in the fundamental representation of the gauge group⁷. Dealing with adjoint indices, it turns out (see appendix A) that they can be thought as formed by a pair of **fundamental and antifundamental indices** (i, j) . In other words, an adjoint index lives in the tensor product of the fundamental and antifundamental representations provided that the singlet component is subtracted, namely:

$$\mathbf{N} \otimes \overline{\mathbf{N}} = \underbrace{(\mathbf{N}^2 - \mathbf{1})}_{\text{adjoint}} \oplus \mathbf{1}. \quad (2.25)$$

Therefore, the gauge-boson fields $A_\mu^a(x)$ can be labeled using two color indices as follows:

$$A_\mu^a(x) = [A_\mu(x)]_j^i \quad i, j = 1, \dots, N, \quad (2.26)$$

where the upper index transforms under the antifundamental representation and the lower under the fundamental one. The propagator for these fields can be easily written using the Fierz identity:

$$[D_{\mu\nu}(p)]_{jl}^{ik} = \sum_{a=1}^{N^2-1} (T^a)_j^i (T^a)_l^k D_{\mu\nu}(x-y) = \left(\delta_l^i \delta_j^k - \frac{1}{N} \delta_j^i \delta_l^k \right) D_{\mu\nu}(x-y). \quad (2.27)$$

Furthermore, the dynamics of QCD that admits a non-trivial $1/N$ expansion is given by the following lagrangian:

$$\mathcal{L} = \frac{N}{g^2} \left\{ -\frac{1}{4} [F_{\mu\nu}(x)]_j^i [F^{\mu\nu}(x)]_i^j + \overline{\psi}^i(x) [\not{D}(x)]_i^j \psi_j(x) - m \overline{\psi}^i(x) \psi_i(x) \right\}. \quad (2.28)$$

This lagrangian is obviously incomplete: we left the gauge fixing term and all those terms involving ghost fields. The term proportional to $1/N$ appears in the propagator (2.27) because of the tracelessness of the gluon field. It would not be present if the gauge group were $U(N)$ rather than $SU(N)$ but, since we are interested in the leading order in the $1/N$ expansion, we can safely drop it and actually work with a $U(N)$ gauge theory. Collecting all these results, we obtain the so called **'t Hooft double line notation**,

⁷For the sake of simplicity we take into account only a single quark flavor omitting the (k) flavor indices we used in the previous chapter.

that allows us to represent the gluon propagator as made up of two straight lines pointing in two opposite directions (because \mathbf{N} and $\overline{\mathbf{N}}$ are **not** equivalent, but they are one the complex conjugate representation of the other, so there is a distinction between upper and lower indices⁸). Thus, a gluon propagates like a quark-antiquark pair (see figure 2.6). The propagator at large N is then given by:

$$[D_{\mu\nu}(p)]_{jl}^{ik} = \delta_l^i \delta_j^k D_{\mu\nu}(x-y). \quad (2.29)$$

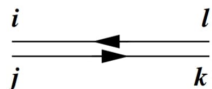


Figure 2.6: The gluon propagator in double line notation [21].

We can similarly rewrite the three and four gluon vertices using the double line notation as shown in figure 2.7 .

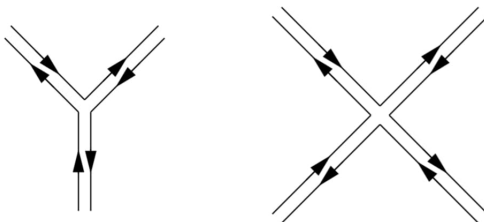


Figure 2.7: The three and four gluon vertices in double line notation [21].

Finally, a quark propagator is represented by a **single** straight line with an arrow pointing from the lower to the upper index (it is proportional to a Kronecker's delta δ_j^i). Using this new notation, we can redraw any Feynman single-line diagram: given a single-line diagram with **assigned** indices, there is only one double-line diagram corresponding to it. Thus, if there are different ways of assigning indices to a single-line diagram, we will have more than one double-line diagram associated with it.

2.3.1 N counting and surface topology

Our main purpose is to assign to every double-line diagram its power of $1/N$. In the following we will realize that this power is determined by the topological properties of the diagram itself. For simplicity, we first focus on vacuum bubbles (diagrams with no external lines). In this case, every line must close to make an index loop. We now have

⁸Nevertheless, if the gauge group were $SO(N)$, for which the fundamental and antifundamental representations are equivalent, we would not have arrows pointing in opposite directions.

to imagine every closed loop as the perimeter of a polygon and interpret the double-line notation as a prescription for sewing these polygons together. More precisely, we identify one edge of a polygon with one edge on another if the both lie on the same double-line (they belong to the **same gluon propagator**). In this way we construct a two-dimensional surface. Furthermore, we can give to it an orientation following the arrows running along the perimeters of each polygon. Thus we end up with an oriented two-dimensional surface.

It is then easy to count the power of $1/N$ for this surface. Let it have V vertices, E edges and F faces. Every interaction vertex corresponds to one of the V vertices of the surface and we can see by direct inspection of (2.28) that it carries a factor of N/g^2 , while every edge carries a factor g^2/N , because the propagator is the inverse of the kinetic term in the lagrangian. Finally, every face carries a factor N because it corresponds to an index loop, whose sum gives the number of colors. Thus, the power counting is given by:

$$N^\chi = N^{V-E+F}, \quad (2.30)$$

where χ is the **Euler characteristic** of the surface. It is a very important topological invariant, meaning that it does **not** change under homeomorphisms between different topological spaces. It also turns out that every two-dimensional oriented surface is homeomorphic⁹ to a sphere with some number of holes and handles stuck onto it. If we label with H the number of handles and with B the number of holes on this surface, we obtain that the Euler characteristic can be expressed as:

$$\chi = 2 - 2H - B. \quad (2.31)$$

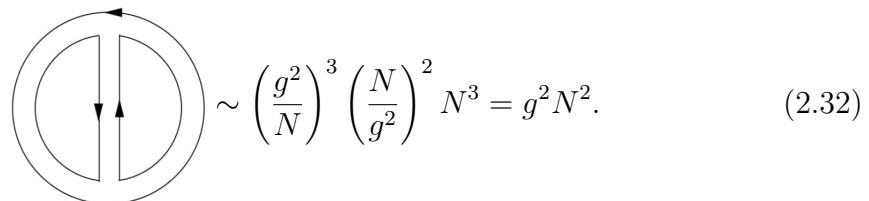
Thus we end up with the following two important results:

- **First result:** the leading connected vacuum bubbles are of order N^2 . They are planar diagrams ($H = 0$) in which we only have double-lines, thus they are made up only of gluons.

The Euler characteristic in this case is that of a sphere, namely $\chi = 2$. This means that a planar double-line bubble diagram without holes and handles is topologically equivalent to a sphere, so it can be suitably inscribed onto it. This is easy to see: given a planar bubble diagram made up only of gluon lines, we can transform it into a double-line one. This transformation divides the plane into disjoint regions. At this point, we have to associate a clockwise orientation to all

⁹Topologically equivalent.

these regions and give the external index line a counterclockwise direction. Finally, we only have to identify the perimeters of these regions. Conversely, given a gluon bubble diagram drawn onto a sphere, we can choose one of its faces and remove it. Then we can flatten what's left onto the plane and use the perimeter of the removed face to envelop it, suitably defining a point at infinity (see figure 2.8). An example of such bubble diagrams is given by:



$$\sim \left(\frac{g^2}{N}\right)^3 \left(\frac{N}{g^2}\right)^2 N^3 = g^2 N^2. \quad (2.32)$$

We incidentally remind that in the 't Hooft limit g^2 is hold fixed. This diagram drawn on a sphere is shown in figure 2.10(a).

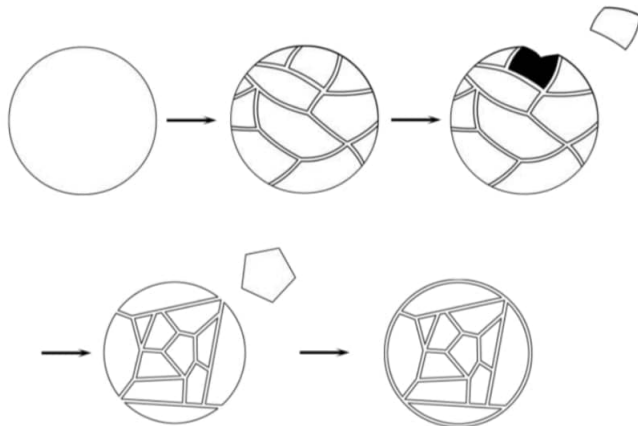
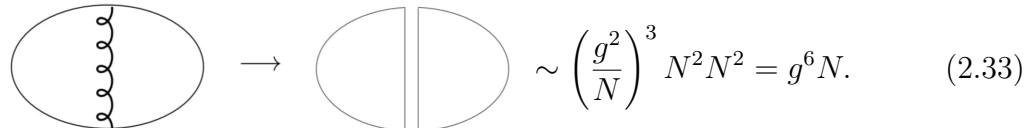


Figure 2.8: Procedure of construction of a gluon double-line bubble diagram inscribed onto a sphere [23].

- **Second result:** the leading connected vacuum bubbles with quark lines are of order N . They are planar diagrams ($H = 0$) with a single quark loop, that represents a hole on the two-dimensional surface; it is necessary that the quark loop runs around the boundary of the diagram, otherwise we would be in presence of an handle and the diagram would be subleading (see figure 2.9).

The Euler characteristic is that of a sphere with a hole, namely $\chi = 1$. This means that the leading bubble diagrams with a single quark line are topologically equivalent to a sphere with a hole, so it can be easily inscribed onto it. The quark

loop index line represents the boundary of the hole. As a matter of fact, a sphere with a hole can be easily flattened on a plane, but this time we do not have a removed face to envelope the flattened ones. The external lines then are unpaired and represent the boundary of the flattened diagram. An example of such diagrams is given by:



$$\sim \left(\frac{g^2}{N}\right)^3 N^2 N^2 = g^6 N. \quad (2.33)$$

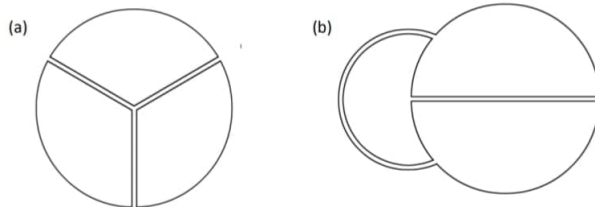
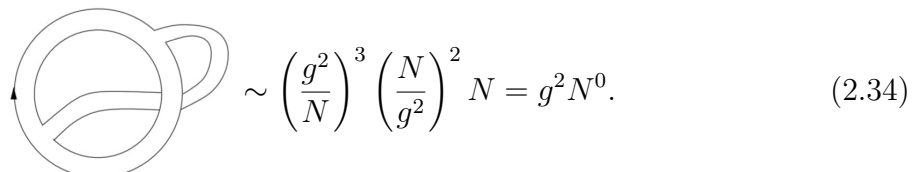


Figure 2.9: Two examples of bubble diagrams involving a single quark loop. Diagram (a) is a leading order one, since the quark loop runs around the boundary and consequently it is topologically equivalent to a sphere with one hole. Diagram (b) is subleading and suppressed at large N , since the quark loop does not run around the boundary. Hence it is non-planar and topologically equivalent to a sphere with a hole and an handle stuck onto it [7].

It is now mandatory to underline that we are actually interested in scattering processes involving **only** gluons. Particularly, we focus our attention on the **tree-level diagrams**. Thus, for the purposes we just mentioned, the only diagrams surviving the $N \rightarrow +\infty$ limit are the planar ones, proportional to N^2 . For example, if we drew a pure gluon diagram ($B = 0$) with one handle ($H = 1$), the power of N would decrease of two units; an example is this kind of diagrams is:



$$\sim \left(\frac{g^2}{N}\right)^3 \left(\frac{N}{g^2}\right)^2 N = g^2 N^0. \quad (2.34)$$

A non-planar diagram like this cannot be drawn on a sphere, but we need a third dimension to succeed in this task. We can easily evaluate the order of this diagram, namely $\chi = 0$, hence $H = 1$. All the oriented surfaces with this Euler characteristic are topologically equivalent to a torus. As a consequence, such a diagram can be drawn on a

torus, as shown in figure 2.10(b). Furthermore, for tree-level pure gluon amplitudes, we will see in the next chapter that the $1/N$ term in the propagator has no effect on the computation: all the terms involving it precisely cancel one with each other. This is **not** due to the large N expansion, the result is exact and prove to be very useful in the following. In other words, the 't Hooft double line notation for gluon propagators is exact for tree-level diagrams, due to the **photon decoupling identity**, as we will see in the next chapter. We remark that this is only a tree-level trick, it cannot be used when loops are present.

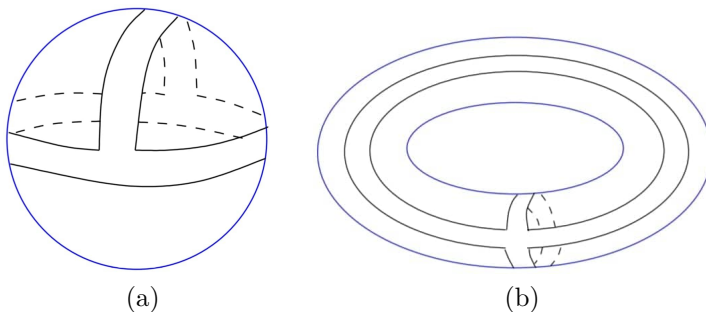


Figure 2.10: The diagrams in (2.32) and (2.34) inscribed on a sphere and on a torus respectively [22].

2.4 The 't Hooft model

The 't Hooft model [6] is nothing but **(1+1)-dimensional QCD** studied in the large N limit. As we will see in the following, restricting QCD to two space-time dimensions will vastly simplify our task. First of all, the lagrangian is given by:

$$\mathcal{L} = \frac{1}{4} [F_{\mu\nu}]_j^i [F^{\mu\nu}]_i^j - \sum_{k=1}^{N_f} \bar{\psi}_i^{(k)} (\not{D} + m_{(k)})^{ij} \psi_j^{(k)}, \quad (2.35)$$

where N_f is the number of quark flavors and $k \in [1, \dots, 6]$ is the label for these flavors, while (i, j) label color indices¹⁰ (since we are at large N , the 't Hooft double-line notation is understood). Furthermore, we have that:

$$F_{\mu\nu} = \partial_\mu A_\nu - \partial_\nu A_\mu + g[A_\mu, A_\nu], \quad (2.36)$$

$$D_\mu = \partial_\mu + gA_\mu. \quad (2.37)$$

For reasons that will become clear in the following, we change set of coordinates using:

¹⁰We will omit color indices from now on.

$$x^\alpha = (x^-, x^+), \quad (2.38)$$

where we suitably define:

$$x^\pm = \frac{1}{\sqrt{2}}(x_0 \pm x_1), \quad (2.39)$$

in place of the usual minkowskian coordinates $x^\mu = (x^0, x^1)$. These coordinates are called **light-cone coordinates**. The space-time line element is expressed in the new coordinates using the following new metric:

$$g = \begin{pmatrix} 0 & 1 \\ 1 & 0 \end{pmatrix}. \quad (2.40)$$

In fact we easily obtain:

$$g_{\alpha\beta} = \frac{\partial x_\alpha}{\partial x^\mu} \frac{\partial x_\beta}{\partial x^\nu} \eta_{\mu\nu} \rightarrow g = \begin{pmatrix} 0 & 1 \\ 1 & 0 \end{pmatrix}, \quad (2.41)$$

and consequently we get:

$$ds^2 = g_{\alpha\beta} dx^\alpha dx^\beta = 2dx^+ dx^-. \quad (2.42)$$

We clearly use the metric (2.40) to suitably raise and lower the light-cone indices:

$$x_- = g_{-\alpha} x^\alpha = x^+, \quad (2.43)$$

$$x_+ = g_{+\beta} x^\beta = x^-. \quad (2.44)$$

Our summation convention then becomes:

$$x^\alpha p_\alpha = x^\alpha g_{\alpha\beta} p^\beta = x^+ p^- + x^- p^+ = x_+ p_- + x_- p_+ = x_- p^- + x_+ p^+. \quad (2.45)$$

The vector-potential A_μ can be decomposed on the new coordinate lines, namely:

$$A^\pm = \frac{1}{\sqrt{2}}(A^0 \pm A^1). \quad (2.46)$$

The F_{+-} component of the strength tensor in the new coordinates is given by:

$$F_{+-} = \partial_+ A_- - \partial_- A_+ + g[A_+, A_-]. \quad (2.47)$$

Now we need to fix a gauge choosing the so called **light-cone gauge**:

$$A_- = A^+ = 0. \quad (2.48)$$

We incidentally remark that in this gauge we fix to zero the values of the **contravariant** component A^+ and the **covariant** component A_- . Furthermore it is also a Lorentz invariant gauge choice. Thus we get:

$$F_{+-} = -\partial_- A_+ = -F_{-+}. \quad (2.49)$$

The strength tensor has only one non-vanishing component and the commutator identically vanishes. Therefore, the gauge we chose makes the theory **abelian**, making the analysis much more easy: non-linear terms disappear from the lagrangian, hence we do **not** have self-interacting gluons any more. This drastically diminishes the number of diagrams that contribute at large N . Furthermore, diagrams become much more simple because any gluon line that connects two quark lines represents an impassable barrier. No other gluon can cross the first interacting with it, because there is no self-interaction between gluons. In addition, since at large N only **planar diagrams** survive, a gluon cannot cross another one without interaction, because it should get under or over it, and this would violate planarity. Writing the strength tensor as a matrix, we find:

$$F_{\alpha\beta} \rightarrow \begin{pmatrix} 0 & \partial_- A_+ \\ -\partial_- A_+ & 0 \end{pmatrix}. \quad (2.50)$$

We can now proceed in our study of the theory. The lagrangian can be rewritten as follows:

$$\mathcal{L} = -\frac{1}{2} \text{Tr}(\partial_- A_+)^2 - \bar{q}_{(k)}(\gamma \cdot \partial + m_{(k)}^2 + g\gamma_- A_+)q_{(k)}, \quad (2.51)$$

where we suitably defined a new set of gamma matrices that have to satisfy the **Clifford's algebra** for the new metric (2.40):

$$\{\gamma_\alpha, \gamma_\beta\} = 2g_{\alpha\beta}, \quad (2.52)$$

where $\alpha, \beta = \pm$. Hence we obtain:

$$(\gamma_+)^2 = (\gamma_-)^2 = 0, \quad (2.53)$$

$$\gamma_+\gamma_- + \gamma_-\gamma_+ = 2. \quad (2.54)$$

The only interaction vertex appearing in the lagrangian is given by $g\bar{q}_k(\gamma_-A_+)q_k$. It only involves the matrix γ_- . On the contrary, the quark propagator involves both the gamma matrices γ_{\pm} . However, in a Feynman diagram, every quark propagator will be sandwiched between two γ_- matrices, because it connects two different vertices.

The free quark propagator is given by:

$$S_0(p) = \frac{m_{(k)} - i\gamma_-p_+ - i\gamma_+p_-}{m_{(k)}^2 + 2p_-p_+ + i\epsilon}. \quad (2.55)$$

Sandwiching the propagator between two vertices, neglecting irrelevant numerical factors, we get:

$$\gamma_- \left(\frac{m_{(k)} - i\gamma_-p_+ - i\gamma_+p_-}{m_{(k)}^2 + 2p_-p_+ + i\epsilon} \right) \gamma_- = \frac{-i\gamma_-(\gamma_+p_-)\gamma_-}{m_{(k)}^2 + 2p_-p_+ + i\epsilon} = \frac{2i\gamma_+p_-}{m_{(k)}^2 + 2p_-p_+ + i\epsilon}. \quad (2.56)$$

Thus, most of the matrix structure is annihilated. In the last step we used the Clifford's algebra for the gamma matrices. As a consequence, we can safely neglect the gamma matrices for every vertex and rewrite the Feynman rules without them. Namely:

- The quark propagator can be rewritten only as a function of the momentum k as follows:

$$\frac{m_{(k)} - i\gamma_-p_+ - i\gamma_+p_-}{m_{(k)}^2 + 2p_-p_+ + i\epsilon} \rightarrow S_0(p) = \frac{-ip_-}{m_{(k)}^2 + 2p_-p_+ + i\epsilon}. \quad (2.57)$$

- The interaction vertex can be rewritten as:

$$-g\gamma_- \rightarrow -2g. \quad (2.58)$$

- Finally, the gluon propagator reads:

$$D_{\alpha\beta}(p) = \delta_{\alpha+}\delta_{\beta+}\mathcal{P}\left(\frac{1}{p_-^2}\right) \rightarrow \mathcal{P}\left(\frac{1}{p_-^2}\right), \quad (2.59)$$

where $\mathcal{P}(\dots)$ is the **principal value**¹¹ of the quantity inside the brackets.

Furthermore, the Euler-Lagrange equation for the field component A_+ is actually a constraint, namely:

$$\partial_-^2 A_+ = g\bar{q}_{(k)}\gamma_- q_{(k)}. \quad (2.60)$$

We can solve this equation and express A_+ in terms of the quark fields, then we substitute this expression into (2.51), obtaining a lagrangian that contains a **linear interaction** between color charges located in two different spatial positions x_+ and y_+ given by:

$$V(x_+, y_+) \propto |x_+ - y_+|. \quad (2.61)$$

This linear interaction implies that the 't Hooft model is **confining**. Thus only colorless particles can freely propagate through our $(1 + 1)$ -dimensional space-time and it would take an infinite amount of energy to separate quarks¹². Collecting all these results, we find that the only diagrams we can have are those of **ladder type**, with free quark lines replaced by dressed propagators.

2.4.1 Dressed propagator

To move further, we actually want to compute the dressed propagator for quarks. Our task is considerably simplified by the planarity of the diagrams in the large N limit and by the absence of interactions between gluons. As a matter of fact, the dressed propagator is nothing but the quark propagator for the interacting theory, and the graphical representation of its defining equation is given in figure 2.12.

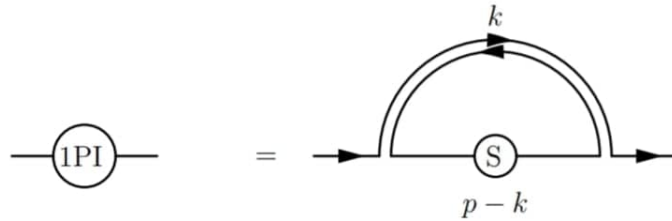


Figure 2.11: Graphical representation of the relation between dressed propagator and quark self-energy known as Dyson equation [23].

¹¹It is defined as: $\mathcal{P}\left(\frac{1}{x^2}\right) = \frac{1}{2} \left[\frac{1}{(x+i\epsilon)^2} + \frac{1}{(x-i\epsilon)^2} \right]$.

¹²This is analogous to what happens in $(1 + 1)$ -dimensional QED, that also exhibits electric charge confinement and thus is a good toy-model for $(3 + 1)$ -dimensional QCD and other confining systems [26].

The planarity of the surviving diagrams and the absence of gluon self-interactions implies that the only diagrams contributing to the dressed propagator are the **rainbow diagrams** also shown in figure 2.12. Labeling as $S(p)$ the dressed propagator and as $-i\Sigma(p)$ the 1PI diagrams surviving at large N and with no self-interactions between gluons, the quark self-energy is related to the dressed propagator through the **Dyson equation**, shown graphically in figure 2.11.

Figure 2.12: First line: graphical representation for the geometric series equation for the dressed quark propagator. Second line: definition of the two-point 1PI diagrams at large N and without self-interaction between gluons; only the rainbow diagrams satisfy both these conditions contributing to the amplitude [23].

The equation in figure 2.12 can be easily iterated to give an exact solution for the dressed propagator, namely:

$$S(p) = S_0(p) - iS_0(p)\Sigma(p)S_0(p) + \dots \quad (2.62)$$

This is a geometric series; its solution is given by:

$$S(p) = \frac{S_0(p)}{1 + i\Sigma(p)S_0(p)} = \frac{ip_-}{m_{(k)}^2 + 2p_-p_+ - p_- \Sigma(p) + i\epsilon}. \quad (2.63)$$

To complete our calculation, we finally should compute the self-energy $\Sigma(k)$. For this purpose, we use the equation in figure 2.11, namely:

$$-i\Sigma(p) = -i\Sigma(p_-) = -i4g^2 \int \frac{dk_- dk_+}{(2\pi)^2} S(p-k) \mathcal{P}\left(\frac{1}{k_-^2}\right) = -\frac{g^2}{\pi p_-}. \quad (2.64)$$

Omitting the details of the computation, it turns out that the dressed propagator has the **same form** of the free propagator, namely:

$$S(p) = \frac{ip_- - M_{(k)}}{p^2 - M_{(k)}^2 + i\epsilon}, \quad (2.65)$$

but with a **renormalized quark mass** $M_{(k)}$ given by:

$$M_{(k)}^2 = m_{(k)}^2 - \frac{g^2}{\pi}. \quad (2.66)$$

It is important to stress that although quarks propagate as free particles, this does not imply that they are not confined. The presence of a pole in the propagators does not prove that free quark (colored) states exist at all. The 't Hooft model is confining, since quarks are subject to a linear potential that is responsible for the binding force the pairs them in color singlet channels. Furthermore, quarks can be tachyonic if g^2 satisfies:

$$g^2 \geq \pi m_{(k)}^2. \quad (2.67)$$

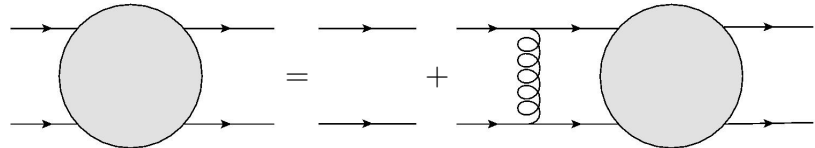
However, we will see in the next section that this problem has no effect on the colorless particles that are free to propagate: mesons.

2.4.2 Bethe-Salpeter equation and mesons

We are now ready to describe **meson bound states**. Mesons are described using Green's functions of two quark bilinears. The starting point of the analysis is the Dyson equation for these kind of Green's functions, namely:

$$G = S_1 S_2 + S_1 S_2 K_{12} G, \quad (2.68)$$

where G is the full four-point Green's function, S_i are the dressed quark propagators and K_{12} encodes all possible 2PI interactions between the two dressed quark lines. By 2PI interactions we mean that the Feynman diagrams contributing to K_{12} cannot be disconnected cutting any two internal **quark** lines. This relation is analogous to that shown in figure 2.12 for the two-point Green's function (dressed propagator). However, in our model gluons cannot interact and cross each other, thus K_{12} collapses into a single diagram given by the exchange of a single gluon line between the two dressed quark lines. In this case the recursive relation (2.68) graphically reads:



$$\text{Diagrammatic representation of equation (2.68):} \quad (2.69)$$

The blobs represent four-point Green's functions and each internal quark line is dressed. The reason is that any gluon line connecting the two upper and lower quark lines forms a

barrier that cannot be passed since all diagrams at large N are planar (furthermore gluon self-interactions are forbidden). Therefore, the key simplifications of our model imply that the four-point Green's function is given by an infinite sum of ladder diagrams. If a meson bound state actually exists, inserting the completeness relation for the Fock basis inside G , it is possible to show that Green's functions always have poles when on-shell intermediate particles are produced (see [27], section 10.2). More precisely, it can be shown that in the vicinity of this pole G is expressed as:

$$G \simeq \frac{\Psi\bar{\Psi}}{P^2 - \mu^2 + i\epsilon} + \text{regular terms as } P^2 \rightarrow \mu^2, \quad (2.70)$$

where μ is the mass of the meson bound state and P is its momentum. The amplitude Ψ is the matrix element of the time-ordered product of two quark fields between the vacuum and the meson bound state, namely:

$$\Psi = \langle \Omega | T \bar{\psi} \psi | P \rangle \neq 0. \quad (2.71)$$

Inserting (2.70) into (2.68) and omitting the explicit computation, we obtain the **Bethe-Salpeter equation**:

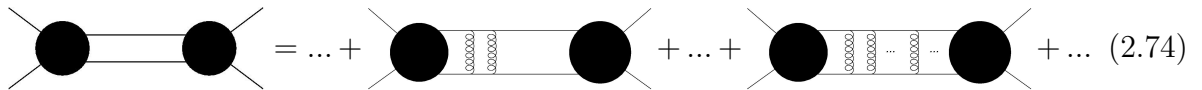
$$\Psi = S_1 S_2 K_{12} \Psi. \quad (2.72)$$

Representing Ψ as a black blob, this equation can be better written graphically as follows:



$$\text{blob} = \text{gluon ladder} \text{ blob} \quad (2.73)$$

As a consequence, the structure of the Green's function approaching the pole is represented as:



$$\text{blob} \text{ blob} = \dots + \text{gluon ladder blob} + \dots + \text{gluon ladder blob gluon ladder} + \dots \quad (2.74)$$

This graphical representation perfectly enlightens the fact that the bound state is given by an infinite exchange of single gluons between the two dressed quarks. Thus we interpret the meson bound state as made up of a quark-antiquark pair interacting infinitely many times with each other. As a consequence, the contribution to the full four-point Green's function given by the meson bound state consists in the sum of an infinite number of Feynman ladder diagrams. Labeling as q the momentum of the quark and with $P - q$ the momentum of the antiquark, namely:

$$(2.75)$$

the mathematical expression satisfied by the amplitude Ψ for the process $q\bar{q} \rightarrow meson$ reads:

$$\Psi(P, q) = -4g^2 i S(P - q) S(-q) \int \frac{d^2 k}{(2\pi)^2} \mathcal{P} \left(\frac{1}{(k_- - q_-)^2} \right) \Psi(P, k). \quad (2.76)$$

Now we suitably define the function:

$$\phi(p, q_-) = \int dq_+ \Psi(P, q). \quad (2.77)$$

Then we can make the following substitutions:

$$2P_+ P_- = \mu^2, \quad x = \frac{q_-}{P_-}, \quad y = \frac{k_-}{P_-}, \quad (2.78)$$

where the variable x represents the fractions of the total light-cone momentum carried by the quark and μ is the meson mass. Finally, after some manipulations, we get the Bethe-Salpeter equation in its final form:

$$\mu^2 \phi(x) = \left(\frac{M^2}{x} + \frac{M^2}{1-x} \right) \phi(x) - \frac{g^2}{\pi} \int_0^1 dy \mathcal{P} \left(\frac{1}{(x-y)^2} \right) \phi(y). \quad (2.79)$$

The function $\phi(x)$ is defined in the interval $[0, 1]$ and vanishes at its end points. More details on the Bethe-Salpeter equation can be found in [25]. However, (2.79) can be interpreted as a non-relativistic light-cone Schrödinger equation describing a quark-antiquark pair interacting through a linear potential enclosed between two infinite potential wells, located in $y = 0$ and $y = 1$. The confinement between two potential wells ensures that the meson spectrum is purely discrete. By the way, for sufficiently high energies the shape of the potential should be negligible and the eigenfunctions should tend towards those of a free particle in a box, namely:

$$\phi_n(x) \simeq \sin(\pi n x), \quad n = 1, 2, \dots \quad (2.80)$$

with eigenvalues given by:

$$\mu_n^2 = g^2 \pi n. \quad (2.81)$$

It is also important to remind that the renormalized quark M^2 can be tachyonic, when g^2 is sufficiently high. However this fact has no consequences on the meson mass, that stills be a positive quantity. To prove it, from (2.79) and using the identity:

$$\int_0^1 dy \mathcal{P} \left(\frac{1}{(x-y)^2} \right) = - \left[\frac{1}{x} + \frac{1}{1-x} \right], \quad (2.82)$$

we get:

$$\mu^2 \int_0^1 |\phi(x)|^2 = m^2 \int_0^1 \left(\frac{1}{x} + \frac{1}{1-x} \right) |\phi(x)|^2 dx + \frac{g^2}{2\pi} \int_0^1 dx \int_0^1 dy \frac{|\phi(x) - \phi(y)|^2}{(x-y)^2}. \quad (2.83)$$

Since m^2 is positive, μ^2 is also positive as we claimed, no matter how large g^2 is: tachyonic quarks do not constitute tachyonic mesons. Finally, as pointed out by Coleman [8], we emphasize again that the free dressed quark propagator we obtained in the previous section tells us nothing about confinement: single quarks propagate as free particles of mass M^2 (sometimes negative), nevertheless the theory is confining, hence it does **not** contain free quarks and tachyons. The location of the pole in our dressed quark propagator cannot be considered an observable quantity if our theory is confining.

Chapter 3

Color decomposition of gluon amplitudes at tree-level

3.1 Preliminary calculations

In this section we perform some calculations that will turn out to be very useful in the following. To start with, we want to prove the equation (1.19) we just mentioned in the first chapter. For this purpose, we recall that the fundamental generators of $SU(N)$ satisfy the following commutation relation:

$$[T^a, T^b] = if^{abc}T^c. \quad (3.1)$$

We can then multiply both sides by a generator T^d and take their trace, obtaining:

$$\text{Tr} \{ [T^a, T^b] T^d \} = if^{abc} \text{Tr} \{ T^c T^d \} = \frac{i}{2} f^{abc} \delta^{cd} = \frac{i}{2} f^{abd}. \quad (3.2)$$

Relabeling $d \leftrightarrow c$, we can easily write:

$$f^{abc} = -2i \text{Tr} \{ [T^a, T^b] T^c \} = -2i \text{Tr} \{ T^a [T^b, T^c] \}. \quad (3.3)$$

Hence equation (1.19) holds and gives us an expression for the structure constants in terms of fundamental generators. Furthermore, it is customary to choose a different set of fundamental generators:

$$\tilde{T}^a = \sqrt{2} \cdot T^a, \quad (3.4)$$

so that they satisfy a simpler normalization condition, namely:

$$\text{Tr} \{ \tilde{T}^a \tilde{T}^b \} = 2 \text{Tr} \{ T^a T^b \} = \delta^{ab}. \quad (3.5)$$

As a consequence, $T_F = 1$. This implies a redefinition of the structure constants:

$$f^{abc} = \frac{(-i)}{\sqrt{2}} \text{Tr} \{ \tilde{T}^a [\tilde{T}^b, \tilde{T}^c] \}. \quad (3.6)$$

In order to simplify calculations we redefine the structure constants as follows:

$$\tilde{f}^{abc} = \sqrt{2} f^{abc}. \quad (3.7)$$

so that from (3.6) we get:

$$\tilde{f}^{abc} = (-i) \text{Tr} \{ \tilde{T}^a [\tilde{T}^b, \tilde{T}^c] \}. \quad (3.8)$$

We will omit the tilde symbol and use these new definitions henceforward. Consider now another important relation, the **Fierz identity**:

$$\sum_{a=1}^{N^2-1} (T^a)_{ij} (T^a)_{kl} = \delta_{il} \delta_{kj} - \frac{1}{N} \delta_{ij} \delta_{kl}. \quad (3.9)$$

It just encodes the completeness relation for the fundamental matrices. Contracting this identity with arbitrary matrices A_{ji} and B_{lk} we obtain the useful relation:

$$\text{Tr} \{ T^a A \} \text{Tr} \{ T^a B \} = \text{Tr} \{ AB \} - \frac{1}{N} \text{Tr} \{ A \} \text{Tr} \{ B \}. \quad (3.10)$$

If instead we contract with matrix elements A_{li} and B_{jk} we have:

$$\text{Tr} \{ A T^a B T^a \} = \text{Tr} \{ A \} \text{Tr} \{ B \} - \frac{1}{N} \text{Tr} \{ AB \}. \quad (3.11)$$

These relations will vastly simplify the calculation of color factors for gluon scattering amplitudes. For example we can calculate the color coefficient for the s -channel in the $gg \rightarrow gg$ process:

$$\begin{aligned} f^{abx} f^{cdx} &= f^{abx} f^{xcd} = -\text{Tr} \{ [T^a, T^b] T^x \} \text{Tr} \{ [T^c, T^d] T^x \} = \\ &= -\text{Tr} \{ [T^a, T^b] [T^c, T^d] \} + \frac{1}{N} \text{Tr} \{ [T^a, T^b] \} \text{Tr} \{ [T^c, T^d] \} = \\ &= -\text{Tr} \{ [T^a, T^b] [T^c, T^d] \}, \end{aligned}$$

where we used equation (3.6) in the first line and equation (3.10) in the last. Finally, we can examine the following peculiar contraction of structure constants:

$$f^{a_1 a_2 x_1} f^{x_1 a_3 x_2} \dots f^{x_{n-4} a_{n-2} x_{n-3}} f^{x_{n-3} a_{n-1} a_n}. \quad (3.12)$$

We want to express this contraction in a suitable way. Using the following property of the trace operation:

$$\text{Tr} \{ [A, B] C \} = \text{Tr} \{ A [B, C] \}, \quad (3.13)$$

where A, B, C are arbitrary square matrices, fixing $n = 2$ we obtain:

$$f^{abx_1} f^{x_1 cd} = -\text{Tr} \left\{ \underbrace{[T^a, T^b]}_{[A,B]} \underbrace{[T^c, T^d]}_C \right\} = (-i)^2 \text{Tr} \left\{ T^a [T^b, [T^c, T^d]] \right\}. \quad (3.14)$$

Therefore we conjecture the following expression for the original product of structure constants:

$$f^{a_1 a_2 x_1} f^{x_1 a_3 x_2} \dots f^{x_{n-3} a_{n-1} a_n} = (-i)^{n-2} \text{Tr} \left\{ T^{a_1} [T^{a_2} [\dots [T^{a_{n-2}} [T^{a_{n-1}}, T^{a_n}] \dots]]] \right\}. \quad (3.15)$$

The proof is very simple, because it is sufficient to replace all the $(n-2)$ nested commutators on the right hand side of (3.15) with the Lie algebra relation (3.1) proceeding from right to left, attaching every $(-i)$ factor to the appropriate commutator. In so doing, step by step we recover the left hand side of the equation. Keeping in mind these results, we are then ready to discuss the main topic of this chapter, the color decomposition of gluon scattering amplitudes at tree-level.

3.2 Gluon scattering amplitudes at tree-level

3.2.1 Trace decomposition

Any tree-level scattering amplitude for the interaction of n gluons can be written as [15]:

$$\mathcal{A} = g^{n-2} \sum_{\sigma \in S_{n-1}} \text{Tr} \left\{ T^1 T^{\sigma(2)} \dots T^{\sigma(n-1)} T^{\sigma(n)} \right\} A[1, \sigma(2), \dots, \sigma(n)]. \quad (3.16)$$

This expression is called **trace decomposition** and the coefficients $A[1, \sigma(2), \dots, \sigma(n)]$ are called **color-ordered partial amplitudes**, because they do not depend on color-

indices but contain all the kinematics of the scattering process. The sum runs over all the $(n - 1)!$ permutations of the $(2, 3, \dots, n)$ indices. The proof of (3.16) runs as follows: we first select one of the Feynman diagrams that contributes to the scattering process¹. Then we replace a certain structure constant f^{abc} associated to some vertex with the equation (3.3):

$$f^{abc} = (-i)\text{Tr} \left\{ T^a [T^b, T^c] \right\}. \quad (3.17)$$

Every line connected to this vertex can be either an external or an internal one. In the latter case, the line is obviously connected to another vertex and carries a certain generator T^c ; the contraction of this generator with the structure constant representing the other vertex (say f^{cde}) can be easily evaluated as:

$$f^{dec} T^c = (-i)[T^d, T^e], \quad (3.18)$$

using the fundamental commutation relations. This procedure allows us to sum over contracted indices and must be performed $V - 1$ times. However, it is well known that for any tree-level diagram we have exactly $I = V - 1$ pairs of contracted indices (\rightarrow internal lines). Thus we finally end up with a single trace of n generators carrying uncontracted indices (\rightarrow external lines). To give an example, we can consider the following tree-level color factor:

$$\begin{aligned} f^{1x_1x_2} f^{x_123} f^{x_245} &= (-i)\text{Tr} \left\{ T^1 [T^{x_1}, T^{x_2}] \right\} f^{x_123} f^{x_245} = \\ &= (-i)\text{Tr} \left\{ T^1 [T^{x_1} f^{x_123}, T^{x_2} f^{x_245}] \right\} = \\ &= (-i)^3 \text{Tr} \left\{ T^1 [[T^2, T^3], [T^4, T^5]] \right\}. \end{aligned}$$

The structure constants can enter inside the trace symbol and be moved between the generators simply because they are numbers with respect to fundamental indices, on which the trace operation is performed. This result also implies that at tree-level the term proportional to $1/N$ in the Fierz identity is completely negligible; it is important to emphasize that this is not due to the large N limit, the computation is exact. Anyway, we incidentally remark that this is true only for tree-level diagrams. For **loop diagrams** we end up with a single trace containing pairs of contracted indices, since in this case we trivially have more than $V - 1$ of these pairs. Thus some of them survive the procedure we described above, appearing inside the final single trace. For example, for $n = 4$ and one loop ($I = V$), we can get terms like:

¹For example the s -channel in the $gg \rightarrow gg$ process.

$$\mathrm{Tr} \{T^1 T^2 T^a T^3 T^4 T^a\} = \mathrm{Tr} \{T^1 T^2\} \mathrm{Tr} \{T^3 T^4\} - \frac{1}{N} \mathrm{Tr} \{T^1 T^2 T^3 T^4\}. \quad (3.19)$$

Therefore we do not have single traces, but **products of traces** of the external generators. Furthermore the term proportional to $1/N$ does not vanish, thus at loop level it cannot be neglected. Returning to tree level-diagrams, we can finally use the cyclic property of traces to collect all the kinematic parts of the amplitude multiplied by traces that differ only up to cyclic permutations of the external color indices $\{1, 2, \dots, n\}$. Hence we only have to sum over non-cyclic permutations of the external indices. However, this procedure turns out to be equivalent to fixing the position of T^{a_1} to the left inside the traces and summing over all the permutations of the other indices $\{2, 3, \dots, n\}$. At this point, all we have to do is to repeat these steps for all the other contributing diagrams. The color-ordered partial amplitudes $A[1, \sigma(2), \dots, \sigma(n)]$ are computed using the **color-ordered Feynman rules** listed below.

- The color-ordered three gluon vertex is given by:

$$\begin{aligned} V_{\mu_1 \mu_2 \mu_3}^{(3)}(p_1, p_2, p_3) &= \\ &= (-i) [\eta_{\mu_1 \mu_2} (p_1 - p_2)_{\mu_3} + \eta_{\mu_3 \mu_1} (p_2 - p_3)_{\mu_2} + \eta_{\mu_2 \mu_3} (p_3 - p_1)_{\mu_1}]. \end{aligned}$$

- The color-ordered four gluon vertex is instead:

$$V_{\mu_1 \mu_2 \mu_3 \mu_4}^{(4)}(p_1, p_2, p_3, p_4) = i [2\eta_{\mu_1 \mu_3} \eta_{\mu_2 \mu_4} - \eta_{\mu_1 \mu_2} \eta_{\mu_3 \mu_4} - \eta_{\mu_1 \mu_4} \eta_{\mu_2 \mu_3}]. \quad (3.20)$$

These amplitudes correspond to planar Feynman diagrams with an ordering of the external gluons given by the permutation $\sigma(2, 3, \dots, n)$. They are also **gauge invariant**². Therefore we can use the spinor representation of polarization vectors (see appendix B) in order to calculate them efficiently, choosing different sets of reference momenta (\rightarrow different gauge fixings) for each color-ordered diagram.

Just to give an example of how color decomposition works, let's consider the simple non trivial process $gg \rightarrow gg$ [13]. Using the standard Feynman rules for QCD, the diagrams contributing to the full scattering amplitude \mathcal{A} are:

$$\mathcal{A} = \mathcal{A}_s + \mathcal{A}_t + \mathcal{A}_u + \mathcal{A}_4, \quad (3.21)$$

²The gauge invariance of partial amplitudes is guaranteed by the exact orthogonality between the traces in (3.16) in the large N limit.

where \mathcal{A}_4 labels the contribution given by the four gluon interaction vertex. However, as long as only color factors are concerned, it is easy to see that the four gluon interaction vertex (1.43) can be considered as the sum of the s , t and u channels together. As a consequence, without loss of generality, any tree-level amplitude can be written in terms of diagrams containing three gluon vertices only. For example, the s -channel reads:

$$\begin{aligned} \mathcal{A}_s &= -\frac{g}{s} f^{a_1 a_2 x} f^{x a_3 a_4} [(\epsilon_1 \cdot \epsilon_2)(p_1 - p_2)^\mu + 2\epsilon_2^\mu(p_2 \cdot \epsilon_1) - 2\epsilon_1^\mu(p_1 \cdot \epsilon_2)] \times \\ &\quad \times [(\epsilon_3 \cdot \epsilon_4)(p_3 - p_4)_\mu + 2\epsilon_{\mu 4}(p_4 \cdot \epsilon_3) - 2\epsilon_{\mu 3}(p_3 \cdot \epsilon_4)] = -g f^{a_1 a_2 x} f^{x a_3 a_4} \tilde{A}_s(1, 2, 3, 4). \end{aligned}$$

The index $i = 1, \dots, 4$ labels momenta and polarizations of the four incoming gluons. Labeling adjoint indices in the same way as $a_i = i$ and concentrating on the color factor, we can alternatively obtain equation (3.14) as:

$$\begin{aligned} f^{12x} f^{x34} &= (-i) [\text{Tr} \{T^1 T^2 T^x\} - \text{Tr} \{T^1 T^x T^2\}] f^{x34} = \\ &= (-i) [\text{Tr} \{T^1 T^2 T^x f^{x34}\} - \text{Tr} \{T^1 T^x f^{x34} T^2\}] = \\ &= (-i)^2 [\text{Tr} \{T^1 T^2 [T^3, T^4]\} - \text{Tr} \{T^1 [T^3, T^4] T^2\}] = \\ &= -[\text{Tr} \{1234\} - \text{Tr} \{2134\} + \text{Tr} \{2143\} - \text{Tr} \{1243\}]. \end{aligned}$$

Hence the s -channel amplitude can be written as:

$$\mathcal{A}_s = [\text{Tr} \{1234\} - \text{Tr} \{2134\} + \text{Tr} \{2143\} - \text{Tr} \{1243\}] \tilde{A}_s(1, 2, 3, 4), \quad (3.22)$$

where $A_s(1, 2, 3, 4)$ includes all the kinematics of the interaction and is called color stripped amplitude³. To proceed further, it is evident by direct inspection that the color stripped amplitude satisfies:

$$\tilde{A}_s(1, 2, 3, 4) = -\tilde{A}_s(2, 1, 3, 4) = \tilde{A}_s(2, 1, 4, 3) = -\tilde{A}_s(1, 2, 4, 3). \quad (3.23)$$

Hence we can rearrange the s -channel amplitude as:

$$\begin{aligned} \mathcal{A}_s &= \text{Tr} \{1234\} \tilde{A}_s(1, 2, 3, 4) + \text{Tr} \{2134\} \tilde{A}_s(2, 1, 3, 4) + \\ &\quad + \text{Tr} \{2143\} \tilde{A}_s(2, 1, 4, 3) + \text{Tr} \{1243\} \tilde{A}_s(1, 2, 4, 3), \end{aligned}$$

³Not to be confused with the partial amplitude.

simply exchanging the outgoing kinematic indices of gluons. The same steps can be repeated for the other channels and the four gluon vertex. For example, the t -channel reads:

$$\mathcal{A}_t = [\text{Tr}\{1432\} - \text{Tr}\{4132\} + \text{Tr}\{4123\} - \text{Tr}\{1423\}] \tilde{A}_t(1, 2, 3, 4). \quad (3.24)$$

The t -channel obviously satisfies:

$$\tilde{A}_t(1, 2, 3, 4) = \tilde{A}_s(1, 4, 3, 2), \quad (3.25)$$

so we can use the antisimmetry properties of A_s to obtain:

$$\begin{aligned} \mathcal{A}_t &= \text{Tr}\{1432\} \tilde{A}_s(1, 4, 3, 2) + \text{Tr}\{4132\} \tilde{A}_s(4, 1, 3, 2) + \\ &+ \text{Tr}\{4123\} \tilde{A}_s(4, 1, 2, 3) + \text{Tr}\{1423\} \tilde{A}_s(1, 4, 2, 3). \end{aligned}$$

Collecting all the color stripped partial amplitudes multiplied by the same trace, we find:

$$\mathcal{A} = \sum_{\sigma \in S_4} \text{Tr}\{T^{\sigma(1)} T^{\sigma(2)} T^{\sigma(3)} T^{\sigma(4)}\} \tilde{A}[\sigma(1), \sigma(2), \sigma(3), \sigma(4)]. \quad (3.26)$$

Here S_4 is the group of all permutations of four indices. However, the traces appearing in the sum are invariant under cyclic permutations, for example:

$$\text{Tr}\{1234\} = \text{Tr}\{4123\}. \quad (3.27)$$

Therefore we can collect all the color stripped amplitudes multiplied by traces with color orderings different up to cyclic permutations, for example:

$$\begin{aligned} \text{Tr}\{1234\} [\tilde{A}_s(1, 2, 3, 4) + \tilde{A}_s(4, 1, 2, 3)] &= \\ \text{Tr}\{1234\} [\tilde{A}_s(1, 2, 3, 4) + \tilde{A}_t(1, 2, 3, 4)] &= \text{Tr}\{1234\} A(1, 2, 3, 4). \end{aligned}$$

because $\tilde{A}_s(4, 1, 2, 3) = \tilde{A}_t(2, 1, 4, 3) = \tilde{A}_t(1, 2, 3, 4)$. Hence, we can restrict the sum to all non-cyclic permutations of four indices or, equivalently, we can fix the first index 1 and then sum over all the permutations of the three other indices left, namely:

$$\mathcal{A} = g^2 \sum_{\sigma \in \mathcal{S}_3} \text{Tr} \left\{ T^1 T^{\sigma(2)} T^{\sigma(3)} T^{\sigma(4)} \right\} A[1, \sigma(2), \sigma(3), \sigma(4)]. \quad (3.28)$$

The kinematic factors $A[1, \sigma(2), \sigma(3), \sigma(4)]$ are what we call color-ordered partial amplitudes. We underline that, as expected, the amplitude $A[1, 2, 3, 4]$ corresponding to the identity permutation is only given by planar diagrams with the same ordering of external indices. The same holds for all the other partial amplitudes.

3.2.2 Reducing the complexity

However, it is not so difficult to realize that the partial amplitudes appearing in equation (3.16) are not independent. Besides the cyclic invariance, traces also have reflection invariance, that implies the following relation between partial amplitudes:

$$A(1, n, \dots, 3, \dots, 2) = A(n, n-1, \dots, 2, 1) = (-1)^n A(1, 2, \dots, n). \quad (3.29)$$

This allows us to reduce the number of independent partial amplitudes from $(n-1)!$ to $(n-1)!/2$. Furthermore, partial amplitudes also satisfy the **$U(1)$ decoupling identity** (also called dual Ward identity) [16] given by:

$$A(1, 2, \dots, n) + A(1, 3, 2, \dots, n) + \dots + A(1, 3, \dots, n, 2) = 0. \quad (3.30)$$

For $n = 4$ we get:

$$A(1, 2, 3, 4) + A(1, 3, 2, 4) + A(1, 3, 4, 2) = 0. \quad (3.31)$$

The vanishing of (3.30) and (3.31) is due to the fact that an amplitude involving an interaction between $(n-1)$ gluons and a 'photon' must be zero. In addition, there are more complicated relations among partial amplitudes discovered by Kleiss and Kuijf [17], namely:

$$A(1, \{\alpha\}, n, \{\beta\}) = (-1)^{n_\beta} \sum_{\sigma \in \text{OP}(\{\alpha\}\{\beta^T\})} A(1, \sigma(\{\alpha\}\{\beta^T\}), n). \quad (3.32)$$

Here the set $\{\alpha\} \cup \{\beta\} = \{2, 3, \dots, n-1\}$, n_β is the cardinality of $\{\beta\}$ and $\{\beta^T\}$ is the set $\{\beta\}$ with all the numbers in reversed order. The sum is over all the ordered permutations (OP) of the set $\{\alpha\} \cup \{\beta^T\}$, where by ordered we mean that they preserve the ordering of the α_i within $\{\alpha\}$ and of β_i within $\{\beta^T\}$, while allowing for all possible relative orderings

between them⁴. To make things clearer, we give two examples of how (3.32) works. First we show that (3.32) **implies the $U(1)$ decoupling identity**. To see this, it is sufficient to choose $\{\alpha\} = \{3, 4, \dots, n-1\}$ and $\{\beta\} = \{\beta^T\} = \{2\}$. For example, fixing $n = 4$, the Kleiss-Kuijff relation reads:

$$A(1, 3, 4, 2) = (-1) [A(1, 2, 3, 4) + A(1, 3, 2, 4)], \quad (3.33)$$

$$A(1, 2, 3, 4) + A(1, 3, 2, 4) + A(1, 3, 4, 2) = 0, \quad (3.34)$$

in perfect accordance with equation (3.31). We now consider $A(1, \{2, 3\}, 5, \{4\})$ obtaining:

$$A(1, 2, 3, 5, 4) = (-1) [A(1, 2, 3, 4, 5) + A(1, 2, 4, 3, 5) + A(1, 4, 2, 3, 5)]. \quad (3.35)$$

3.2.3 The adjoint color decomposition

At this point, we are ready to introduce another color decomposition capable of describing the full gluon scattering amplitude at tree-level as the sum of only $(n-2)!$ independent partial amplitudes, called **adjoint representation decomposition** [18]. It reads as follows:

$$\begin{aligned} \mathcal{A} &= (ig)^{n-2} \sum_{\sigma \in S_{n-2}} f^{a_1 a_{\sigma(2)} x_1} f^{x_1 a_{\sigma(3)} x_2} \dots f^{x_{n-3} a_{\sigma(n-1)} a_n} A(1, \sigma(2), \dots, \sigma(n-1), n) = \\ &= g^{n-2} \sum_{\sigma \in S_{n-2}} (F^{a_{\sigma(2)}} \dots F^{a_{\sigma(n-1)}})_{a_1 a_n} A(1, \sigma(2), \dots, \sigma(n-1), n), \end{aligned}$$

where $(F^a)_{bc} = (if^a)_{bc} = i(T_{\text{adj}}^a)_{bc}$ is a generator of the adjoint representation of $SU(N)$. This is the reason why it is called adjoint representation decomposition. Furthermore, it turns out to be equivalent to inserting the Kleiss-Kuijff relations inside the standard trace decomposition (3.16). The proof runs as follows: we first use relation (3.15) to replace the color factor of the new decomposition with a sum a single traces of n fundamental matrices as we have in the standard decomposition,

$$f^{a_1 a_{\sigma(2)} x_1} f^{x_1 a_{\sigma(3)} x_2} \dots f^{x_{n-3} a_{\sigma(n-1)} a_n} = (-i)^{n-2} \text{Tr} \{ T^{a_1} [T^{a_{\sigma(2)}}] [\dots [T^{a_{\sigma(n-1)}}, T^{a_n}] \dots] \}. \quad (3.36)$$

⁴These permutations are also called mergings. For example, if $\{\alpha\} = \{2\}$ and $\{\beta^T\} = \{4, 3\}$, the mergings are given by $\{2, 4, 3\}$, $\{4, 2, 3\}$ and $\{4, 3, 2\}$. The reason why they are called mergings should now be clear: the two sets interpenetrate themselves preserving their internal ordering.

Now we want to identify all the partial amplitudes corresponding to a trace factor of the form:

$$\text{Tr} \left\{ T^1 T^{\alpha_1} \dots T^{\alpha_{n-2-q}} T^n T^{\beta_1} \dots T^{\beta_q} \right\}, \quad (3.37)$$

because they should give rise to the amplitude $A(1, \{\alpha\}, n, \{\beta\})$ by virtue of (??), as established by the Kleiss-Kuijf relations. Relation (3.36) contains $(n-2)$ commutators and 2^{n-2} terms, but only $\binom{n-2}{q}$ of these terms contain exactly q fundamental matrices on the right of T^n . By direct inspection of (3.36), it is evident that all these q matrices are forced to come in reversed order with respect to $\{\beta\} = \{\beta_1, \dots, \beta_q\}$, while the fundamental indices on the left $\{\alpha\} = \{\alpha_1, \dots, \alpha_{n-2-q}\}$ conserve their original ordering. Anyway, the two sets can be merged in any relative order with respect to each other. In other words, we have that, for any ordered permutation $\sigma(\{\alpha\}\{\beta^T\})$, the amplitude $A(1, \sigma(\{\alpha\}\{\beta^T\}), n)$ appearing in the adjoint decomposition results to be multiplied by the trace (3.37). The relative $(-1)^q$ sign appears because we need to exchange exactly $n_\beta = q$ commutators in order to arrange q fundamental matrices to the right of T^n , and this procedure trivially carries a product of q minus signs. Finally, collecting all these amplitudes one easily obtains the Kleiss-Kuijf relations (3.32), successfully establishing its equivalence to the new adjoint decomposition.

The adjoint decomposition further reduces the number of independent amplitudes to $(n-2)!$, fixing the indices of the first and the last leg. This decomposition can be obtained as follows: we already mentioned that every four gluon vertex can be expressed as the sum of the three channels s , t and u . Therefore we can consider only Feynman diagrams containing three gluon vertices. The color factor appearing in the adjoint decomposition can be represented graphically as shown in figure 3.1.

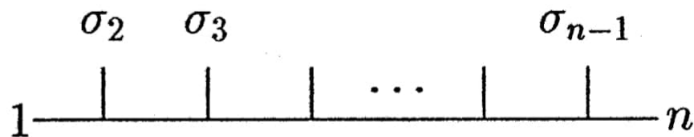


Figure 3.1: Graphical representation of the adjoint color decomposition coefficient $f^{a_1 a_{\sigma(2)} x_1} f^{x_1 a_{\sigma(3)} x_2} \dots f^{x_{n-3} a_{\sigma(n-1)} a_n}$ from [18]. Continuous lines now represent gluons.

These diagrams are called **multi-peripheral**, meaning that every permuted external line is directly connected to the line extending from 1 to n . In other words, all the permuted external lines are connected to the 1- n line without passing through any other internal line. However, it is trivial to realize that the set of all multi-peripheral tree-level color diagrams is only a subset of all the possible ones. For example, the color factor:

$$f^{a_1 x_2 x_1} f^{x_2 a_2 a_3} f^{x_1 a_4 a_5} \quad (3.38)$$

represents a tree-level diagram, but it is not multi-peripheral. Conversely, the following factors:

$$f^{a_1 x_1 x_2} f^{x_1 x_2 x_3} f^{x_3 a_2 a_3}, \quad f^{a_1 x_1 x_3} f^{x_1 a_2 x_2} f^{x_2 a_3 x_3} \quad (3.39)$$

even involve one loop (they contain the same number of f factors and contracted indices), hence they do not correspond to a tree-level diagram and will not be considered. In order to circumvent this problem, we recall the Jacobi identity:

$$f^{abx} f^{xcd} + f^{bcx} f^{xad} + f^{cax} f^{xbd} = 0, \quad (3.40)$$

that we can suitably recast as:

$$f^{abx} f^{xcd} = f^{cax} f^{xbd} - f^{cbx} f^{xad}, \quad (3.41)$$

shown graphically in figure 3.2. It is evident that the left hand side is the color factor for a t -channel diagram, while the other two are color factors for s and u channel respectively.

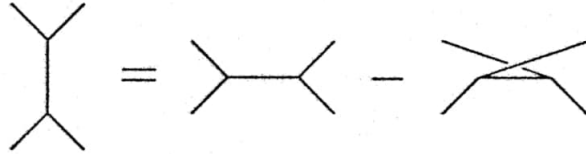
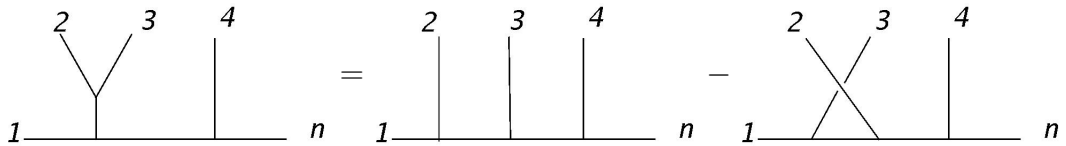


Figure 3.2: The Jacobi identity in graphical notation [18].

This identity can be used to convert an arbitrary tree-level gluon diagram made up only of three vertices into a multi-peripheral one. To give a graphical example of how the Jacobi identity can be used to make tree-level color factors multi-peripheral, we can consider the factor (3.38) (containing a Y-fork tree):



Therefore it is evident that the two diagrams on the right hand side are both multi-peripheral, the only difference between them being the permuted couple of indices (2, 3). A more complicated tree-level color diagram is shown in figure 3.3. The first step of the conversion into a sum of multi-peripheral diagrams is also shown.

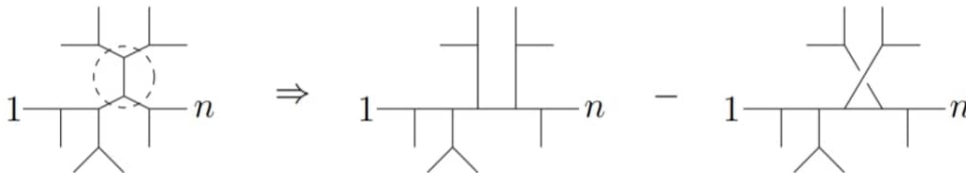


Figure 3.3: First step of the conversion of a specific tree-level diagram into a sum of multi-peripheral ones for $n = 10$ [18]. The two diagrams on the right hand side are of the Y-fork type as the factor (3.38).

Therefore, we can establish that in the adjoint decomposition only those partial amplitudes that are **not** connected through the Jacobi identity are summed, each of them being suitably weighted by the correspondent multi-peripheral color factor. However, in the formula we have written the kinematic factors $A(1, \sigma(2), \dots, \sigma(n-1), n)$ using the same notation we previously used to indicate the color-ordered partial amplitudes in the standard trace decomposition. We made this choice simply because we can easily prove that they coincide. The proof of this statement is simple: we first consider as unknown coefficients the kinematic terms in the adjoint decomposition, then we equate it to the standard trace decomposition, namely:

$$\sum_{\sigma \in S_{n-2}} (F^{a_{\sigma(2)}} \dots F^{a_{\sigma(n-1)}})_{a_1 a_n} X(1, \sigma(2), \dots, \sigma(n-1), n) = \sum_{\sigma \in S_{n-1}} \text{Tr} \left\{ T^1 T^{\sigma(2)} \dots T^{\sigma(n-1)} T^{\sigma(n)} \right\} A(1, \sigma(2), \dots, \sigma(n)).$$

Notice we changed the label for the partial amplitudes in the first line. Then we can contract both terms with the trace $\text{Tr} \left\{ T^1 T^{\tilde{\sigma}(2)} \dots T^{\tilde{\sigma}(n-1)} T^n \right\}$ for a fixed permutation $\tilde{\sigma}$ that leaves the first and the last leg unchanged. Since the kinematic factors do not depend on the number of colors N , we take the large N limit on both sides, dropping all the positive powers of $1/N$ and retaining only the leading contraction terms. It is very well known that single traces satisfy an exact orthogonality relation at large N [19], therefore only those color factors with legs labeled as $\{1, \tilde{\sigma}(i), n\}$ survive the contraction. As a consequence, the contraction selects a single term on both sides of the equation. Thanks to the arbitrariness of the permutation $\tilde{\sigma}$, this indeed proves that the amplitudes in the adjoint decomposition are given by:

$$X(1, \sigma(2), \dots, \sigma(n-1), n) = A(1, \sigma(2), \dots, \sigma(n-1), n), \quad (3.42)$$

as we claimed. We finally remark that all the results we obtained in this section do not rely on any kinematic properties of the color-ordered amplitudes. We only used group-theoretic considerations such as the Jacobi identity and the properties of single traces in the large N limit.

3.2.4 Calculating the cross-section

In order to calculate the cross-section for the process at tree-level, we have to square the amplitude \mathcal{A} , then sum over the final color and helicity states and average over the initial ones [18]. Using both the standard and the adjoint decomposition of the scattering amplitude, we can express the cross-section in two equivalent ways:

$$\begin{aligned} \sum_{\text{col.}} |\mathcal{A}^{\text{tree}}(1, 2, \dots, n)|^2 &= (g^2)^{n-2} \sum_{i,j=1}^{(n-1)!} C_{ij} A_i^{\text{tree}}(A_j^{\text{tree}})^* = \\ &= (g^2)^{n-2} \sum_{i,j=1}^{(n-2)!} \tilde{C}_{ij} A_i^{\text{tree}}(A_j^{\text{tree}})^*. \end{aligned}$$

Obviously, the paired indices (i, j) take values from S_{n-1} in the first line and from S_{n-2} in the second. Employing the usual shorthand notation, the color matrix C_{ij} is given by:

$$C_{ij} = \sum_{\text{col.}} \text{Tr} \{1, \sigma_i(2, \dots, n)\} [\text{Tr} \{1, \sigma_j(2, \dots, n)\}]^*, \quad (3.43)$$

while \tilde{C}_{ij} reads:

$$\tilde{C}_{ij} = \sum_{\text{col.}} \left[F^{\sigma_i(2)} \dots F^{\sigma_i(n-1)} \right]_{a_1 a_n} \left[F^{\sigma_j(2)} \dots F^{\sigma_j(n-1)} \right]_{a_1 a_n}^*. \quad (3.44)$$

The expressions of \tilde{C}_{ij} for $n = 4, 5, 6$ are presented explicitly in appendix C. Finally, if we want to express the cross-section at large N - the **leading color approximation (LCA)** - it is more fruitful to use the expression (3.43) together with the orthogonality relation between single traces. When we square the full amplitude, products of traces can be easily computed graphically. One of these products, for $n = 4$, is given by:

$$\text{Tr}(1, 2, 3, 4) \text{Tr}(1, 2, 4, 3)^* = \left(\begin{array}{c} \text{1} \\ \text{2} \\ \text{3} \\ \text{4} \end{array} \right) \times \left(\begin{array}{c} \text{1} \\ \text{2} \\ \text{4} \\ \text{3} \end{array} \right) = \left(\begin{array}{c} \text{1} \\ \text{2} \\ \text{3} \\ \text{4} \end{array} \right) = N^2. \quad (3.45)$$

Every factor of N is given by each single-line loop $\delta_i^i = N$. Hence we obtain:

$$\sum_{\text{col.}} |\mathcal{A}^{\text{tree}}(1, 2, \dots, n)|^2 = (g^2)^{n-2} C_n(N) \sum_{\sigma \in \mathcal{S}_{n-1}} \left[|A^{\text{tree}}(1, \sigma(2), \dots, \sigma(n))|^2 + \mathcal{O}(N^{-2}) \right], \quad (3.46)$$

where we suitably defined:

$$C_n(N) = N^{n-2}(N^2 - 1). \quad (3.47)$$

3.2.5 BCJ relations and color-kinematics duality at tree-level

In this section we finally introduce another set of linear relations, called **BCJ relations**, introduced by Bern, Carrasco and Johansson in [20], that further reduce the number of independent color-ordered partial amplitudes at tree-level from $(n-2)!$ to $(n-3)!$. First of all, we remind that from the point of view of color degrees of freedom the four gluon vertex can be written as the sum of the s , t and u channel. Hence, we can write every full color-dressed amplitude at tree-level as the sum of diagrams with only **three gluon vertices**, namely:

$$\mathcal{A} = \sum_{i \in \Gamma} \frac{c_i n_i}{\prod_{\beta_i} p_{\beta_i}^2}, \quad (3.48)$$

where Γ is the set of all different trivalent diagrams, while c_i is the color factor associated to the i -th diagram and n_i is its **kinematic numerator**. These numerators contain all the kinematic information of the diagram (it depends on Lorentz invariant contractions of polarization vectors and momenta). The denominator is simply the product of all the internal propagators. The statement of color-kinematics duality is that any scattering amplitude for gluons at tree-level can be expressed using numerators n_i satisfying the same algebraic properties of the corresponding color factors c_i . In practice, we state that we can find a suitable representation of the n_i such that they satisfy the following relations:

$$c_i = -c_j, \quad \longleftrightarrow \quad n_i = -n_j, \quad \forall i, j \in \Gamma, \quad (3.49)$$

$$c_i + c_j + c_k = 0, \quad \longleftrightarrow \quad n_i + n_j + n_k = 0, \quad \forall i, j, k \in \Gamma. \quad (3.50)$$

The existence of such a representation of the n_i may seem highly **non-trivial** at first sight. After all, the Jacobi identities encoded on the left in (3.50) are consequences of the intrinsic properties of the underlying $SU(N)$ color symmetry. Apparently there is no

reason for the numerators to reflect the same structure of color factors. To start with, it is sufficient to have a look at the above expression for the full amplitude (3.48). As a matter of fact, the following transformations:

$$\epsilon(p_i) \longrightarrow \epsilon(p_i) + \alpha_i p_i, \quad (3.51)$$

has obviously no effect on the full amplitude \mathcal{A} , since it is gauge invariant. However, they clearly change the single numerators. Hence the n_i are **not** gauge invariant. This first result suggests us that we are allowed to manipulate the numerators n_i in such a way that the full amplitude remains unchanged. For this purpose, we choose any three diagrams (c_i, c_j, c_k) in Γ such that their color factors are not independent but constrained by the Jacobi identity:

$$c_i + c_j + c_k = 0. \quad (3.52)$$

Why shouldn't we take advantage of this relation to construct a transformation that leaves \mathcal{A} unchanged? After all, the Jacobi identity only allows us to rewrite a certain channel in terms of the other two, thus the three diagrams differ only by a single propagator defining the channel. Labeling the squared momenta flowing through the channels by s_i, s_j and s_k , it turns out that the transformations:

$$n_i \longrightarrow n_i + s_i \Delta, \quad n_j \longrightarrow n_j + s_j \Delta, \quad n_k \longrightarrow n_k + s_k \Delta, \quad (3.53)$$

leave (3.48) unchanged, since the shifting is proportional to the Jacobi identity. We remark that the function Δ is arbitrary and must be the same for the three numerators. For this reason (3.53) is called **generalized gauge transformation**. Until now we proved that the n_i are not unique nor gauge invariant. However this is not a real problem: what actually matters is that \mathcal{A} is gauge invariant and unchanged by our manipulations. To move further, from section 3.2.4, we know that there are only $(n-2)!$ diagrams that are not related by the Jacobi identity. Thus we wrote a color decomposition of \mathcal{A} in terms of only $(n-2)!$ color-ordered amplitudes. On the other hand, every Jacobi identity between diagrams implies a relation between the kinematic numerators. Thus we have $(n-2)!$ independent numerators as well. Furthermore, as shown in [28], we write any independent partial amplitude in terms of the independent numerators as follows:

$$A_{(i)} = \sum_{j=1}^{(n-2)!} \Theta_{ij} \tilde{n}_j. \quad (3.54)$$

The square $(n-2)! \times (n-2)!$ matrix Θ_{ij} is called **propagator matrix**. The linear relation (3.54), if inverted, could allow us to find the color-ordered independent amplitudes

very easily in terms of the independent numerators. If this were the case, we would only have re-stated the adjoint color decomposition in a different fashion, and color-kinematics duality would be in some sense trivial and useless. By the way, it is not the case. In fact it can be shown [20] that Θ_{ij} is **not invertible** for 4-dimensional Yang-Mills theories. As a consequence, we do not have unique \tilde{n}_i . An immediate consequence of this is that there exist a certain number of further linear relations between the color-ordered partial amplitudes.

As a matter of fact, the number of independent partial amplitudes coincides with the rank of Θ_{ij} , given by $(n - 3)!$. The **general BCJ relations** read:

$$A(1, 2, \{\alpha\}, 3, \{\beta\}) = \sum_{\sigma \in \text{POP}(\{\alpha, \beta\})} A(1, 2, 3, \sigma) \mathcal{F}_\sigma, \quad (3.55)$$

where $\text{POP}(\{\alpha, \beta\})$ is the set of all partially ordered permutations of $\{\alpha\} \cup \{\beta\}$, the ones preserving the relative order between the elements of $\{\beta\}$, while \mathcal{F}_σ indicates some dynamical factors whose definitions can be found in [20]. For $n = 4$ we get:

$$A(1, 2, \{4\}, 3) = \frac{s_{14}}{s_{24}} A(1, 2, 3, 4), \quad (3.56)$$

while for $n = 5$ we get two non-trivial relations:

$$A(1, 2, \{4, 5\}, 3) = \frac{-A(1, 2, 3, 4, 5)s_{34}s_{15} - A(1, 2, 3, 5, 4)(s_{245} + s_{35})}{s_{24}s_{245}},$$

$$A(1, 2, \{4\}, 3, \{5\}) = \frac{A(1, 2, 3, 4, 5)(s_{14} + s_{45}) + A(1, 2, 3, 5, 4)s_{14}}{s_{24}}.$$

Equation (3.55) have been proven using both the BCFW recursion relations [29, 30] and string theory [31]. When the set $\{\alpha\}$ contains only one index we obtain the **fundamental BCJ relations**, while when $\{\alpha\} = \emptyset$ we get a trivial result. As a matter of fact, it can be shown that the only relevant relations are the fundamental ones: to be more specific, we can show that, combining the Kleiss-Kuijff and fundamental BCJ relations, any amplitude can be written as a sum of amplitudes of the form $A(1, 2, 3, \sigma(4, \dots, n))$ provided by (3.55) [30].

In fact, consider an arbitrary amplitude of the form $A(1, \alpha_2, \dots, \alpha_{|\alpha|}, 2, \beta_1, \dots, \beta_{|\beta|})$, where $|\alpha|$ and $|\beta|$ are the cardinalities of the two sets respectively and where the only index fixed in position is 1, using the cyclic invariance of traces. Then:

- We can use the Kleiss-Kuijff relation to write this arbitrary amplitude as:

$$A(1, \alpha_2, \dots, \alpha_{|\alpha|}, 2, \beta_1, \dots, \beta_{|\beta|}) = (-1)^{|\beta|} \sum_{\sigma} A(1, \sigma(\{\alpha\} \cup \{\beta^T\}), 2), \quad (3.57)$$

where σ is an arbitrary ordered permutation of the union of the two sets of indices. We can then use the reflection property of the amplitudes to fix the index 2 on the right of 1.

- The resulting independent amplitudes are of the form:

$$A(1, 2, t_1, t_2, \dots, t_{|\gamma|}, 3, l_1, \dots, l_{|\delta|}), \quad (3.58)$$

thus exactly the amplitudes on the left hand side of (3.55). We want to prove that these amplitudes can be expressed through amplitudes of the form $A(1, 2, 3, \sigma(4, \dots, n))$, $\sigma \in \text{POP}(\{\gamma\} \cup \{\delta\})$, using the fundamental BCJ relations. Following [30], we consider the amplitudes with $|\delta| = 0$. The amplitudes are given by:

$$A(1, 2, t_1, t_2, \dots, t_{n-3}, 3). \quad (3.59)$$

Considering t_2 as **fixed** along the string, we can write $(n-3)!$ different fundamental BCJ equations (each for any set of $\{t_i\}$). To the right hand side of each of these equations, the index 3 can be positioned on the n -th or $(n-1)$ -th site along the string of color ordered indices. Therefore, we can treat them as a system of equations and solve all configurations with 3 at the n -th site by the ones at the $(n-1)$ -th site. We consider next the configuration:

$$A(1, 2, t_1, t_2, \dots, t_{n-4}, 3, l_1), \quad (3.60)$$

with $|\delta| = 1$. Repeating the above procedure, we can solve the amplitudes with 3 at the $(n-1)$ -th site by the ones at the $(n-2)$ -th site and so on, until we solved the ones with 3 at fourth site by the ones at the third site. To sum up, we proved that any amplitude on the left hand side of (3.55) can actually be expressed as a sum on the partially ordered permutations of the amplitudes $A(1, 2, 3, \sigma(4, \dots, n))$, each one weighted by a suitable dynamical factors.

3.2.6 Proof of the fundamental BCJ relations

At last, we need to prove the fundamental BCJ relations. We will follow [30] using induction on the number of external gluons n through the very powerful tool given by the BCFW recursion relations⁵. In fact, they allow us to express a given amplitude as

⁵See the last paragraph of appendix B.

a product of two on-shell sub-amplitudes with $(n - 1)$ or less gluons connected to them. We focus on $n = 6$ without loss of generality, since the computation for general n will follow the same path. The idea is to consider the following combination of amplitudes:

$$\begin{aligned}\mathcal{I}_6 &= A(2, 4, 3, 5, 6, 1)(s_{43} + s_{45} + s_{46} + s_{41}) \\ &\quad + A(2, 3, 4, 5, 6, 1)(s_{45} + s_{46} + s_{41}) \\ &\quad + A(2, 3, 5, 4, 6, 1)(s_{46} + s_{41}) + A(2, 3, 5, 6, 4, 1)s_{41},\end{aligned}$$

and deform it shifting the two external momenta p_1 and p_2 . Then we expand each amplitude through BCFW recursion, obtaining terms with different splittings⁶. We call $\mathcal{I}_6^{[m]}$ the sum of all terms with m gluons connected to the sub-amplitude on the left. For example:

$$\begin{aligned}\mathcal{I}_6^{[2]} &= A(\hat{2}, 4, -\hat{P}_{24}|\hat{P}_{24}, 3, 5, 6, \hat{1})(s_{43} + s_{45} + s_{46} + s_{41}) \\ &\quad + A(\hat{2}, 3, -\hat{P}_{23}|\hat{P}_{23}, 4, 5, 6, \hat{1})(s_{45} + s_{46} + s_{41}) \\ &\quad + A(\hat{2}, 3, -\hat{P}_{23}|\hat{P}_{23}, 5, 4, 6, \hat{1})(s_{46} + s_{41}) \\ &\quad + A(\hat{2}, 3, -\hat{P}_{23}|\hat{P}_{23}, 5, 6, 4, \hat{1})s_{41}.\end{aligned}$$

We will prove the fundamental BCJ relation for $n = 6$ if the combination \mathcal{I}_6 identically vanishes. The inductive hypothesis is that the fundamental BCJ relations hold for $n = 3, 4, 5$. The above terms can be divided into two groups: the ones where the index 4 is on the left and the one where it is on the right. The last three terms are of the latter type. In order to apply the inductive step, we need the factorized amplitudes to be multiplied by deformed dynamical factors such as $s_{\hat{1}3}$ *et cetera*. For this purpose, we write each dynamical factor as:

$$s_{ij} = s_{ij}, \quad \text{for } \{i, j\} \neq \{1, 2\},$$

$$s_{\hat{i}j} = s_{ij} - (s_{ij} - s_{ij}), \quad \text{for } i = 1, 2.$$

⁶From now on we will use the same notation for the amplitude splittings employed in the last paragraph of [30].

The last three terms can be rearranged as:

$$\begin{aligned}
& A(\hat{2}, 3, -\hat{P}_{23}|\hat{P}_{23}, 4, 5, 6, \hat{1})(s_{45} + s_{46} + s_{4\hat{1}}) + A(\hat{2}, 3, -\hat{P}_{23}|\hat{P}_{23}, 5, 4, 6, \hat{1})(s_{46} + s_{4\hat{1}}) \\
& + A(\hat{2}, 3, -\hat{P}_{23}|\hat{P}_{23}, 5, 6, 4, \hat{1})s_{4\hat{1}} + [A(\hat{2}, 3, -\hat{P}_{23}|\hat{P}_{23}, 4, 5, 6, \hat{1}) + A(\hat{2}, 3, -\hat{P}_{23}|\hat{P}_{23}, 5, 4, 6, \hat{1}) \\
& + A(\hat{2}, 3, -\hat{P}_{23}|\hat{P}_{23}, 5, 6, 4, \hat{1})](s_{41} - s_{4\hat{1}}(z_{23})).
\end{aligned}$$

Since the inductive step implies the validity of the fundamental BCJ relations for the amplitude on the right ($n = 5$), we have that the first three terms are summed to zero, thus only the term between square brackets survives. Finally, the first term can be rewritten as:

$$\begin{aligned}
& -s_{24}A(\hat{2}, 4, -\hat{P}_{24}|\hat{P}_{24}, 3, 5, 6, \hat{1}) = \\
& = -s_{\hat{2}4}A(\hat{2}, 4, -\hat{P}_{24}|\hat{P}_{24}, 3, 5, 6, \hat{1}) - (s_{24} - s_{\hat{2}4}(z_{24}))A(\hat{2}, 4, -\hat{P}_{24}|\hat{P}_{24}, 3, 5, 6, \hat{1}),
\end{aligned}$$

using momentum conservation. The first term identically vanishes using the inductive step on the sub-amplitudes on the left ($n = 3$). Repeating the same procedure for $\mathcal{I}_6^{[3]}$ and $\mathcal{I}_6^{[4]}$, we finally get:

$$\begin{aligned}
\mathcal{I}_6 & = s_{41}[A(2, 4, 3, 5, 6, 1) + A(2, 3, 4, 5, 6, 1) + A(2, 3, 5, 4, 6, 1) + A(2, 3, 5, 6, 4, 1)] \\
& + \oint_{z \neq 0} \frac{dz s_{\hat{1}4}}{z} [A(\hat{2}, 4, 3, 5, 6, \hat{1}) + A(\hat{2}, 3, 4, 5, 6, \hat{1}) + A(\hat{2}, 3, 5, 4, 6, \hat{1}) + A(\hat{2}, 3, 5, 6, 4, \hat{1})].
\end{aligned}$$

The contour integral is the sum of all the residues corresponding to all simple poles except $z = 0$. Thus the contour is large enough to contain all finite poles, namely:

$$\oint_{z \neq 0} dz(\dots) = \sum_{\text{poles} \neq 0} \text{Res}(\dots). \quad (3.61)$$

We can now use the Kleiss-Kuijff relations to simplify (3.62) as:

$$\mathcal{I}_6 = -s_{41}A(4, 2, 3, 5, 6, 1) - \oint_{z \neq 0} \frac{dz s_{\hat{1}4}}{z} A(4, \hat{2}, 3, 5, 6, \hat{1}). \quad (3.62)$$

Evaluating the contour integral is now straightforward. In fact, we know from complex analysis that the sum of all the residues of an holomorphic function (including the residue at infinity) must vanish. Thus we write:

$$0 = \oint_{z \neq 0} \frac{dz s_{\hat{1}4}}{z} A(4, \hat{2}, 3, 5, 6, \hat{1}) + \underbrace{s_{14} A(4, 2, 4, 5, 6, 1)}_{\text{residue at } z=0} + \oint_{z=\infty} \frac{dz s_{\hat{1}4}}{z} A(4, \hat{2}, 3, 5, 6, \hat{1}). \quad (3.63)$$

Since in (3.62) the shifted indices are not nearby, the integrand goes to zero faster than $1/z$ as $|z| \rightarrow +\infty$, and this implies that the residue at infinity vanishes. As a consequence, we get:

$$\oint_{z \neq 0} \frac{dz s_{\hat{1}4}}{z} A(4, \hat{2}, 3, 5, 6, \hat{1}) = -s_{41} A(4, 2, 3, 5, 6, 1). \quad (3.64)$$

The insertion of this equation in (3.62) implies the vanishing of \mathcal{I}_6 and proves that the fundamental BCJ relations hold for $n = 6$. The proof for general n is exactly the same.

Just to give an example of computation using BCJ relations, consider the amplitude for $n = 4$ gluons at tree level. Here we have only one independent amplitude: $A(1, 2, 3, 4)$. Using the BCJ relation (3.56) and the adjoint decomposition, the amplitude is given by:

$$\begin{aligned} \mathcal{A}_4 &= f^{13x} f^{x42} A_4(1, 3, 4, 2) + f^{14y} f^{y32} A_4(1, 4, 3, 2) = \\ &= f^{13x} f^{x42} A_4(1, 2, 4, 3) + f^{14y} f^{y32} A_4(1, 2, 3, 4) = \\ &= \left[\frac{t}{u} f^{13x} f^{x42} + f^{14y} f^{y32} \right] A(1, 2, 3, 4). \end{aligned}$$

In the last step we used reflection invariance. Reminding that:

$$\begin{aligned} (f^{13x} f^{x42})^2 &= N^2(N^2 - 1), \\ (f^{13x} f^{x42})(f^{14y} f^{y32}) &= \frac{N^2(N^2 - 1)}{2}, \end{aligned}$$

squaring this amplitude we get:

$$\sum_{\text{colors}} |\mathcal{A}_4|^2 = 4N^2(N^2 - 1) \left[\frac{t^2}{u^2} + 1 + \frac{t}{u} \right] |A_4(1, 2, 3, 4)|^2. \quad (3.65)$$

Since for $n = 4$ the only non-vanishing amplitudes are the MHV ones⁷, considering the

⁷The details are shown in appendix B.

configuration $(-, -, +, +)$ and using the Parke-Taylor formula we obtain:

$$|A_4(1^-, 2^-, 3^+, 4^+)|^2 = \frac{(\langle 12 \rangle [21])^4}{\langle 12 \rangle \langle 23 \rangle \langle 34 \rangle \langle 41 \rangle [21] [32] [43] [14]} = \frac{s^2}{t^2}. \quad (3.66)$$

Inserting (3.66) into (3.65), we finally get:

$$\sum_{\text{colors}} |\mathcal{A}_4|^2 = 4N^2(N^2 - 1)s^2 \left(\frac{t^2 + u^2 + ut}{t^2 u^2} \right) = 4N^2(N^2 - 1) \left(\frac{s^4}{t^2 u^2} - \frac{s^2}{tu} \right), \quad (3.67)$$

in perfect accordance with [13]. Summing over all helicity configurations and averaging over the different initial states, we easily get the well-known total cross-section:

$$\frac{1}{256} \sum_{\text{pols., col.}} |\mathcal{A}_4|^2 = \frac{9}{2} g^4 \left(3 - \frac{us}{t^2} - \frac{ut}{s^2} - \frac{st}{u^2} \right). \quad (3.68)$$

Chapter 4

Large N expansion at work

4.1 Tree-level partial amplitudes up to $n = 7$

Here we list the analytic expressions of partial amplitudes for different external helicity configurations and $n = 6, 7$. For MHV amplitudes¹ the Parke-Taylor formula holds:

$$A(1^+, \dots, i^-, \dots, j^-, \dots, n^+) = \frac{\langle ij \rangle^4}{\langle 12 \rangle \langle 23 \rangle \dots \langle (n-1)n \rangle \langle n1 \rangle}, \quad \forall n. \quad (4.1)$$

For $n = 4, 5$, all partial amplitudes are MHV. The simplicity of this formula cannot be generalized to NMHV helicity configurations. In fact, using the Mathematica package **GGT.m**[37], for $n = 6$ we get:

$$A(1^-, 2^-, 3^-, \dots, 6^+) = \left(\frac{1}{\langle 12 \rangle \langle 23 \rangle \langle 34 \rangle \langle 45 \rangle \langle 56 \rangle \langle 61 \rangle} \right) \cdot$$

$$\left\{ \frac{\langle 21 \rangle \langle 43 \rangle \left[-\langle 31 \rangle \langle 6|x_{64}|x_{42}|2 \rangle - \frac{\langle 21 \rangle \langle 32 \rangle \langle 6|x_{64}|x_{42}|3 \rangle}{\langle 23 \rangle} \right]^4}{s_{24} \langle 6|x_{62}|x_{24}|3 \rangle \langle 6|x_{62}|x_{24}|4 \rangle \langle 6|x_{64}|x_{42}|1 \rangle \langle 6|x_{64}|x_{42}|2 \rangle} \right.$$

$$+ \frac{\langle 21 \rangle \langle 54 \rangle \left[-\langle 31 \rangle \langle 6|x_{65}|x_{52}|2 \rangle - \frac{\langle 21 \rangle \langle 32 \rangle \langle 6|x_{65}|x_{52}|3 \rangle}{\langle 23 \rangle} \right]^4}{s_{25} \langle 6|x_{62}|x_{25}|4 \rangle \langle 6|x_{62}|x_{25}|5 \rangle \langle 6|x_{65}|x_{52}|1 \rangle \langle 6|x_{65}|x_{52}|2 \rangle}$$

$$\left. + \frac{\langle 21 \rangle^4 \langle 32 \rangle^5 \langle 54 \rangle \langle 6|x_{65}|x_{53}|3 \rangle^3}{s_{35} \langle 23 \rangle^4 \langle 6|x_{63}|x_{35}|4 \rangle \langle 6|x_{63}|x_{35}|5 \rangle \langle 6|x_{65}|x_{53}|2 \rangle} \right\}.$$

¹Amplitudes with 2 negative and $(n-2)$ positive helicities, see appendix B.

Here we suitably defined $x_{ij} = \sum_{k=i}^{j-1} p_k$ and $s_{ij} = x_{ij}^2$. For $n = 7$ we get the following NMHV amplitude:

$$\begin{aligned}
A(1^-, 2^-, 3^-, \dots, 7^+) &= \left(\frac{1}{\langle 12 \rangle \langle 23 \rangle \langle 34 \rangle \langle 45 \rangle \langle 56 \rangle \langle 67 \rangle \langle 71 \rangle} \right) \cdot \\
&\left\{ \frac{\langle 21 \rangle \langle 43 \rangle \left[-\langle 31 \rangle \langle 7 | x_{74} | x_{42} \rangle 2 - \frac{\langle 21 \rangle \langle 32 \rangle \langle 7 | x_{74} | x_{42} \rangle 3}{\langle 23 \rangle} \right]^4}{s_{24} \langle 7 | x_{72} | x_{24} \rangle 3 \langle 7 | x_{72} | x_{24} \rangle 4 \langle 7 | x_{74} | x_{42} \rangle 1 \langle 7 | x_{74} | x_{42} \rangle 2} \right. \\
&+ \frac{\langle 21 \rangle \langle 54 \rangle \left[-\langle 31 \rangle \langle 7 | x_{75} | x_{52} \rangle 2 - \frac{\langle 21 \rangle \langle 32 \rangle \langle 7 | x_{75} | x_{52} \rangle 3}{\langle 23 \rangle} \right]^4}{s_{25} \langle 7 | x_{72} | x_{25} \rangle 4 \langle 7 | x_{72} | x_{25} \rangle 5 \langle 7 | x_{75} | x_{52} \rangle 1 \langle 7 | x_{75} | x_{52} \rangle 2} \\
&+ \frac{\langle 21 \rangle^4 \langle 32 \rangle^5 \langle 54 \rangle \langle 7 | x_{75} | x_{53} \rangle 3^3}{s_{35} \langle 23 \rangle^4 \langle 7 | x_{73} | x_{35} \rangle 4 \langle 7 | x_{73} | x_{35} \rangle 5 \langle 7 | x_{75} | x_{53} \rangle 2} \\
&+ \frac{\langle 21 \rangle \langle 65 \rangle \left[-\langle 31 \rangle \langle 7 | x_{76} | x_{62} \rangle 2 - \frac{\langle 21 \rangle \langle 32 \rangle \langle 7 | x_{76} | x_{62} \rangle 3}{\langle 23 \rangle} \right]^4}{s_{26} \langle 7 | x_{72} | x_{26} \rangle 5 \langle 7 | x_{72} | x_{26} \rangle 6 \langle 7 | x_{76} | x_{62} \rangle 1 \langle 6 | x_{76} | x_{62} \rangle 2} \\
&\left. + \frac{\langle 21 \rangle^4 \langle 32 \rangle^5 \langle 65 \rangle \langle 7 | x_{76} | x_{63} \rangle 3^3}{s_{36} \langle 23 \rangle^4 \langle 7 | x_{73} | x_{36} \rangle 5 \langle 7 | x_{73} | x_{36} \rangle 6 \langle 7 | x_{76} | x_{63} \rangle 2} \right\}.
\end{aligned}$$

To obtain numerical values of the amplitudes, the GGT.m package uses the **S@M.m** package, see [38] for further details.

4.2 Color coefficients classification

In this section we classify all color coefficients for $n = 5, 6, 7, 8, 9, 10$ external gluons at tree-level. These coefficients have been computed numerically, for $N = 3$, using a code written in Fortran. Then the values we obtained have been matched with their expressions as functions of powers of $1/N$ using the Mathematica package **ColorMath**[39]. Starting from $n = 5$, the color matrix is given by:

$$\tilde{C}_{ij} = N^2(N^2 - 1) \begin{pmatrix} 8 & 4 & 4 & 2 & 2 & 0 \\ 4 & 8 & 2 & 0 & 4 & 2 \\ 4 & 2 & 8 & 4 & 0 & 2 \\ 2 & 0 & 4 & 8 & 2 & 4 \\ 2 & 4 & 0 & 2 & 8 & 4 \\ 0 & 2 & 2 & 4 & 4 & 8 \end{pmatrix}, \quad A_i = \begin{pmatrix} A(1, 2, 3, 4, 5) \\ A(1, 2, 4, 3, 5) \\ A(1, 3, 2, 4, 5) \\ A(1, 3, 4, 2, 5) \\ A(1, 4, 2, 3, 5) \\ A(1, 4, 3, 2, 5) \end{pmatrix}, \quad i \in S_3. \quad (4.2)$$

No NLC coefficients are present, thus the LC amplitude is exact.

4.2.1 Six gluons

For six external gluons, the classification reads:

Full coefficient	LC coefficient	Occurrence
16	16	1
8	8	3
4	4	5
2	2	4
$2 + 24/N^2$	2	1
0	0	6
$24/N^2$	0	4

We note that NLC corrections hit only 0 and 2. Retaining only LC contributions, only 14 coefficients survive. We put the coefficients in powers of 2 in descending order: terms proportional to $1/N^2$ are in some sense interpreted as ‘corrections’ to the powers of 2 and 0.

4.2.2 Seven gluons

For seven gluons, we get:

Full coefficient	LC coefficient	Occurrence
32	32	1
16	16	4
8	8	9
4	4	12
$4 + 48/N^2$	4	2
2	2	8

$2 + 24/N^2$	2	4
$2 + 32/N^2$	2	2
0	0	27
$48/N^2$	0	8
$\pm 32/N^2$	0	3, 1
$24/N^2$	0	16
$16/N^2$	0	7
$\pm 8/N^2$	0	10, 6

The number of non-vanishing coefficients is 93. In this case only 0, 2 and 4 are ‘corrected’ by NLC powers of $1/N$.

4.2.3 Eight gluons

For eight external gluons, the full amplitude displays corrections proportional to $1/N^4$. The classification of adjoint color coefficients and their occurrences is the following:

Full coefficient	LC coefficient	Occurrence
64	64	1
32	32	5
16	16	14
8	8	25
$8 + 96/N^2$	8	3
4	4	28
$4 + 48/N^2$	4	10
$4 + 64/N^2$	4	4
2	2	16
$2 + 24/N^2$	2	12
$2 + 32/N^2$	2	8
$2 + 64/N^2 + 96/N^4$	2	2
$2 + 28/N^2 - 48/N^4$	2	4
0	0	137
$96/N^2$	0	12
$\pm 64/N^2$	0	6, 2
$48/N^2$	0	40
$24/N^2$	0	48
$\pm 32/N^2$	0	26, 4

$\pm 16/N^2$	0	48, 12
$\pm 8/N^2$	0	56, 32
$64/N^2 + 96/N^4$	0	4
$28/N^2 + 48/N^4$	0	24
$32/N^2 + 96/N^4$	0	20
$\pm(4/N^2 + 48/N^4)$	0	30, 8
$\pm(12/N^2 + 48/N^4)$	0	28, 10
$\pm(-12/N^2 + 48/N^4)$	0	10, 4
$\pm(20/N^2 + 48/N^4)$	0	12, 2
$24/N^2 + 96/N^4$	0	12
$40/N^2 + 96/N^4$	0	1

The number of non-vanishing coefficients is 583. Curiously, now only 0 and 2 are ‘corrected’ by N^2 LC powers of $1/N$, while NLC terms hit 4 and 8. As a consequence, we guess that, increasing the number of external gluons, for even n the lowest order color contribution hits 0 and 2, while for odd n it hits 0, 2 and 4.

4.2.4 Nine gluons

Let’s see if our guess is correct. For nine gluons we get:

Full coefficient	LC	Occ.	Full coefficient	LC	Occ.
128	128	1	$\pm(24/N^2 + 96/N^4)$	0	104, 20
64	64	6	$\pm(-8/N^2 + 96/N^4)$	0	20, 8
32	32	20	$\pm(40/N^2 + 96/N^4)$	0	28, 4
16	16	44	$48/N^2 + 192/N^4$	0	24
$16 + 192/N^2$	16	4	$80/N^2 + 192/N^4$	0	2
8	8	66	$\pm(14/N^2 + 8/N^4)$	0	22, 8
$8 + 128/N^2$	8	6	$\pm(12/N^2 - 80/N^4)$	0	8, 8
$8 + 96/N^2$	8	18	$\pm(-8/N^2 + 160/N^4)$	0	60, 14
4	4	64	$64/N^2 + 96/N^4$	0	16
$4 + 64/N^2$	4	20	$-6/N^2 + 120/N^4$	0	6
$4 + 48/N^2$	4	36	$\pm(20/N^2 + 176/N^4)$	0	8, 4
$4 + 128/N^2 + 192/N^4$	4	4	$\pm(32/N^2 - 64/N^4)$	0	15, 10
$4 + 56/N^2 - 96/N^4$	4	8	$32/N^2 + 96/N^4$	0	80
2	2	32	$\pm(-4/N^2 + 48/N^4)$	0	40, 16
$2 + 32/N^2$	2	24	$24/N^2 + 288/N^4$	0	16

$2 + 24/N^2$	2	32	$\pm(20/N^2 + 16/N^4)$	0	22, 14
$2 + 44/N^2 + 80/N^4$	2	6	$\pm(12/N^2 + 80/N^4)$	0	9, 9
$2 + 32/N^2 + 32/N^4$	2	8	$\pm 32/N^4$	0	16, 12
$2 + 64/N^2 + 96/N^4$	2	8	$24/N^2 + 256/N^4$	0	16
$2 + 28/N^2 - 48/N^4$	2	16	$20/N^2 + 208/N^4$	0	28
$2 + 48/N^2 + 288/N^4$	2	2	$\pm(16/N^2 + 128/N^4)$	0	40, 14
$2 + 128/N^2 + 128/N^4$	2	2	$\pm(16/N^2 - 32/N^4)$	0	66, 38
$2 + 22/N^2 - 56/N^4$	2	2	$\pm(8/N^2 + 128/N^4)$	0	128, 14
0	0	818	$\pm(6/N^2 + 8/N^4)$	0	10, 6
$192/N^2$	0	16	$\pm(-2/N^2 + 40/N^4)$	0	64, 44
$\pm 128/N^2$	0	9, 3	$\pm(32/N^2 - 32/N^4)$	0	8, 2
$\pm 64/N^2$	0	51, 10	$\pm(6/N^2 + 40/N^4)$	0	24, 20
$48/N^2$	0	144	$\pm(8/N^2 - 32/N^4)$	0	12, 10
$\pm 32/N^2$	0	168, 30	$\pm(10/N^2 - 40/N^4)$	0	4, 12
$24/N^2$	0	128	$24/N^2 - 32/N^4$	0	8
$\pm 16/N^2$	0	216, 76	$22/N^2 + 8/N^4$	0	16
$\pm 8/N^2$	0	200, 120	$14/N^2 + 168/N^4$	0	22
$\pm(12/N^2 + 48/N^4)$	0	216, 68	$\pm(10/N^2 + 88/N^4)$	0	78, 18
$\pm(4/N^2 + 48/N^4)$	0	120, 32	$36/N^2 + 176/N^4$	0	7
$\pm(8/N^2 + 96/N^4)$	0	60, 16	$18/N^2 + 88/N^4$	0	28
$\pm(-4/N^2 + 80/N^4)$	0	106, 44	$16/N^2 + 256/N^4$	0	6
$\pm(4/N^2 + 80/N^4)$	0	52, 36	$6/N^2 + 168/N^4$	0	10
$\pm(128/N^2 + 128/N^4)$	0	3, 1	$12/N^2 + 208/N^4$	0	6
$\pm(64/N^2 + 32/N^4)$	0	20, 6	$64/N^2 + 192/N^4$	0	40
$44/N^2 + 16/N^4$	0	26	$56/N^2 + 96/N^4$	0	48
$\pm(20/N^2 + 80/N^4)$	0	10, 4	$128/N^2 + 192/N^4$	0	8
$\pm(20/N^2 + 48/N^4)$	0	86, 8	$\pm(4/N^2 + 208/N^4)$	0	44, 8
$\pm(32/N^2 + 256/N^4)$	0	9, 1	$28/N^2 + 48/N^4$	0	96
$96/N^2$	0	72			T: 5040

The number of non-vanishing coefficients is 4222. We underline the presence of two coefficients in which N^2 LC corrections are **not** paired to NLC ones, namely $\pm 32/N^4$. We call them **pure** N^2 LC coefficients. Furthermore, our guess is confirmed, N^2 LC corrections hit only 0, 2 and 4. For ten gluons we expect that only 0 and 2 will be corrected by N^3 LC contributions.

4.2.5 Ten gluons

Our expectations for ten gluons are confirmed, since only 0 and 2 display corrections involving terms proportional to $1/N^6$. In order to simplify the classification, we explicitly list all coefficients giving a non-vanishing contribution at LC and their occurrences, while we do not list all the others² singularly:

Full coefficient	LC coefficient	Occurrence
256	256	1
128	128	7
64	64	27
32	32	70
$32 + 192/N^2$	16	5
16	16	129
$16 + 192/N^2$	16	28
$16 + 256/N^2$	16	8
8	8	168
$8 + 96/N^2$	8	75
$8 + 128/N^2$	8	36
$8 + 256/N^2 + 384/N^4$	8	6
$8 + 112/N^2 - 192/N^4$	8	12
4	4	144
$4 + 48/N^2$	4	112
$4 + 64/N^2$	4	72
$4 + 128/N^2 + 192/N^4$	4	20
$4 + 56/N^2 - 96/N^4$	4	40
$4 + 96/N^2 + 576/N^4$	4	5
$4 + 256/N^2 + 256/N^4$	4	4
$4 + 64/N^2 + 64/N^4$	4	16
$4 + 88/N^2 + 160/N^4$	4	12
$4 + 44/N^2 - 112/N^4$	4	84
2	2	64
$2 + 24/N^2$	2	80
$2 + 32/N^2$	2	64
$2 + 64/N^2 + 96/N^4$	2	24
$2 + 28/N^2 - 48/N^4$	2	48
$2 + 48/N^2 + 288/N^4$	2	12
$2 + 128/N^2 + 128/N^4$	2	8

²The lowest order corrections of 0.

$2 + 32/N^2 + 32/N^4$	2	32
$2 + 44/N^2 + 80/N^4$	2	24
$2 + 22/N^2 - 56/N^4$	2	8
$2 + 56/N^2 + 384/N^4$	2	8
$2 + 256/N^2 + 256/N^4 + 384/N^6$	2	2
$2 + 48/N^2 + 48/N^4 - 192/N^6$	2	12
$2 + 76/N^2 + 64/N^4 - 192/N^6$	2	6
$2 + 36/N^2 + 216/N^4 + 96/N^6$	2	12
$2 + 30/N^2 + 32/N^4 - 96/N^6$	2	8
$2 + 60/N^2 + 528/N^4 + 384/N^6$	2	3
$2 + 40/N^2 + 232/N^4 + 96/N^6$	2	7
$2 + 22/N^2 + 112/N^4 + 96/N^6$	2	3
$2 + 24/N^2 + 64/N^4$	2	4
0	0	5449

The remaining coefficients are of the form:

$$\frac{a}{N^2} + \frac{b}{N^4} + \frac{c}{N^6}. \quad (4.3)$$

Furthermore, some of them give **pure** NLC and N²LC contributions, namely:

$$\frac{\alpha}{N^2}, \quad \frac{\beta}{N^4}. \quad (4.4)$$

As a consequence, N³LC contributions are always mixed with at least one term of lower order. In other words, we do not have pure $1/N^6$ contributions.

4.2.6 An additional comment on numerators

For all numbers of external gluons $n \leq 10$, each color coefficient listed above can be trivially expressed as:

$$a + \frac{b}{N^2} + \frac{c}{N^4} + \frac{d}{N^6}. \quad (4.5)$$

where a can be zero or a power of 2 such that $a \leq 2^{n-2}$. By direct inspection of the

above tables³ we note that the highest coefficient appearing as numerator to all orders in even powers of $1/N$ is given by:

$$\begin{aligned} n = 6, & \longrightarrow 24 = 2^3 \cdot 3^1, & n = 7, & \longrightarrow 48 = 2^4 \cdot 3^1, \\ n = 8, & \longrightarrow 96 = 2^5 \cdot 3^1, & n = 9, & \longrightarrow 288 = 2^5 \cdot 3^2, \\ n = 10, & \longrightarrow 576 = 2^6 \cdot 3^2, & n = 11, & \longrightarrow 1152 = 2^7 \cdot 3^2 (?). \end{aligned}$$

Obviously the question mark means that the value for $n = 11$ is a guess. Noticing that the sum of the exponents is given by $n - 2$, we guess that, for n external gluons, the highest numerator is:

$$C_0^{\max}(n) = 2^{n-2-\lfloor \frac{n-3}{3} \rfloor} 3^{\lfloor \frac{n-3}{3} \rfloor} = 2^{n-1-\lfloor \frac{n}{3} \rfloor} 3^{\lfloor \frac{n}{3} \rfloor - 1}. \quad (4.6)$$

Here we checked this guess for less than 11 external gluons. This means that terms of highest order in $1/N$ can at most be:

$$\begin{aligned} n = 6, & \longrightarrow 24/N^2 \simeq 2.\bar{6}, & n = 7, & \longrightarrow 48/N^2 \simeq 5.\bar{3}, \\ n = 8, & \longrightarrow 96/N^4 \simeq 1.18\bar{6}, & n = 9, & \longrightarrow 288/N^4 \simeq 3.\bar{5}, \\ n = 10, & \longrightarrow 576/N^6 \simeq 0.79, & n = 11, & \longrightarrow 1152/N^6 \simeq 1.58 (?). \end{aligned}$$

If our guess is correct, the behaviour of these terms would be:

$$R_0^{\max}(n) = \frac{2^{n-2-\lfloor \frac{n-3}{3} \rfloor} 3^{\lfloor \frac{n-3}{3} \rfloor}}{3^{2\lfloor \frac{n-4}{2} \rfloor}} = \frac{2^{n-1-\lfloor \frac{n}{3} \rfloor} 3^{\lfloor \frac{n}{3} \rfloor - 1}}{3^{2(\lfloor \frac{n}{2} \rfloor - 2)}}. \quad (4.7)$$

These terms have to be compared to the LC coefficients, especially the highest one 2^{n-2} . Thus we decide to normalize them by this coefficient, so that the greatest coefficient is one, namely:

$$R_{0,\text{norm}}^{\max}(n) = \frac{2^{1-\lfloor \frac{n}{3} \rfloor} 3^{\lfloor \frac{n}{3} \rfloor - 1}}{3^{2(\lfloor \frac{n}{2} \rfloor - 2)}}. \quad (4.8)$$

In addition:

- The highest numerators for the next lower order power of $1/N$ are instead:

³Including all non-listed coefficients for $n = 10$.

$$\begin{aligned}
n = 8, & \longrightarrow 96 = 2^5 \cdot 3^1, & n = 9, & \longrightarrow 192 = 2^6 \cdot 3^1, \\
n = 10, & \longrightarrow 576 = 2^6 \cdot 3^2, & n = 11, & \longrightarrow 1152 = 2^7 \cdot 3^2 (?).
\end{aligned}$$

To reproduce these terms we guess another formula, similar to (4.7):

$$C_1^{\max}(n) = \begin{cases} 2^{n-2-\lfloor \frac{(n-3)-1}{3} \rfloor} 3^{\lfloor \frac{(n-3)-1}{3} \rfloor} & \text{if } n \geq 8 \text{ is even,} \\ 2^{n-2-\lfloor \frac{(n-3)-2}{3} \rfloor} 3^{\lfloor \frac{(n-3)-2}{3} \rfloor} & \text{if } n \geq 8 \text{ is odd.} \end{cases} \quad (4.9)$$

- Finally, the highest numerators for further lower order power of $1/N$ are:

$$n = 10, \longrightarrow 384 = 2^7 \cdot 3^1, \quad n = 11, \longrightarrow 768 = 2^8 \cdot 3^1 (?).$$

Again, to reproduce these terms we guess the following formula, namely:

$$C_2^{\max}(n) = \begin{cases} 2^{n-2-\lfloor \frac{(n-3)-3}{3} \rfloor} 3^{\lfloor \frac{(n-3)-3}{3} \rfloor} & \text{if } n \geq 10 \text{ is even,} \\ 2^{n-2-\lfloor \frac{(n-3)-4}{3} \rfloor} 3^{\lfloor \frac{(n-3)-4}{3} \rfloor} & \text{if } n \geq 10 \text{ is odd.} \end{cases} \quad (4.10)$$

Thus, moving through all orders in powers of $1/N$ in descending order, we decrease $n - 3$ by odd numbers when n is even and by even numbers when it is odd.

We collect our results in the following table, also providing the values we would obtain for $n = 11, 12$ if our guess itself holds true:

# gluons	$1/N^0$	$1/N^2$	$1/N^4$	$1/N^6$	$1/N^8$
$n = 3$	$2^1 \cdot 3^0 = 2$	0	0	0	0
$n = 4$	$2^2 \cdot 3^0 = 4$	0	0	0	0
$n = 5$	$2^3 \cdot 3^0 = 8$	0	0	0	0
$n = 6$	$2^4 \cdot 3^0 = 16$	$2^3 \cdot 3^1 = 24$	0	0	0
$n = 7$	$2^5 \cdot 3^0 = 32$	$2^4 \cdot 3^1 = 48$	0	0	0
$n = 8$	$2^6 \cdot 3^0 = 64$	$2^5 \cdot 3^1 = 96$	$2^5 \cdot 3^1 = 96$	0	0
$n = 9$	$2^7 \cdot 3^0 = 128$	$2^6 \cdot 3^1 = 192$	$2^5 \cdot 3^2 = 288$	0	0
$n = 10$	$2^8 \cdot 3^0 = 256$	$2^7 \cdot 3^1 = 384$	$2^6 \cdot 3^2 = 576$	$2^6 \cdot 3^2 = 576$	0
$n = 11(?)$	$2^9 \cdot 3^0 = 512$	$2^8 \cdot 3^1 = 768$	$2^7 \cdot 3^2 = 1152$	$2^7 \cdot 3^2 = 1152$	0
$n = 12(?)$	$2^{10} \cdot 3^0 = 1024$	$2^9 \cdot 3^1 = 1536$	$2^8 \cdot 3^2 = 2304$	$2^8 \cdot 3^2 = 2304$	$2^7 \cdot 3^3 = 3456$

Inspecting the above table, let us make two comments.

- First of all, the fact that these coefficients are given by suitable powers of **only** 3 (number of QCD colors) and 2 (they are all even numbers) up to ten external gluons is at least curious.
- Furthermore, we can consider all the highest LC powers⁴ of 2 as trivial products of the form:

$$2^{n-2} \cdot 3^0. \quad (4.11)$$

As a consequence, they are easily described by the above mentioned products of powers of 2 and 3 anyway.

4.3 Expansion efficacy for MHV amplitudes up to eight external gluons in the adjoint basis

In this section our purpose is to compare the squared and color-summed gluon scattering amplitudes at tree level with their values obtained at leading, next-to-leading and next-to-next-to leading order in powers of $1/N$. From now on we will denote them as LC, NLC and N²LC as customary. As previously stated, up to $n \leq 5$ we can easily see that no NLC and N²LC contributions to the amplitude are present, thus at leading order in color we get exact results.

4.3.1 Six gluons

For $n = 6$, the color matrix has dimension 24×24 . Instead of giving the entire matrix, we can recognize that all the information is contained in the first row, given by $\tilde{C}_{(123456)(1\sigma(2345)6)} = C_6(N)\gamma(\sigma(2345))$:

$$\begin{aligned} \gamma(2345) &= 16, & \gamma(3245) &= 8, & \gamma(4235) &= 4, & \gamma(5234) &= 2, \\ \gamma(2354) &= 8, & \gamma(3254) &= 4, & \gamma(4253) &= 2, & \gamma(5243) &= 0, \\ \gamma(2435) &= 8, & \gamma(3425) &= 4, & \gamma(4325) &= 0, & \gamma(5324) &= 0, \\ \gamma(2453) &= 4, & \gamma(3452) &= 2, & \gamma(4352) &= 0, & \gamma(5342) &= a, \\ \gamma(2534) &= 4, & \gamma(3524) &= 2, & \gamma(4523) &= b, & \gamma(5423) &= a, \\ \gamma(2543) &= 0, & \gamma(3542) &= 0, & \gamma(4532) &= a, & \gamma(5432) &= a, \end{aligned} \quad (4.12)$$

⁴We can alternatively think of them as multiplied by the even power $1/N^0 = 1$.

where $a = 24/N^2$ and $b = 2 + a$. As a consequence, the first row contribution to the full and LO tree-level amplitudes read:

$$\begin{aligned} \mathcal{A}_{\text{FULL}}^{\text{tree}} = & N^4 (N^2 - 1) A_{123456}^* \left[16A_{123456} + 8N^2 A_{123546} + 8A_{124356} + \right. \\ & 4A_{124536} + 4A_{125346} + 8A_{132456} + 4A_{132546} + \\ & 4A_{134256} + 2A_{134526} + 2A_{135246} + 4A_{142356} + \\ & 2A_{142536} + 2A_{145236} + 2A_{152346} + \frac{24}{N^2} A_{145236} + \\ & \left. \frac{24}{N^2} A_{145326} + \frac{24}{N^2} A_{153426} + \frac{24}{N^2} A_{154236} + \frac{24}{N^2} A_{154326} \right], \end{aligned}$$

$$\begin{aligned} \mathcal{A}_{\text{LC}}^{\text{tree}} = & N^4 (N^2 - 1) A_{123456}^* [16A_{123456} + 8A_{123546} + 8A_{124356} + 4A_{124536} + \\ & 4A_{125346} + 8A_{132456} + 4A_{132546} + 4A_{134256} + 2A_{134526} + 2A_{135246} + \\ & 4A_{142356} + 2A_{142536} + 2A_{145236} + 2A_{152346}]. \end{aligned}$$

Using Mathematica, we implemented a very simple function to sum all the different contributions coming from the 24 rows of both the full and LC matrix. We then compared the results for MHV amplitudes with fixed helicities: $(-, +, \dots, +, -)$. In order to obtain numerical values for the partial amplitudes, we used the function `GenMomenta[...]` included in [38] to generate a valid pseudo-random set of six external momenta, then got numerical values through the function `GGTtoSpinors[...]/N`. Finally, we called `GenMomenta[...]` 100 times to obtain a mean value of the color-summed squared amplitude on the phase space. Here we report the first twenty values of both the full and LC amplitudes we obtained for twenty different phase space points:

FULL = 27230.8,	LC = 26923.4,	Ratio = 0.988708,
FULL = 394930.0,	LC = 384992.0,	Ratio = 0.974837,
FULL = $1.28108 \cdot 10^7$,	LC = $1.28071 \cdot 10^7$,	Ratio = 0.999708,
FULL = $2.89343 \cdot 10^8$,	LC = $2.88893 \cdot 10^8$,	Ratio = 0.998444,
FULL = 452909.0,	LC = 452870.0,	Ratio = 0.999914,
FULL = 35167.1,	LC = 35026.3,	Ratio = 0.995988,
FULL = 39801.7,	LC = 39655.5,	Ratio = 0.996327,
FULL = 333179.0,	LC = 328767.0,	Ratio = 0.986759,
FULL = 511.921,	LC = 511.891,	Ratio = 0.999942,
FULL = 2168.84,	LC = 2168.03,	Ratio = 0.999625,
FULL = 28883.8,	LC = 28293.4,	Ratio = 0.97956,
FULL = 220.89,	LC = 218.824,	Ratio = 0.990647,
FULL = 406540.0,	LC = 403950.0,	Ratio = 0.993628,
FULL = 590901,	LC = 588495,	Ratio = 0.995928,
FULL = $8.17026 \cdot 10^6$,	LC = $8.14478 \cdot 10^6$,	Ratio = 0.996881,
FULL = 54828.6,	LC = 54801.3,	Ratio = 0.999501,
FULL = 126783.0,	LC = 121835.0,	Ratio = 0.960971,
FULL = $1.20998 \cdot 10^6$,	LC = $1.20972 \cdot 10^6$,	Ratio = 0.999789,
FULL = 4077.38,	LC = 4067.33,	Ratio = 0.997534,
FULL = $2.25875 \cdot 10^6$,	LC = $2.22828 \cdot 10^6$,	Ratio = 0.986513.

Therefore, the LC approximation gives an average error of 1% over the pseudo-randomly selected phase space points.

4.3.2 Seven gluons

For $n = 7$ we continue to get only NLC corrections. Using a similar Mathematica code, we obtained 100 full and LC amplitudes. We report again the first twenty values of both the full and LC amplitudes:

FULL = $3.16578 \cdot 10^9$,	LC = $2.98795 \cdot 10^9$,	Ratio = 0.943827,
FULL = $8.16687 \cdot 10^8$,	LC = $7.52012 \cdot 10^8$,	Ratio = 0.920808,
FULL = $4.59454 \cdot 10^7$,	LC = $4.54689 \cdot 10^7$,	Ratio = 0.989628,
FULL = $1.26928 \cdot 10^7$,	LC = $1.13688 \cdot 10^7$,	Ratio = 0.895691,
FULL = 697036,	LC = 667346,	Ratio = 0.957405,
FULL = $1.99 \cdot 10^6$,	LC = $1.84555 \cdot 10^6$,	Ratio = 0.927414,
FULL = $8.12467 \cdot 10^6$,	LC = $7.71536 \cdot 10^6$,	Ratio = 0.949621,
FULL = $4.07664 \cdot 10^7$,	LC = $4.05576 \cdot 10^7$,	Ratio = 0.994878,
FULL = 6190.13,	LC = 6061.45,	Ratio = 0.979213,
FULL = $1.07534 \cdot 10^{11}$,	LC = $1.07031 \cdot 10^{11}$,	Ratio = 0.995321,
FULL = $1.21092 \cdot 10^7$,	LC = $1.17029 \cdot 10^7$,	Ratio = 0.966443,
FULL = 453893,	LC = 419789,	Ratio = 0.924863,
FULL = 8021.32,	LC = 7285.55,	Ratio = 0.908274,
FULL = 576004,	LC = 573496,	Ratio = 0.995647,
FULL = $1.57023 \cdot 10^7$,	LC = $1.42651 \cdot 10^7$,	Ratio = 0.908474,
FULL = 717694,	LC = 696527,	Ratio = 0.970506,
FULL = 128624,	LC = 127713,	Ratio = 0.992918,
FULL = $2.89073 \cdot 10^7$,	LC = $2.87604 \cdot 10^7$,	Ratio = 0.99492,
FULL = $1.73362 \cdot 10^6$,	LC = $1.51124 \cdot 10^6$,	Ratio = 0.871727,
FULL = 85806.9,	LC = 80093.4,	Ratio = 0.933414.

In this case the LC approximation is not satisfactory, since we get an average error of 5% over all 100 phase space points.

4.3.3 Eight gluons

For $n = 8$, neglecting all $1/N^4$ contributions to the tree-level amplitude, we get that our NLC approximation gives a value differing from the exact one by one part per mil on average. We report here the first twenty values of the full amplitude and the ratios we obtained for both the LC and NLC approximation for twenty different phase space points, namely:

FULL = $1.58706 \cdot 10^{10}$,	Ratio _{LC} = 0.822465,	Ratio _{NLC} = 0.997494,
FULL = $1.56476 \cdot 10^{12}$,	Ratio _{LC} = 0.986549,	Ratio _{NLC} = 0.999929,
FULL = $4.37443 \cdot 10^8$,	Ratio _{LC} = 0.921011,	Ratio _{NLC} = 0.999614,
FULL = $2.35873 \cdot 10^8$,	Ratio _{LC} = 0.969267,	Ratio _{NLC} = 0.999964,
FULL = $1.56476 \cdot 10^6$,	Ratio _{LC} = 0.991875,	Ratio _{NLC} = 0.999977,
FULL = $4.37443 \cdot 10^{10}$,	Ratio _{LC} = 0.98727,	Ratio _{NLC} = 0.999989,
FULL = $2.95491 \cdot 10^7$,	Ratio _{LC} = 0.930747,	Ratio _{NLC} = 0.999928,
FULL = $1.14142 \cdot 10^9$,	Ratio _{LC} = 0.934263,	Ratio _{NLC} = 0.999242,
FULL = $3.18545 \cdot 10^7$,	Ratio _{LC} = 0.858419,	Ratio _{NLC} = 0.998719,
FULL = $4.54754 \cdot 10^8$,	Ratio _{LC} = 0.890643,	Ratio _{NLC} = 0.999297,
FULL = $1.31524 \cdot 10^6$,	Ratio _{LC} = 0.779917,	Ratio _{NLC} = 0.996694,
FULL = $3.16123 \cdot 10^{11}$,	Ratio _{LC} = 0.92231,	Ratio _{NLC} = 0.999626,
FULL = $2.77371 \cdot 10^{10}$,	Ratio _{LC} = 0.858758,	Ratio _{NLC} = 0.998966,
FULL = $7.28107 \cdot 10^9$,	Ratio _{LC} = 0.817419,	Ratio _{NLC} = 0.998861,
FULL = $9.23245 \cdot 10^8$,	Ratio _{LC} = 0.93888,	Ratio _{NLC} = 0.999624,
FULL = $8.78216 \cdot 10^9$,	Ratio _{LC} = 0.97915,	Ratio _{NLC} = 0.999869,
FULL = $1.62271 \cdot 10^6$,	Ratio _{LC} = 0.867123,	Ratio _{NLC} = 0.999456,
FULL = $2.51064 \cdot 10^{10}$,	Ratio _{LC} = 0.99718,	Ratio _{NLC} = 0.999996,
FULL = $8.56096 \cdot 10^9$,	Ratio _{LC} = 0.987968,	Ratio _{NLC} = 0.999991,
FULL = $5.39079 \cdot 10^7$,	Ratio _{LC} = 0.880421,	Ratio _{NLC} = 0.998863.

As a consequence, the NLC approximation turns out to be very good: over the 100 phase space points generated we get an average error less than 0.1%. On the other hand, the LC approximation is definitely unsatisfactory, since it gives an average error of 10%.

Chapter 5

NLO corrections and large N expansion

5.1 Definition

The one-loop color decomposition for n -gluon amplitudes expressed in terms of adjoint generator matrices reads [18]:

$$\mathcal{A}^{1\text{-L}} = g^n \sum_{\sigma} \left[\text{Tr}(F^{a_{\sigma_1}} \dots F^{a_{\sigma_n}}) A_{n;1}^{[1]}(\sigma_1, \dots, \sigma_n) + 2N_f \text{Tr}(T^{a_{\sigma_1}} \dots T^{a_{\sigma_n}}) A_{n;1}^{[1/2]}(\sigma_1, \dots, \sigma_n) \right], \quad (5.1)$$

where σ lives in the set of all non-cyclic permutations of the n external gluons up to reflections¹ and N_f is the numbers of quark flavors. The superscript $[s]$ denotes the spin of the particle circulating in the loop. Therefore the number of independent subamplitudes is $(n-1)!/2$. One-loop amplitudes contribute to NLO QCD cross-sections interfering with the tree-level part of the full amplitude, namely:

$$\begin{aligned} \sum_{\text{colors}} \mathcal{A}(1, \dots, n) \mathcal{A}^*(1, \dots, n)|_{\text{NLO}} &= 2 \sum_{\text{colors}} \text{Re} \left[\mathcal{A}^{\text{tree}}(\mathcal{A}^{1\text{-loop}})^* \right] = \\ &= 2(g^2)^{n-1} \text{Re} \left\{ \sum_{i=1}^{(n-2)!} \sum_{j=1}^{(n-1)!/2} A_i^{\text{tree}} \left[\hat{c}_{ij}(A_j^{[1]})^* + 2N_f \hat{d}_{ij}(A_j^{[1/2]})^* \right] \right\}. \end{aligned}$$

The elements of the two $(n-2)! \times (n-1)!/2$ color matrices appearing above read:

$$\hat{c}_{ij} = \sum_{\text{colors}} (P_i \{F^{a_2} \dots F^{a_{n-1}}\})_{a_1 a_n} [\text{Tr}(F^{a_1} P_j \{F^{a_2} \dots F^{a_n}\})]^*, \quad (5.2)$$

¹We denote this set as S_{n-1}/\mathcal{R} .

$$\hat{d}_{ij} = \sum_{\text{colors}} (P_i \{F^{a_2} \dots F^{a_{n-1}}\})_{a_1 a_n} [\text{Tr}(T^{a_1} P_j \{T^{a_2} \dots T^{a_n}\})]^*, \quad (5.3)$$

where $i \in S_{n-2}$ and $j \in S_{n-1}/\mathcal{R}$. For example, when $n = 4$, we get:

$$\hat{c}_{11} = \sum_{\text{colors}} (f^{a_1 a_2 l} f^{l a_3 a_4}) (f^{x a_1 y} f^{y a_2 z} f^{z a_3 k} f^{k a_4 x}), \quad (5.4)$$

$$\hat{d}_{11} = \sum_{\text{colors}} (f^{a_1 a_2 x} f^{x a_3 a_4}) (T_{ij}^{a_1} T_{jk}^{a_2} T_{kl}^{a_3} T_{li}^{a_4}). \quad (5.5)$$

For $n = 4, 5$ these matrices are explicitly given in [18]. We report them here for completeness. For $n = 4$ we get:

$$\hat{c}_{ij} = N^3(N^2 - 1) \begin{pmatrix} 2 & -2 & 0 \\ 0 & -2 & 2 \end{pmatrix}, \quad \hat{d}_{ij} = N^2(N^2 - 1) \begin{pmatrix} 1 & -1 & 0 \\ 0 & -1 & 1 \end{pmatrix}, \quad (5.6)$$

while for $n = 5$ we get:

$$\hat{c}_{ij} = N^4(N^2 - 1) \begin{pmatrix} 2 & -2 & 0 & -2 & 0 & 2 & 0 & 0 & a & -a & a & a \\ 0 & -2 & 2 & -2 & 2 & 0 & a & a & a & 0 & 0 & a \\ 0 & 0 & a & -2 & -a & 2 & 2 & -2 & 0 & 0 & a & a \\ a & a & a & 0 & 0 & 2 & 0 & -2 & 2 & 2 & a & 0 \\ a & -2 & 0 & 0 & 2 & -a & a & 0 & a & 2 & 2 & 0 \\ a & 0 & a & a & 2 & 0 & a & -2 & 0 & 2 & 0 & 2 \end{pmatrix}, \quad (5.7)$$

$$\hat{d}_{ij} = N^3(N^2 - 1) \begin{pmatrix} 1 & -1 & 0 & -1 & 0 & 1 & 0 & 0 & b & -b & b & b \\ 0 & -1 & 1 & -1 & 1 & 0 & b & b & b & 0 & 0 & b \\ 0 & 0 & b & -1 & -b & 1 & 1 & -1 & 0 & 0 & b & b \\ b & b & b & 0 & 0 & 1 & 0 & -1 & 1 & 1 & b & 0 \\ b & -1 & 0 & 0 & 1 & -b & b & 0 & b & 1 & 1 & 0 \\ b & 0 & b & b & 1 & 0 & b & -1 & 0 & 1 & 0 & 1 \end{pmatrix}, \quad (5.8)$$

where we suitably set $a = 24/N^2$ and $b = 2/N^2$. In the following, we present the first row of these matrices for $n = 6$ and only classify the coefficients for $n = 7, 8$. All coefficients have been computed using the Mathematica package **ColorMath**[39].

5.2 Six gluons

For six gluons, the first row of the \hat{c}_{ij} matrix, normalized by a factor $N^5(N^2 - 1)$, reads:

$$\hat{c}_{1j} = \left\{ 2, -2, 0, -2, 0, 2, 0, 0, \frac{24}{N^2}, -2, -\frac{24}{N^2}, 2, \frac{24}{N^2}, \frac{24}{N^2}, \frac{24}{N^2}, 0, 0, 2, -\frac{24}{N^2}, -\frac{24}{N^2}, -\frac{24}{N^2}, \right.$$

$$0, 0, -2, 0, 0, 0, 0, 0, 0, \frac{24}{N^2}, -\frac{24}{N^2}, \frac{32}{N^2}, -\frac{32}{N^2}, \frac{16}{N^2}, -\frac{8}{N^2}, \frac{8}{N^2}, -\frac{24}{N^2}, -\frac{16}{N^2}, \frac{8}{N^2},$$

$$-\frac{8}{N^2}, \frac{24}{N^2}, \frac{24}{N^2}, -\frac{24}{N^2}, \frac{16}{N^2}, -\frac{16}{N^2}, \frac{24}{N^2}, -\frac{24}{N^2}, \frac{8}{N^2}, -\frac{8}{N^2}, \frac{16}{N^2}, -\frac{8}{N^2}, -\frac{16}{N^2}, \frac{8}{N^2}, \frac{32}{N^2},$$

$$\left. \frac{8}{N^2}, \frac{8}{N^2}, -\frac{8}{N^2}, -\frac{8}{N^2}, -\frac{32}{N^2} \right\}.$$

The classification is given by:

Full coefficient	LC coefficient	Occurrence
± 2	± 2	4, 4
0	0	14
$\pm 32/N^2$	0	2, 2
$\pm 24/N^2$	0	8, 8
$\pm 16/N^2$	0	3, 3
$\pm 8/N^2$	0	6, 6

Furthermore, the first row of \hat{d}_{ij} , normalized by a factor $N^4(N^2 - 1)$, is:

$$\hat{d}_{1j} = \left\{ 1, -1, 0, -1, 0, 1, 0, 0, \frac{2}{N^2}, -1, -\frac{2}{N^2}, 1, \frac{2}{N^2}, \frac{2}{N^2}, \frac{2}{N^2}, 0, 0, 1, -\frac{2}{N^2}, -\frac{2}{N^2}, -\frac{2}{N^2}, \right.$$

$$0, 0, -1, 0, 0, 0, 0, 0, 0, \frac{2}{N^2}, -\frac{2}{N^2}, \frac{1}{N^2}, -\frac{1}{N^2}, \frac{3}{N^2}, \frac{1}{N^2}, -\frac{1}{N^2}, -\frac{2}{N^2}, -\frac{3}{N^2}, -\frac{1}{N^2},$$

$$\frac{1}{N^2}, \frac{2}{N^2}, \frac{2}{N^2}, -\frac{2}{N^2}, -\frac{2}{N^2}, \frac{2}{N^2}, \frac{2}{N^2}, -\frac{2}{N^2}, -\frac{1}{N^2}, \frac{1}{N^2}, \frac{3}{N^2}, \frac{1}{N^2}, -\frac{3}{N^2}, -\frac{1}{N^2}, \frac{1}{N^2},$$

$$\left. -\frac{1}{N^2}, -\frac{1}{N^2}, \frac{1}{N^2}, \frac{1}{N^2}, -\frac{1}{N^2} \right\}.$$

The classification is:

Full coefficient	LC coefficient	Occurrence
± 1	± 1	4, 4
0	0	14
$\pm 3/N^2$	0	2, 2
$\pm 2/N^2$	0	9, 9
$\pm 1/N^2$	0	8, 8

5.3 Seven gluons

For seven external gluons, the dimension of the color matrices is 120×360 , making the writing of their first rows cumbersome. We restrict ourselves to classify their coefficients. Normalizing each term by $N^6(N^2 - 1)$, for the first row of \hat{c}_{ij} we get:

Full coefficient	LC coefficient	NLC coefficient	Occurrence
± 2	± 2	± 2	8, 8
0	0	0	68
$\pm 24/N^2$	0	$\pm 24/N^2$	24, 24
$\pm 32/N^2$	0	$\pm 32/N^2$	8, 8
$\pm 16/N^2$	0	$\pm 16/N^2$	12, 12
$\pm 8/N^2$	0	$\pm 8/N^2$	34, 34
$\pm(24/N^2 + 96/N^4)$	0	$\pm 24/N^2$	7, 5
$\pm(4/N^2 + 48/N^4)$	0	$\pm 4/N^2$	21, 11
$\pm(12/N^2 + 48/N^4)$	0	$12/N^2$	14, 14
$\pm(64/N^2 + 96/N^4)$	0	$64/N^2$	3, 1
$\pm(28/N^2 + 48/N^4)$	0	$\pm 28/N^2$	8, 8
$\pm(-4/N^2 + 48/N^4)$	0	$\mp 4/N^2$	8, 4
$\pm(32/N^2 + 96/N^4)$	0	$\pm 32/N^2$	11, 5

Normalizing each term by $N^5(N^2 - 1)$, for the first row of \hat{d}_{ij} we obtain the following classification:

Full coefficient	LC coefficient	NLC coefficient	Occurrence
± 1	± 1	± 1	8, 8
0	0	0	72
$\pm 2/N^2$	0	$\pm 2/N^2$	32, 32
$\pm 1/N^2$	0	$\pm 1/N^2$	36, 36
$\pm 3/N^2$	0	$\pm 3/N^2$	8, 8
$\pm(1/N^2 + 2/N^4)$	0	$\pm 1/N^2$	20, 12
$\pm(2/N^2 + 2/N^4)$	0	$\pm 2/N^2$	4, 4
$\pm 2/N^4$	0	0	32, 16
$\pm(1/N^2 - 2/N^4)$	0	$\pm 1/N^2$	10, 10
$\pm(2/N^2 - 2/N^4)$	0	$\pm 2/N^2$	4, 4
$\pm(3/N^2 - 2/N^4)$	0	$\pm 3/N^2$	2, 2

5.4 Eight gluons

The classification confirms our guess again, since we only get ‘corrections’ of 0. For the matrix \hat{c}_{ij} , normalizing each coefficient by $N^7(N^2 - 1)$, we obtain:

Full coefficient	LC coefficient	NLC coefficient	Occurrence
± 2	± 2	± 2	16, 16
0	0	0	396
$\pm 32/N^2$	0	$\pm 32/N^2$	24, 24
$\pm 24/N^2$	0	$\pm 24/N^2$	64, 64
$\pm 16/N^2$	0	$\pm 16/N^2$	36, 36
$\pm 8/N^2$	0	$\pm 8/N^2$	120, 120
$\pm(64/N^2 + 96/N^4)$	0	$\pm 64/N^2$	8, 8
$\pm(28/N^2 + 48/N^4)$	0	$\pm 28/N^2$	32, 32
$\pm(12/N^2 + 48/N^4)$	0	$\pm 12/N^2$	116, 116
$\pm(32/N^2 + 96/N^4)$	0	$\pm 32/N^2$	32, 32
$\pm(4/N^2 - 48/N^4)$	0	$\pm 4/N^2$	24, 24
$\pm(4/N^2 + 48/N^4)$	0	$\pm 4/N^2$	64, 64
$\pm(24/N^2 + 96/N^4)$	0	$\pm 24/N^2$	26, 26
$\pm(128/N^2 + 128/N^4)$	0	$\pm 128/N^2$	2, 2
$\pm 32/N^4$	0	0	12, 12
$\pm 288/N^4$	0	0	16, 16
$\pm(64/N^2 + 32/N^4)$	0	$\pm 64/N^2$	10, 10

$\pm(20/N^2 + 16/N^4)$	0	$\pm 20/N^2$	16, 16
$\pm(12/N^2 + 80/N^4)$	0	$\pm 12/N^2$	8, 8
$\pm(20/N^2 + 208/N^4)$	0	$\pm 20/N^2$	4, 4
$\pm(18/N^2 + 88/N^4)$	0	$\pm 18/N^2$	6, 6
$\pm(32/N^2 - 32/N^4)$	0	$\pm 32/N^2$	2, 2
$\pm(32/N^2 + 256/N^4)$	0	$\pm 32/N^2$	4, 4
$\pm(8/N^2 - 80/N^4)$	0	$\pm 8/N^2$	18, 18
$\pm(4/N^2 + 208/N^4)$	0	$\pm 4/N^2$	12, 12
$\pm(14/N^2 + 168/N^4)$	0	$\pm 14/N^2$	8, 8
$\pm(6/N^2 + 168/N^4)$	0	$\pm 6/N^2$	6, 6
$\pm(10/N^2 - 40/N^4)$	0	$\pm 10/N^2$	8, 8
$\pm(6/N^2 - 120/N^4)$	0	$\pm 6/N^2$	4, 4
$\pm(4/N^2 - 80/N^4)$	0	$\pm 4/N^2$	36, 36
$\pm(2/N^2 - 40/N^4)$	0	$\pm 2/N^2$	22, 22
$\pm(6/N^2 + 8/N^4)$	0	$\pm 6/N^2$	8, 8
$\pm(20/N^2 + 48/N^4)$	0	$\pm 20/N^2$	16, 16
$\pm(44/N^2 + 16/N^4)$	0	$\pm 44/N^2$	8, 8
$\pm(32/N^2 - 64/N^4)$	0	$\pm 32/N^2$	12, 12
$\pm(16/N^2 - 32/N^4)$	0	$\pm 16/N^2$	44, 44
$\pm(8/N^2 + 128/N^4)$	0	$\pm 8/N^2$	54, 54
$\pm(20/N^2 + 176/N^4)$	0	$\pm 20/N^2$	6, 6
$\pm(14/N^2 + 8/N^4)$	0	$\pm 14/N^2$	18, 18
$\pm(8/N^2 - 32/N^4)$	0	$\pm 8/N^2$	12, 12
$\pm(10/N^2 + 88/N^4)$	0	$\pm 10/N^2$	48, 48
$\pm(6/N^2 + 40/N^4)$	0	$\pm 6/N^2$	24, 24
$\pm(4/N^2 + 80/N^4)$	0	$\pm 4/N^2$	32, 32
$\pm(20/N^2 + 80/N^4)$	0	$\pm 20/N^2$	6, 6
$\pm(16/N^2 + 128/N^4)$	0	$\pm 16/N^2$	18, 18

Furthermore, for the matrix \hat{d}_{ij} , normalized by $N^6(N^2 - 1)$, we get the following coefficients:

Full coefficient	LC coefficient	NLC coefficient	Occurrence
± 1	± 1	± 1	16, 16
0	0	0	416
$\pm 2/N^2$	0	$\pm 2/N^2$	100, 100
$\pm 1/N^2$	0	$\pm 1/N^2$	122, 122

$\pm 3/N^2$	0	$\pm 3/N^2$	24, 24
$\pm(1/N^2 + 2/N^4)$	0	$\pm 1/N^2$	70, 70
$\pm(2/N^2 + 2/N^4)$	0	$\pm 2/N^2$	18, 18
$\pm 2/N^4$	0	0	148, 148
$\pm(1/N^2 - 2/N^4)$	0	$\pm 1/N^2$	40, 40
$\pm(2/N^2 - 2/N^4)$	0	$\pm 2/N^2$	18, 18
$\pm(3/N^2 - 2/N^4)$	0	$\pm 3/N^2$	8, 8
$\pm 4/N^4$	0	0	60, 60
$\pm(1/N^2 + 1/N^4)$	0	$\pm 1/N^2$	32, 32
$\pm(2/N^2 + 3/N^4)$	0	$\pm 2/N^2$	4, 4
$\pm 1/N^4$	0	0	132, 132
$\pm 3/N^4$	0	0	118, 118
$\pm(1/N^2 + 5/N^4)$	0	$\pm 1/N^2$	6, 6
$\pm(1/N^2 + 3/N^4)$	0	$\pm 1/N^2$	16, 16
$\pm(1/N^2 - 1/N^4)$	0	$\pm 1/N^2$	22, 22
$\pm(2/N^2 - 1/N^4)$	0	$\pm 2/N^2$	8, 8
$\pm(2/N^2 + 1/N^4)$	0	$\pm 2/N^2$	8, 8
$\pm(1/N^2 - 3/N^4)$	0	$\pm 1/N^2$	10, 10
$\pm 5/N^4$	0	0	44, 44
$\pm 7/N^4$	0	0	6, 6
$\pm(1/N^2 - 5/N^4)$	0	$\pm 1/N^2$	8, 8
$\pm(1/N^2 + 4/N^4)$	0	$\pm 1/N^2$	4, 4
$\pm(1/N^2 - 4/N^4)$	0	$\pm 1/N^2$	4, 4
$\pm(2/N^2 - 3/N^4)$	0	$\pm 2/N^2$	4, 4
$\pm(3/N^2 - 1/N^4)$	0	$\pm 3/N^2$	2, 2

We give just two comments.

- By direct inspection of the above 1-loop tables for the \hat{c}_{ij} matrices, it is evident that the highest numerators up to $n = 8$ are given again by products of powers of 2 and 3, as we had for tree-level color coefficients, namely:

$$\begin{aligned}
n = 5, & \longrightarrow 24 = 2^3 \cdot 3^1, & n = 6, & \longrightarrow 32 = 2^5 \cdot 3^0, \\
n = 7, & \longrightarrow 96 = 2^5 \cdot 3^1, & n = 8, & \longrightarrow 288 = 2^5 \cdot 3^2.
\end{aligned}$$

- Furthermore, the sum of the exponents of 2 and 3 is $(n - 1)$. For tree-level coefficients the same sum gave $(n - 2)$.

Chapter 6

Color-flow decomposition

6.1 Definition

The color-flow decomposition [40] of an n -gluon amplitude reads:

$$\mathcal{A} = \sum_{\sigma(2,\dots,n)} \delta_{j\sigma_2}^{i_1} \delta_{j\sigma_3}^{i_{\sigma_2}} \dots \delta_{j_1}^{i_{\sigma_n}} A(1, \sigma_2, \dots, \sigma_n). \quad (6.1)$$

The sum is over all $(n-1)!$ permutations of $(2, \dots, n)$ and the partial amplitudes are the same as in both the trace and adjoint decompositions. It is based on treating the $SU(N)$ gluon field as an $N \times N$ matrix $(A_\mu)_j^i$, with $(i, j) = 1, \dots, N$, rather than as a one-index field A_μ^a with $a = 1, 2, \dots, N^2 - 1$. More details can be found in Appendix A. To obtain the cross-section, we square the amplitude and sum over colors. The leading term in $1/N$ is trivially given by the square of each term. In other words, if we concentrate on the first row of the color-matrix, the leading color contribution in the color-flow decomposition comes from the contraction in which external gluons are ordered in the same way, hence:

$$\left(\delta_{j_2}^{i_1} \delta_{j_3}^{i_2} \dots \delta_{j_1}^{i_n} \right) \cdot \left(\delta_{j_2}^{i_1} \delta_{j_3}^{i_2} \dots \delta_{j_1}^{i_n} \right)^\dagger = \left(\delta_{j_2}^{i_1} \delta_{j_3}^{i_2} \dots \delta_{j_1}^{i_n} \right) \cdot \left(\delta_{i_1}^{j_2} \delta_{i_2}^{j_3} \dots \delta_{i_n}^{j_1} \right) = N^n. \quad (6.2)$$

Terms involving the contraction a deltas associated to different color-flows will give rise to factors N^{n-2r} , where $r = 1, \dots, \lfloor \frac{n-1}{2} \rfloor$. This decomposition, as the name suggests, is based on the flow of color, so it has a simple physical interpretation and furnishes a very natural way to express an arbitrary QCD amplitude.

6.2 Number of NLC contributions

In this section we aim to prove that the number of color coefficients contributing to NLO in powers of $1/N$ for tree-level gluon amplitudes is equal to:

$$\#_{\text{NLC}} = \binom{n+1}{4}, \quad (6.3)$$

for any row of the color-matrix.

6.2.1 Proof

Concentrating on the first row of the color-matrix, our reference permutation is given by $(1, 2, 3, \dots, n-1, n)$. We denote an arbitrary permutation of the external legs as $(1, \sigma_2, \sigma_3, \dots, \sigma_n)$. All the indices having on their right side the same index they had in the reference ordering produce contractions of the form $\delta_{jl}^{i_k} \delta_{i_k}^j = \delta_{i_k}^{i_k} = N$. We denote the number of these terms as m and call them **contracted**. The remaining strings of coupled Kronecker's deltas give rise¹ to a single string of $(n-m)$ deltas of the form:

$$\prod_{\{k\}} \delta_{i_{L(i_{k+1})}}^{i_k}, \quad (6.4)$$

where $L(i_{k+1})$ denotes the index on the left side of i_{k+1} in the permuted set of indices. Therefore, by definition, $L(i_{k+1}) \neq i_{k+1}$. For example, if we contract $(123456) \cdot (135642)$, we get:

$$\delta_{i_4}^{i_1} \delta_{i_1}^{i_2} \delta_{i_6}^{i_3} \delta_{i_3}^{i_4} \delta_{i_5}^{i_5} \delta_{i_2}^{i_6} = N^2. \quad (6.5)$$

We neglect the case in which $m = n$, since it is associated to the only LC color coefficient. Focusing on NLC coefficients, consider $n \geq 4$ gluons. It is easy to show that we get NLC coefficients if and only if:

$$n - m = 3 \quad \vee \quad n - m = 4. \quad (6.6)$$

To prove it, remind that the maximum power of N for an arbitrary cross term is trivially given by:

$$n_{\text{max}}(m) = m + \left\lfloor \frac{n-m}{2} \right\rfloor. \quad (6.7)$$

The power of N for the NLC contributions is $(n-2)$. If we write the following inequality:

$$n - 2 > n_{\text{max}}(m) = m + \left\lfloor \frac{n-m}{2} \right\rfloor, \quad (6.8)$$

¹Once we contracted the $\{j_k\}$.

and easily rearrange it, we end up with:

$$n - m > 2 + \left\lfloor \frac{n - m}{2} \right\rfloor. \quad (6.9)$$

This inequality holds for all $(n - m) \geq 5$. Hence we get NLC coefficients only when $n - m \leq 4$, therefore we can have a string of **at most** 4 uncontracted deltas left. Since the minimum number of uncontracted deltas for the simplest non-trivial permutations² of the external gluons is 3, we get:

$$3 \leq n - m \leq 4. \quad (6.10)$$

By the way, in order to get a power N^{n-2} , a string of 3 uncontracted deltas should give a factor N , while a string of 4 deltas should give a factor N^2 . This is always true, since, relabeling indices and writing the deltas with upper i 's in ascending order, the only contractions we could have are given by:

$$\delta_{i_3}^{i_1} \delta_{i_1}^{i_2} \delta_{i_2}^{i_3} = N, \quad \delta_{i_3}^{i_1} \delta_{i_4}^{i_2} \delta_{i_1}^{i_3} \delta_{i_2}^{i_4} = N^2. \quad (6.11)$$

As a consequence, the total number of permutations of the external gluon indices giving NLC coefficients is given by all possible ways to combine them in groups of three **and** four, namely:

$$\binom{n}{3} + \binom{n}{4} = \binom{n+1}{4}, \quad (6.12)$$

as we claimed. For example, the contraction given by (6.5) does not give NLC contribution, since $(n - m) = (6 - 1) = 5$. The same does the contraction $(12345678) \cdot (16483752)$, since $m = 0$:

$$\delta_{i_5}^{i_1} \delta_{i_1}^{i_5} \delta_{i_8}^{i_2} \delta_{i_2}^{i_8} \delta_{i_6}^{i_3} \delta_{i_3}^{i_6} \delta_{i_7}^{i_4} \delta_{i_4}^{i_7} = N^4, \quad (6.13)$$

while $(12345678) \cdot (17845623)$ gives the desired result, since $m = 4$, namely:

$$\delta_{i_6}^{i_1} \delta_{i_1}^{i_6} \delta_{i_2}^{i_2} \delta_{i_4}^{i_4} \delta_{i_5}^{i_5} \delta_{i_7}^{i_7} \delta_{i_3}^{i_3} \delta_{i_8}^{i_8} = N^6. \quad (6.14)$$

²They are given by the exchange of two adjacent indices, for example: $(12345) \rightarrow (12435)$.

Chapter 7

Summary and conclusions

Finally, we first sum up all the steps we moved in this work, collecting the results we obtained.

- In chapter 1 we gave the basics of Quantum Chromodynamics: we first described the properties of the $SU(N)$ group and its generators. Then we described the QCD lagrangian, derived the Feynman rules and underlined the key features of the theory, in particular its asymptotic freedom at high energy scales.
- In chapter 2 we introduced the large N limit and applied it to the Gross-Neveu model and to QCD. This non-perturbative technique was introduced in order to avoid the breakdown of perturbation theory for QCD at low energy scales, where $g_S \simeq 1$. Thus, the idea is to replace g_S with another parameter, given by $1/N$, and use it to suitably expand QCD amplitudes. Furthermore, we pointed out the relation between the order in powers of N of an arbitrary Feynman diagram and the topology of surfaces. Then, as a further application, we studied the so called 't Hooft model, that is nothing but $(1 + 1)$ -dimensional QCD at large N : the simplifications introduced by the large N limit allow us to prove that in this model quarks are confined, to compute the dressed quark propagator and to describe meson bound states using the formalism of the Bethe-Salpeter equation.
- In chapter 3 we first described both the standard and adjoint color decompositions of gluon scattering amplitudes at tree-level. The first one, also called trace-based decomposition, expresses a given amplitude as a superposition of $(n - 1)!$ color-ordered partial amplitudes, each weighted by a suitable color coefficient given by traces of $SU(N)$ generators. The second one expresses the same amplitude as a superposition of only $(n - 2)!$ partial amplitudes, in which the first and the last external gluons are fixed in position and all the others are permuted. Each of them is weighted by color coefficients given by strings of structure constants contracted in a multi-peripheral way. Finally, we described further relations between partial

amplitudes, called BCJ relations, allowing us to reduce the number of independent partial amplitudes to $(n - 3)!$.

- In chapter 4, we first classified all the adjoint color coefficients up to ten external gluons. Furthermore, inspecting their structures and classifications, we made some guesses about their structure for an higher number of gluons: in particular we guessed that, for an even number of gluons, only 0's and 2's are hit by the highest order color contributions, while for an odd number of gluons, even 4's are hit. Furthermore, we conjectured formulas for the highest numerators appearing in the coefficients singularly for each order in color. Then we studied the goodness of the LC and NLC approximations up to eight gluons: for six gluons the LC amplitude makes an average error of 1%, while for seven gluons we get an average error of the 5%. Finally, for eight gluons the NLC amplitude turns out to be very good, since the approximation gives an error of 0.1%.
- In chapter 5, we first introduced the adjoint color decomposition for 1-loop gluon amplitudes, then we classified all color coefficients up to eight external gluons.
- Finally, in chapter 6 we introduced another important color decomposition, named color-flow decomposition, by which we write a gluon tree-level amplitude as a superposition of $(n - 1)!$ partial amplitudes, as the trace-based decomposition does. However, in this case color coefficients are given by strings of Kronecker's deltas, thus they are easier to compute. Then we proved that the total number of NLC coefficients are given by $\binom{n+1}{4}$, where n is the number of gluons. Therefore, increasing n , only a tiny percentage of all the $(n - 1)!$ permutations of the external gluons gives a NLC contribution to a given amplitude.

In conclusion, the study of the accuracy of the $1/N$ expansion up to eight external gluons at tree-level, the classification of the adjoint color coefficients and the proof of the binomial rate of growth of the number of NLC coefficients for the color-flow decomposition constitute the original contributions of this work. The NLC approximation turns out to be very accurate at tree-level (at least up to eight gluons), and the validity of this result for an higher number of gluons would allow us to obtain a more efficient way of computing scattering amplitudes in QCD. It will be also interesting to test the NLC approximation accuracy and the validity of our guess on the structure of color coefficients for an higher number of gluons. We defer this discussion to future works.

Appendix A

Color factors computations

It is very well known that QCD Feynman rules involving matter fields (quarks) are almost the same as the QED ones. The only difference is due to the presence of color factors. In this appendix we describe a technology to evaluate color factors in graphical form. To start with, we remind that the gauge fields are given by:

$$A_\mu(x) = A_\mu^a(x)T^a. \quad (\text{A.1})$$

The gauge boson propagator gets simpler if we choose to work in the Feynman gauge $\xi = 1$ and reads:

$$D_{\mu\nu}^{ab}(p) = \delta^{ab} \left(\frac{-i\eta_{\mu\nu}}{p^2 + i\epsilon} \right), \quad (\text{A.2})$$

where δ^{ab} encodes color conservation. In other words, we have 8 different gluons $A_\mu^a(x)$ each living in the adjoint representation and carrying 8 different color combinations. However, things can be easier if we note that the adjoint representation $\mathbf{8}$ satisfies:

$$\mathbf{3} \otimes \bar{\mathbf{3}} = \mathbf{1} \oplus \mathbf{8}. \quad (\text{A.3})$$

From the relations (1.23) and (1.25) we see that color transforms under $\mathbf{3}$ while anticolor transforms under $\bar{\mathbf{3}}$. Hence, if we contract a fundamental index with an antifundamental one we obtain a color singlet or a color octet. The latter acts on the Hilbert space where gluons live in. Furthermore, combining a color and anticolor we can form an uncolored quantum state given by the singlet. Being these two representations not equivalent, any tensor belonging to $\mathbf{3} \otimes \bar{\mathbf{3}}$ will be written as $B(x)_j^i$, where the upper index transforms under the antifundamental representation and the lower one under the fundamental. As usual, an upper index can only be contracted with a lower one. By virtue of the tensorial

equation (A.3), a tensor object living in the adjoint representation $\mathbf{8}$ can be thought as having a pair of fundamental and antifundamental indices to which the contribution of the trace (uncolored) part given by the singlet must be subtracted. Hence, instead of expressing the gauge field $A_\mu(x)$ and the Feynman rules using adjoint indices, we can use the fundamental and antifundamental ones:

$$A_\mu(x) = [A_\mu(x)]_j^i = [A_\mu^a(x)T^a]_j^i. \quad (\text{A.4})$$

Writing the gauge fields in this way, the gluon propagator takes the form:

$$[D_{\mu\nu}(p)]_{jl}^{ik} = (T^a)_j^i (T^a)_l^k \left(\frac{-i\eta_{\mu\nu}}{p^2 + i\epsilon} \right) = \frac{1}{2} \left(\delta_l^i \delta_j^k - \frac{1}{N} \delta_j^i \delta_l^k \right) \left(\frac{-i\eta_{\mu\nu}}{p^2 + i\epsilon} \right), \quad (\text{A.5})$$

where in the last step we used the Fierz identities making the adjoint index to disappear from the propagator. We can represent this propagator as showed in figure A.1, where the first term given by $\delta_l^i \delta_j^k$ encodes the conservation of color from l to i and from j to k , and the second term $\delta_j^i \delta_l^k$ encodes the same conservation from j to i and from l to k .

$$\begin{array}{c} i \\ \leftarrow \\ \hline \hline \rightarrow \\ j \end{array} \begin{array}{c} l \\ \leftarrow \\ \hline \hline \rightarrow \\ k \end{array} - \frac{1}{N} \begin{array}{c} i \\ \leftarrow \\ \hline \hline \rightarrow \\ j \end{array} \begin{array}{c} l \\ \leftarrow \\ \hline \hline \rightarrow \\ k \end{array}$$

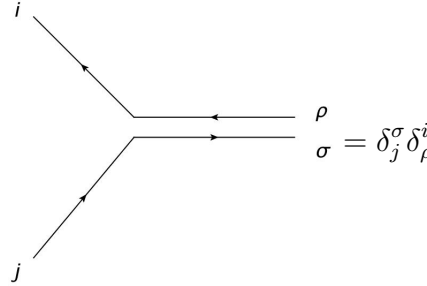
Figure A.1: Double line notation for the gluon propagator. N is the number of colors and the term proportional to N^{-1} is due to the tracelessness of the gauge field $A_\mu(x)$. The arrows point from the lower index to the upper index.

The structure for the propagator we just obtained is known as double line notation. Hence it is evident that we can think to the gluon propagator as two quark propagators pointing in opposite directions. The gluon carries the combination of a color and an anticolor, but one of the nine possible combinations, the uncolored one, given by the quantum state in the color part of the quark Hilbert space:

$$|\text{Singlet}\rangle = \frac{1}{\sqrt{3}} |\bar{R}R + \bar{B}B + \bar{G}G\rangle, \quad (\text{A.6})$$

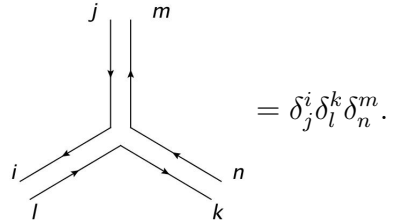
formed by the sum of all equal color-anticolor pairs is subtracted away. The arrows can be defined because $\mathbf{3}$ and $\bar{\mathbf{3}}$ are not equivalent (so there is a distinction between upper and lower indices). In order to compute color factors using these results we just have to replace any gluon propagator with the expression given by (A.5) and use the new Feynman rules for color established by the selected decomposition of the gauge field, indeed:

- For the quark-antiquark-gluon vertex we have:



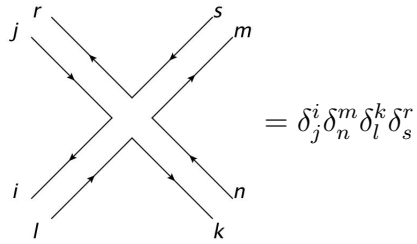
$$\sigma = \delta_j^\sigma \delta_\rho^i. \quad (\text{A.7})$$

- For the three gluon vertex we get:



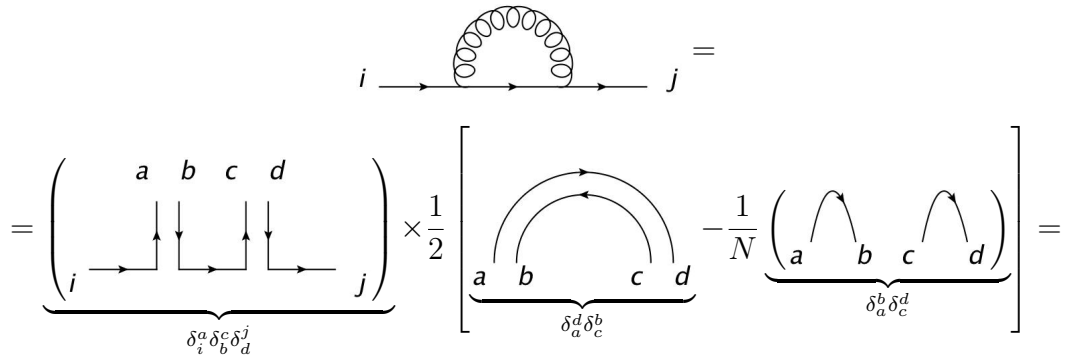
$$= \delta_j^i \delta_l^k \delta_n^m. \quad (\text{A.8})$$

- Finally, for the four gluon vertex we have:



$$= \delta_j^i \delta_n^m \delta_l^k \delta_s^r. \quad (\text{A.9})$$

The first letters of the latin alphabet must not be confused with adjoint indices, they are fundamental and antifundamental ones. In the following we give some examples of color factors computations taken by [11] and [12]. We first restrict our analysis to graphs containing only quarks or photons as external particles. To begin with, we try to find the color factor for the quark self-energy, namely:



$$= \left(\underbrace{\begin{array}{c} a \quad b \quad c \quad d \\ \downarrow \quad \downarrow \quad \downarrow \quad \downarrow \\ i \rightarrow \quad \quad \quad \quad \rightarrow j \end{array}}_{\delta_i^a \delta_b^c \delta_d^j} \right) \times \frac{1}{2} \left[\underbrace{\begin{array}{c} \text{diagram with lines } a, b, c, d \\ \text{and } a, c \end{array}}_{\delta_a^d \delta_c^b} - \frac{1}{N} \underbrace{\begin{array}{c} \text{diagram with lines } a, b, c, d \\ \text{and } b, d \end{array}}_{\delta_a^b \delta_c^d} \right] =$$

$$= \frac{1}{2} \left[\underbrace{\text{Diagram 1}}_{\delta_i^j \delta_c^c = N \delta_i^j} - \frac{1}{N} \underbrace{\left(\text{Diagram 2} \right)}_{\delta_i^j} \right] = \frac{\delta_i^j}{2} \left(N - \frac{1}{N} \right) = C_F \delta_i^j.$$

In the last step we used the fact that the color loop in the first diagram gives a factor of N , because we sum over the number of colors, given by δ_c^c . Another example of computation is given by the scattering $q\bar{q} \rightarrow q\bar{q}$:

$$\begin{aligned} & \text{Diagram 3} = \underbrace{\left(\text{Diagram 4} \right)}_{\delta_i^\alpha \delta_b^j \delta_l^d \delta_c^k} \times \frac{1}{2} \left[\underbrace{\text{Diagram 5}}_{\delta_a^c \delta_d^b} - \frac{1}{N} \underbrace{\left(\text{Diagram 6} \right)}_{\delta_a^b \delta_d^c} \right] = \\ & = \frac{1}{2} \left(\text{Diagram 7} - \frac{1}{N} \text{Diagram 8} \right) = \frac{1}{2} \left(\delta_i^k \delta_l^j - \frac{1}{N} \delta_i^j \delta_l^k \right) = (T^a)_i^j (T^a)_l^k. \end{aligned}$$

Hence, by direct inspection we recovered the Fierz identity. As a further example we can compute the following graph:

$$\text{Diagram 9} = \underbrace{\left(\text{Diagram 10} \right)}_{\delta_i^\alpha \delta_b^i \delta_l^d \delta_c^i} \times \frac{1}{2} \left[\underbrace{\text{Diagram 11}}_{\delta_a^b \delta_d^c} - \frac{1}{N} \underbrace{\left(\text{Diagram 12} \right)}_{\delta_a^c \delta_d^b} \right] =$$

$$= \frac{1}{2} \left[\underbrace{\text{Diagram 1}}_{N^2} - \frac{1}{N} \underbrace{\text{Diagram 2}}_N \right] = \frac{N^2 - 1}{2}.$$

As a matter of fact, we have safely neglected the incoming and outgoing photons for the obvious reason that they do not carry color charge. Then we substituted the internal gluon line with (A.5) and suitably connected the different legs together. Finally, we can calculate the color factor for the following one loop correction involving the interaction with a photon:

$$\begin{aligned}
& \text{Diagram with photon} = \underbrace{\left(\text{Diagram with internal lines } a, b, c, d \right)}_{\delta_i^a \delta_c^j \delta_b^d} \times \frac{1}{2} \left[\underbrace{\text{Diagram with lines } a, c}_{\delta_a^c \delta_d^b} - \frac{1}{N} \underbrace{\left(\text{Diagram with lines } a, b \right)}_{\delta_a^b \delta_d^c} \right] = \\
& = \frac{1}{2} \left[\text{Diagram 1} - \frac{1}{N} \text{Diagram 2} \right] = \frac{1}{2} \left(N - \frac{1}{N} \right) \delta_i^j = C_F \delta_i^j.
\end{aligned}$$

Again the presence of the emitted photon turns out to be completely irrelevant. Until now all the gluon lines we encountered were internal and consequently described by propagators. We now want to consider graphs with a single external gluon. In this case, we have to project the external gluon line on the octet representation using the projector given by the Fierz identity. In so doing we replace the adjoint index carried by the external gluon with the double line notation given by the Fierz identity and then we suitably connect every line to the double line interaction vertex. Consider for example:

$$\begin{aligned}
\text{Diagram} &= \frac{1}{2} \left[\underbrace{\begin{array}{c} b \longleftarrow d \\ a \longrightarrow c \end{array}}_{\delta_a^c \delta_d^b} - \frac{1}{N} \left(\begin{array}{c} b \\ a \end{array} \right) \underbrace{\left(\begin{array}{c} d \\ c \end{array} \right)}_{\delta_a^b \delta_c^d} \right] \times \underbrace{\left(\begin{array}{c} d \\ c \end{array} \right)}_{\delta_c^d} = \\
&= \frac{1}{2} \left[\begin{array}{c} b \\ a \end{array} \right] - \frac{1}{N} \left(\begin{array}{c} b \\ a \end{array} \right) \left(\begin{array}{c} d \\ c \end{array} \right) \right] = \frac{1}{2} (\delta_a^b - \delta_a^b) = 0.
\end{aligned}$$

The same result could be obtained simply using the ordinary Feynman rules for QCD, making use of the adjoint index a carried by the incoming gluon, namely:

$$\text{Tr} \{T^a\} = (T^a)_i^i = 0, \quad (\text{A.10})$$

by virtue of the tracelessness of the fundamental generators. We remark that the first factor is the projection operator on the adjoint representation (octet) applied to the external gluon in order to correctly substitute its adjoint index and give the right null color factor for the diagram. As a final remarkable example, we can consider the correction to the quark-gluon vertex, that contains both an internal and external gluon:

$$\begin{aligned}
\text{Diagram} &= \left(\begin{array}{c} k \quad l \\ b \quad d \\ i \quad a \quad c \quad j \end{array} \right) \times \frac{1}{2} \left[\begin{array}{c} b \longleftarrow d \\ a \longrightarrow c \end{array} - \frac{1}{N} \left(\begin{array}{c} b \\ a \end{array} \right) \left(\begin{array}{c} d \\ c \end{array} \right) \right] \times \\
&\times \frac{1}{2} \left[\begin{array}{c} r \quad s \\ k \quad l \end{array} - \frac{1}{N} \left(\begin{array}{c} r \\ k \end{array} \right) \left(\begin{array}{c} s \\ l \end{array} \right) \right] = -\frac{1}{2N} \left(\begin{array}{c} \text{Diagram} \\ i \quad j \end{array} \right).
\end{aligned}$$

In the last example we suppressed the Kronecker's deltas for the sake of clarity and calculations are not explicitly performed. They can be easily completed connecting all the legs together in a suitable way following the arrows as usual.

Appendix B

Spinor-helicity formalism

In this appendix we want to introduce the spinor-helicity formalism, a technique that is largely used to calculate scattering amplitudes nowadays. We will follow the developments of the topic given in [13] and [14].

B.1 Momenta

It is very well known that 4-momenta p_μ live in the following 4-dimensional representation of the Lorentz group $SO(3,1)$:

$$R_{\text{Vector}} = \left(\frac{1}{2}, \frac{1}{2} \right) = \tau_{\frac{1}{2}\frac{1}{2}}, \quad (\text{B.1})$$

called **vector representation** (or alternatively **spin 1 representation**). However, it is also well known from the Clebsch-Gordan-Racah multiplication and decomposition rule that:

$$R_{\text{Vector}} = \tau_{\frac{1}{2}\frac{1}{2}} = \left(\frac{1}{2}, 0 \right) \otimes \left(0, \frac{1}{2} \right) = \tau_{\frac{1}{2}0} \otimes \tau_{0\frac{1}{2}}. \quad (\text{B.2})$$

Hence, the spin 1 representation is the direct product of the left and right-handed spinor representations. As a consequence, we can express a momentum vector in terms a 2×2 matrix labeled by two spinor indices:

$$p^{a\dot{a}} = (\sigma_\mu)^{a\dot{a}} p^\mu = \begin{pmatrix} p^0 - p^3 & -p^1 + ip^2 \\ -p^1 - ip^2 & p^0 + p^3 \end{pmatrix}. \quad (\text{B.3})$$

Dotted and undotted indices label left and right-handed Weyl spinors and consequently they transform with respect to $\left(\frac{1}{2}, 0 \right)$ and $\left(0, \frac{1}{2} \right)$ respectively. Obviously $(\sigma^\mu)^{a\dot{a}} =$

$(\delta^{a\dot{a}}, \vec{\sigma}^{a\dot{a}})$, where $\vec{\sigma}$ are the usual Pauli matrices. As we use the Lorentz metric $\eta_{\mu\nu}$ to raise and lower vector indices, for spinor indices we use two different dotted and undotted metrics defined as follows:

$$\epsilon^{ab} = -\epsilon_{ab} = \epsilon^{\dot{a}\dot{b}} = -\epsilon_{\dot{a}\dot{b}} = \begin{pmatrix} 0 & 1 \\ -1 & 0 \end{pmatrix}. \quad (\text{B.4})$$

In addition, using the fundamental relation:

$$\epsilon_{ab}\epsilon_{\dot{a}\dot{b}}(\sigma_\mu)^{b\dot{b}} = (\bar{\sigma}_\mu)_{\dot{a}a}, \quad (\text{B.5})$$

whose inverse is given by:

$$(\sigma^\mu)^{a\dot{a}} = \epsilon^{ab}\epsilon^{\dot{a}\dot{b}}(\bar{\sigma}^\mu)_{\dot{b}b}, \quad (\text{B.6})$$

we can write the momentum with both lower indices as:

$$p_{\dot{a}a} = \epsilon_{ab}\epsilon_{\dot{a}\dot{b}}(\sigma_\mu)^{b\dot{b}}p^\mu = (\bar{\sigma}_\mu)_{\dot{a}a}p^\mu, \quad (\text{B.7})$$

where $(\bar{\sigma}^\mu)^{\dot{a}a} = (\delta^{\dot{a}a}, -\vec{\sigma}^{\dot{a}a})$. We incidentally stress that the order of the spinor indices is essential. It is interesting to obtain the inverse relation of (B.3). To this purpose, we use the following equality:

$$\eta^{\mu\nu}(\sigma_\mu)^{a\dot{a}}(\sigma_\nu)^{b\dot{b}} = 2\epsilon^{ab}\epsilon^{\dot{a}\dot{b}}, \quad (\text{B.8})$$

to find by direct substitution that the inverse of (B.3) is given by the relation:

$$p^\mu = \frac{1}{2}(\sigma^\mu)^{a\dot{a}}p_{\dot{a}a}. \quad (\text{B.9})$$

Namely:

$$p^{a\dot{a}} = (\sigma_\mu)^{a\dot{a}}p^\mu = \frac{1}{2}\eta^{\mu\nu}(\sigma_\mu)^{a\dot{a}}(\sigma_\nu)^{b\dot{b}}p_{b\dot{b}} = \epsilon^{ab}\epsilon^{\dot{a}\dot{b}}p_{b\dot{b}} = \underbrace{\epsilon^{ab}\epsilon^{\dot{a}\dot{b}}(\bar{\sigma}_\mu)_{\dot{b}b}}_{(\sigma_\mu)^{a\dot{a}}}p^\mu = p^{a\dot{a}}, \quad (\text{B.10})$$

as we claimed. Analogously, we find the inverse relation:

$$p^\mu = \frac{1}{2}(\bar{\sigma}^\mu)_{\dot{a}a}p^{a\dot{a}}. \quad (\text{B.11})$$

All the equations we listed above allow us to convert from the R_{Vector} representation of momenta to the bispinor one and vice versa. Furthermore, we can calculate the determinant of the $p^{a\dot{a}}$ matrix finding the well known mass-shell relation:

$$\det(p^{a\dot{a}}) = p_\mu p^\mu = m^2. \quad (\text{B.12})$$

The momentum matrix is singular if and only if we are dealing with massless particles like photons and gluons. However, if we are in the high-energy limit, we can safely neglect the masses of particles. In fact, in this case quarks are ultra-relativistic and the energy scale of the process is much greater than their masses. This is certainly true for LHC, where we have a center of mass energy $E_{\text{cm}} = 13\text{TeV} = 13000\text{GeV}$, an energy scale that is much greater than the mass of the heaviest quark, the **top** quark:

$$m_{\text{top}} \simeq 173\text{GeV}. \quad (\text{B.13})$$

Hence, we can safely consider all quarks massless.

B.1.1 Helicity spinors and light-like momenta

We are now arrived to the heart of the matter: we define **helicity spinors** as doublets of real numbers transforming in the $\tau_{\frac{1}{2}0}$ and $\tau_{0\frac{1}{2}}$ representations of the Lorentz group.

Any left-handed helicity spinor will be conventionally labeled with upper undotted indices as λ^a , while right-handed ones with lower dotted indices $\tilde{\psi}_{\dot{a}}$. Choosing this convention, we can write the inner product between left handed helicity spinor as:

$$\langle \psi \chi \rangle = \epsilon_{ab} \psi^a \chi^b = \psi^a \chi_a = -\epsilon_{ba} \psi^a \chi^b = -\chi^b \epsilon_{ba} \psi^a = -\chi^b \psi_b = -\langle \chi \psi \rangle, \quad (\text{B.14})$$

since ψ^a and χ^b are real (therefore commuting) numbers. Notice that if they were Grassmann (anticommuting) numbers, we would have:

$$\langle \psi \chi \rangle = \langle \chi \psi \rangle. \quad (\text{B.15})$$

Furthermore, it is clear from (B.14) that we have to be careful in raising and lowering contracted indices, because $\psi^a \chi_a \neq \psi_a \chi^a$. In the same way, we can define the inner product between right-handed spinors (that we denote using a tilde symbol), namely:

$$[\tilde{\psi}\tilde{\chi}] = \epsilon^{\dot{a}\dot{b}}\tilde{\psi}_{\dot{a}}\tilde{\chi}_{\dot{b}} = \tilde{\psi}_{\dot{a}}\tilde{\chi}^{\dot{a}} = -\epsilon^{\dot{b}\dot{a}}\tilde{\psi}_{\dot{a}}\tilde{\chi}_{\dot{b}} = -\tilde{\chi}_{\dot{b}}\epsilon^{\dot{b}\dot{a}}\tilde{\psi}_{\dot{a}} = -\tilde{\chi}_{\dot{b}}\tilde{\psi}^{\dot{b}} = -[\tilde{\chi}\tilde{\psi}]. \quad (\text{B.16})$$

Finally, if we take $\psi = \chi$ and $\tilde{\psi} = \tilde{\chi}$, by virtue of (B.14) and (B.16) we easily find:

$$\langle\psi\psi\rangle = [\tilde{\psi}\tilde{\psi}] = 0. \quad (\text{B.17})$$

The choice of using angle and square brackets to denote the two inner products will be clear in a moment. To proceed further, it is well known from linear algebra that every singular 2×2 matrix can be expressed as an outer product, namely:

$$p^{a\dot{a}} = \lambda^a\tilde{\lambda}^{\dot{a}}, \quad (\text{B.18})$$

where $\lambda^a = (\tilde{\lambda}^{\dot{a}})^\dagger$, because the momentum is real. This is exactly the case of light-like momenta. As a consequence, we can express the Lorentz contraction of two light-like momenta $p^{a\dot{a}} = \lambda^a\tilde{\lambda}^{\dot{a}}$ and $q^{a\dot{a}} = \chi^a\tilde{\chi}^{\dot{a}}$ as:

$$p_\mu q^\mu = \frac{1}{4}(\bar{\sigma}_\mu)_{\dot{a}a}(\bar{\sigma}^\mu)_{b\dot{b}}\lambda^a\tilde{\lambda}^{\dot{a}}\chi^b\tilde{\chi}^{\dot{b}} = \frac{1}{2}\epsilon_{ab}\epsilon_{\dot{a}\dot{b}}\lambda^a\tilde{\lambda}^{\dot{a}}\chi^b\tilde{\chi}^{\dot{b}} = \frac{1}{2}\langle\lambda\chi\rangle[\tilde{\chi}\tilde{\lambda}]. \quad (\text{B.19})$$

At this point we can introduce a very useful notation:

$$\lambda^a = |p\rangle, \quad \tilde{\lambda}_{\dot{a}} = [p], \quad \lambda_a = \langle p|, \quad \tilde{\lambda}^{\dot{a}} = [p|, \quad (\text{B.20})$$

so that:

$$p^{a\dot{a}} = |p\rangle[p|, \quad p_{a\dot{a}} = [p|\langle p|. \quad (\text{B.21})$$

Therefore, contracting Lorentz indices can be seen as taking a trace over spinor indices, namely:

$$p_\mu q^\mu = \frac{1}{2}p_{\dot{a}a}q^{a\dot{a}} = \frac{1}{2}\text{Tr}\{|p\rangle\langle pq|[q|\} = \frac{1}{2}\langle pq\rangle[qp|. \quad (\text{B.22})$$

B.2 Polarizations

The true power of the spinor-helicity formalism comes when applied to vector bosons polarizations. We first recall that physical polarization satisfy:

- The transverse wave condition,

$$p_\mu \epsilon^\mu = -1. \quad (\text{B.23})$$

- The light-like condition,

$$\epsilon_\mu \epsilon^\mu = 0. \quad (\text{B.24})$$

- Finally, we have the following result for the contraction of a polarization and its complex conjugate:

$$\epsilon_\mu^* \epsilon^\mu = -1. \quad (\text{B.25})$$

If we take the momentum along the x -direction, we have only two physical polarizations, namely:

$$p^\mu = (E, 0, 0, E), \quad \epsilon_+^\mu = \frac{1}{\sqrt{2}}(0, 1, i, 0), \quad \epsilon_-^\mu = \frac{1}{\sqrt{2}}(0, 1, -i, 0). \quad (\text{B.26})$$

We can also notice that $\epsilon_\mu^+ \epsilon^{-\mu} = -1$. The light-like condition allows us to express the polarization as an outer product of helicity spinors, as we did above for the momenta. In order to find the expression of polarizations using spinor indices, we introduce another light-like arbitrary momentum r^μ not aligned with p^μ , called **reference momentum**. Therefore, we can express the two physical polarizations as follows:

$$[\epsilon_p^-(r)]^{a\dot{a}} = \sqrt{2} \frac{|p\rangle[r]}{[pr]}, \quad [\epsilon_p^+(r)]^{a\dot{a}} = \sqrt{2} \frac{|r\rangle[p]}{\langle pr\rangle}. \quad (\text{B.27})$$

We can easily check that these definitions are consistent with the constraint we listed above. For example:

$$p_\mu \epsilon_p^\mu(r) = p_{\dot{a}a} [\epsilon_p^-(r)]^{a\dot{a}} = \sqrt{2} \frac{|p\rangle\langle pp\rangle[r]}{[pr]} = 0, \quad (\text{B.28})$$

as it should be because of the transverse wave condition. All the other constraints can be analogously checked. Finally, it is also very important to underline that:

- The arbitrariness of the reference vector $r^\mu \neq c \cdot p^\mu$ reflects the gauge freedom: selecting a certain reference vector in place of another encodes a specific gauge fixing choice.
- Furthermore, polarization vectors differing only by the reference vectors r^μ and $(r')^\mu$ are related as:

$$\epsilon_p^{\pm\mu}(r') = \epsilon_p^{\pm\mu}(r) + \alpha^\pm p^\mu, \quad (\text{B.29})$$

where:

$$\alpha^+ = (\alpha^-)^* = \frac{\sqrt{2}\langle rr' \rangle}{\langle pr \rangle \langle pr' \rangle}. \quad (\text{B.30})$$

If we take $(r')^\mu = r^\mu + p^\mu$, we get:

$$\alpha^+ = (\alpha^-)^* = \frac{\sqrt{2}}{\langle pr \rangle}. \quad (\text{B.31})$$

Because of the arbitrariness of the reference vector, the amplitude cannot depend on its value. Therefore this implies that the Ward identity $p^\mu \mathcal{A}_\mu(p) = 0$ automatically holds. In other words, the longitudinal component of the polarization vector is not physical and consequently the probability amplitude cannot depend on it.

The power of the helicity formalism arises from the arbitrariness of r^μ . As we stated in the third chapter, the color ordered-partial amplitudes are gauge invariant. This is very useful, since for each partial amplitude we are free to choose the reference momenta in different (and clever) ways, in order to simplify the computation as much as possible.

B.3 Dirac spinors

Finally, it is very simple to use helicity spinors to define Dirac spinors. First of all, we write the gamma matrices using spinor indices as follows:

$$(\gamma^\mu)_{a\dot{a}} = \begin{pmatrix} 0 & (\sigma^\mu)^{a\dot{a}} \\ (\bar{\sigma}^\mu)_{\dot{a}a} & 0 \end{pmatrix}, \quad (\text{B.32})$$

so that the Feynman's slashed momentum is given by:

$$\not{p} = \begin{pmatrix} 0 & p^{a\dot{a}} \\ p_{\dot{a}a} & 0 \end{pmatrix} = \begin{pmatrix} 0 & (\sigma^\mu)^{a\dot{a}} p_\mu \\ (\bar{\sigma}^\mu)_{\dot{a}a} p_\mu & 0 \end{pmatrix}. \quad (\text{B.33})$$

Using our convention, a left-handed helicity spinor has upper undotted indices, while a right-handed one has lower dotted indices. Therefore, we can identify left and right-handed incoming Dirac fermions as:

$$u_+(p) = \begin{pmatrix} \lambda^a \\ 0 \end{pmatrix} = \begin{pmatrix} |p\rangle \\ 0 \end{pmatrix}, \quad u_-(p) = \begin{pmatrix} 0 \\ \tilde{\lambda}_{\dot{a}} \end{pmatrix} = \begin{pmatrix} 0 \\ |p] \end{pmatrix}. \quad (\text{B.34})$$

The \pm symbols label positive and negative helicity. Furthermore, employing the **crossing symmetry**, we have $u_{\pm}(p) = v_{\mp}(p)$, finding the expressions for outgoing left and right-handed Dirac antifermions. To proceed further, we can construct both outgoing left and right-handed fermions and incoming antifermions taking the Dirac conjugate of $u_{\pm}(p)$ using the above expression for the γ^0 matrix, finding:

$$\bar{u}_+(p) = \bar{v}_-(p) = (\langle p|, 0), \quad \bar{u}_-(p) = \bar{v}_+(p) = (0, [p|). \quad (\text{B.35})$$

We can easily check that these definitions are consistent. As an example, if we consider the left-handed incoming fermion $u_+(p)$, we see that it trivially satisfies the Weyl equation:

$$\not{p}u_+(p) = p_{\dot{a}a}|p\rangle^a = |p\rangle\langle pp\rangle = 0. \quad (\text{B.36})$$

The same result holds for an outgoing left-handed fermion $\bar{u}_+(p)$:

$$\bar{u}_+(p)\not{p} = \langle p|_a p^{a\dot{a}} = \langle pp\rangle[p| = 0, \quad (\text{B.37})$$

and for all the other helicity states. We can now proceed to calculate some useful expressions focusing on fermions for simplicity (the relations for antifermions can be easily deduced by crossing). First of all, it is trivial to see that:

$$\bar{u}_+(p)\gamma^\mu u_+(q) = \langle p|\gamma^\mu|q\rangle = 0 = [p|\gamma^\mu|q\rangle = \bar{u}_-(p)\gamma^\mu u_-(q). \quad (\text{B.38})$$

Hence, we can only have fermions with different helicities meeting at an interaction vertex. Furthermore we have:

$$\bar{u}_+(p)\gamma^\mu u_-(q) = \langle p|\gamma^\mu|q\rangle = \langle p|\sigma^\mu|q\rangle = [q|\bar{\sigma}^\mu|p\rangle = [q|\gamma^\mu|p\rangle = \bar{u}_-(q)\gamma^\mu u_+(p). \quad (\text{B.39})$$

Furthermore we get:

$$[\bar{u}_+(p)\gamma^\mu u_-(q)][\bar{u}_+(r)\gamma_\mu u_-(s)] = \langle p|\gamma^\mu|q\rangle\langle r|\gamma_\mu|s\rangle = 2\langle pr\rangle[sq], \quad (\text{B.40})$$

and similarly:

$$\bar{u}_+(p)\gamma^\mu k_\mu u_-(q) = \langle p|\not{k}|q\rangle = \langle pk\rangle[kq]. \quad (\text{B.41})$$

These relations turn out to be very useful in calculating cross-sections involving fermions in the high-energy limit.

B.4 Examples of calculation

B.4.1 Example from QED

Following [13], we give here a simple example of scattering amplitude calculation at high energy taken by QED which involves only Dirac spinors: the unpolarized $e^+e^- \rightarrow \mu^+\mu^-$ scattering at lowest order in the coupling constant e . Since we are in the high-energy limit, we can safely treat the both electron (positron) and the muon (antimuon) as massless. We have $2^4 = 16$ possible different helicity amplitudes, but it turns out that we are free to fix only the helicities of the incoming electron and the outgoing muon, because in doing so we automatically fix the helicities of the other two particles. Hence we end up with only four amplitudes to calculate. Let's consider first a specific configuration of the incoming and outgoing helicities. For example, we can take the incoming electron as $|1\rangle$ ($h_1 = -$) and the outgoing muon as $\langle 3|$ ($h_3 = +$). This forces the amplitude to be:

$$i\mathcal{A}(1^-, 2^+, 3^-, 4^+) = (-ie)^2 \langle 2|\gamma^\mu|1\rangle \left(\frac{-i\eta_{\mu\nu}}{s}\right) \langle 3|\gamma^\nu|4\rangle = 2\frac{ie^2}{s}[41]\langle 23\rangle. \quad (\text{B.42})$$

Squaring this amplitude we get:

$$|\mathcal{A}(1^-, 2^+, 3^-, 4^+)|^2 = 4e^2 \frac{[41]\langle 14\rangle\langle 23\rangle[32]}{s^2} = 16e^2 \frac{(p_1 \cdot p_4)(p_2 \cdot p_3)}{s^2} = 4e^4 \left(\frac{u^2}{s^2}\right). \quad (\text{B.43})$$

The amplitude $\mathcal{A}(1^+, 2^-, 3^+, 4^-)$ is identical by parity (that flips all helicities). The last two amplitudes give the same thing but with $1 \leftrightarrow 2$:

$$|\mathcal{A}(1^-, 2^+, 3^+, 4^-)|^2 = 4e^4 \left(\frac{t^2}{s^2}\right). \quad (\text{B.44})$$

We now have to sum over final helicities and average over the initial ones, namely:

$$\frac{1}{4} \sum_{\text{hel.}} |\mathcal{A}|^2 = 2e^4 \left(\frac{t^2 + u^2}{s^2}\right), \quad (\text{B.45})$$

as it should be when we set $m_e = m_\mu = 0$.

B.4.2 Pure gluon tree-level amplitudes

We now want to apply all the relations we developed to the pure gluon tree-level scattering amplitudes [13]. First of all, consider an amplitude with all the helicities of the incoming particles (we take them incoming for convention¹) having the same value, say $+$. It is very easy to see that amplitudes with all positive (or negative) helicities vanish at tree-level in QCD, for any number of external gluons, namely:

$$\mathcal{A}(+, +, \dots, +, +) = 0. \quad (\text{B.46})$$

The proof is very simple: first of all we choose the same reference vector r^μ for all the n external gluons, provided that it is different from all the incoming momenta p_i^μ . In every diagram, we have exactly n polarization vectors, that can be contracted either with another polarization vector or with a momentum. At tree level, a single vertex can provide at most a single momentum factor (none for the four gluon vertex). Furthermore, any diagram has always fewer vertices than external lines. As a consequence, for each term in the amplitude there is at least one contraction of the form:

$$\epsilon_{i\mu}^+(r) \cdot \epsilon_j^{+\mu}(r) = \frac{\langle rr \rangle [ji]}{\langle ri \rangle \langle rj \rangle} = 0, \quad (\text{B.47})$$

so that the amplitude itself trivially vanishes. This first example clearly shows how a clever choice of the reference vectors can make the computation much simpler. Another interesting case is that of an amplitude with a single external gluon with positive (or negative) helicity, for example:

$$\mathcal{A}(-, +, \dots, +, +). \quad (\text{B.48})$$

In this case, it is sufficient to choose the reference vector of all the gluons with positive helicity to be equal to the momentum of the one with negative helicity, $r_i^\mu = p_1^\mu$, $\forall i$. Repeating the steps above, every term in the amplitude contains vanishing contractions between polarization vectors, namely:

¹As a consequence, the helicities we write for the amplitude are **not** the physical ones. If we write $\mathcal{A}(+, +, +, +)$ for a $2 \rightarrow 2$ gluon process, we are actually calculating the **physical amplitude** $\mathcal{A}_{\text{phys}}(+, +, -, -)$, because the gluons in the final state are actually outgoing: as the momentum flips the helicity flips.

$$\begin{aligned}\epsilon_{i\mu}^+(1) \cdot \epsilon_j^{+\mu}(1) &= \frac{\langle 11 \rangle [ji]}{\langle 1i \rangle \langle 1j \rangle} = 0, \quad \forall i, j \neq 1, \\ \epsilon_{i\mu}^+(1) \cdot \epsilon_1^{-\mu}(r) &= \frac{[ir] \langle 11 \rangle}{\langle 1i \rangle [1r]} = 0, \quad \forall i \neq 1.\end{aligned}$$

This trick works for all the amplitudes with a number of external gluons greater than three. Hence, we found that amplitudes with all but one positive (or negative) helicity vanish at tree-level in QCD for any number of external gluons greater than three:

$$\mathcal{A}(+, -, \dots, -, -) = 0. \quad (\text{B.49})$$

For all the other configurations of helicities there is no general rule and the amplitudes do not all vanish. Therefore, the leading non-vanishing amplitudes have at least two positive or two negative helicities. These amplitudes are called **maximally helicity violating (MHV)**, and they can be expressed through the **Parke-Taylor formula**[24]:

$$A(1^+, 2^+, \dots, j^-, \dots, k^-, \dots, n^+) = \frac{\langle jk \rangle^4}{\langle 12 \rangle \langle 23 \rangle \dots \langle (n-1)n \rangle \langle n1 \rangle}, \quad (\text{B.50})$$

where (j, k) labels the couple of external gluons that have negative (or positive) helicity.

B.5 Little-group scaling

The **little-group** is the group of all Lorentz transformations leaving a certain p_μ unchanged. In the environment of spinor-helicity formalism, these transformations act on spinor variables in order to leave $p^{a\dot{a}}$ invariant:

$$|p\rangle \longrightarrow z|p\rangle, \quad [p] \longrightarrow z^{-1}[p], \quad (\text{B.51})$$

where $z \in \mathbb{C}$. Note that if momenta are real:

$$|p\rangle = ([p])^\dagger, \longrightarrow z|p\rangle = \frac{1}{z^*}([p])^\dagger. \quad (\text{B.52})$$

Hence $zz^* = |z| = 1$, then z is a pure phase, hence it cannot change the full amplitude squared. As a consequence, polarization vectors transforms as follows:

$$\epsilon_p^+(r) \longrightarrow z^{-2}\epsilon_p^+(r), \quad \epsilon_p^-(r) \longrightarrow z^2\epsilon_p^-(r). \quad (\text{B.53})$$

Therefore polarizations describing different helicities transform in different ways under the little-group. Since spinors allow us to express through angle and square parenthesis both polarizations and external momenta, collecting the above transformation laws, a color-ordered amplitude with n external gluons scales as:

$$A(h_1, h_2, \dots, h_n) \longrightarrow \prod_{i=1}^n z^{-2h_i} A(h_1, h_2, \dots, h_n), \quad (\text{B.54})$$

where $h_i = \pm$. This scaling property furnishes a useful non-perturbative constraint. For example, if we consider the MHV amplitude $A(-, -, +, +)$, we can easily state that it can be given by expressions like:

$$\frac{\langle 12 \rangle^3}{\langle 23 \rangle \langle 34 \rangle \langle 41 \rangle}, \quad \frac{\langle 21 \rangle [34]^2}{[21] [14] \langle 41 \rangle}. \quad (\text{B.55})$$

but cannot be given by $\langle 12 \rangle \langle 34 \rangle$, since this contraction does not scale as required by (B.50).

B.6 Complex momenta

B.6.1 Three-point amplitude

In the above sections we imposed a reality condition on helicity spinors. However, it turns out to be convenient to consider momenta as complex. In this case, the angle and square brackets are independent, since:

$$\lambda^a = |p\rangle \neq ([p])^\dagger = (\tilde{\lambda}^a)^\dagger. \quad (\text{B.56})$$

Thus we get:

$$\langle ij \rangle^* \neq [ij]. \quad (\text{B.57})$$

To see a first application, consider the three gluon amplitude. Momentum conservation reads:

$$p_1 + p_2 + p_3 = |1\rangle[1] + |2\rangle[2] + |3\rangle[3] = 0. \quad (\text{B.58})$$

Contracting with $\langle 1|$, $\langle 2|$, $|1]$ and $|2]$ on both sides we obtain:

$$\langle 12 \rangle [2] = -\langle 13 \rangle [3], \quad \langle 21 \rangle [1] = -\langle 23 \rangle [3]. \quad (\text{B.59})$$

These equations are satisfied if $\langle 12 \rangle = 0$, that implies $\langle 13 \rangle = \langle 23 \rangle = 0$. Furthermore, if we contract by $[1]$ and $[2]$ we get $[12] = [13] = [23] = 0$. If momenta are real, the vanishing of angle parenthesis implies the vanishing of the square ones since $\langle ji \rangle^* = [ij]$. All possible contractions vanish, consequently we have a trivially **vanishing** three gluon scattering amplitude. However, if we consider all momenta as complex, we find that the three gluon amplitude can be given only by $\langle ij \rangle$ or $[ij]$, hence it does **not** vanish at all. Considering the little group scaling behaviour, MHV three point amplitudes turn out to be:

$$\mathcal{A}^{abc}(1^-, 2^-, 3^+) = C^{abc} \frac{\langle 12 \rangle^3}{\langle 12 \rangle \langle 32 \rangle} \quad \text{and} \quad \mathcal{A}^{abc}(1^+, 2^+, 3^-) = C^{abc} \frac{[12]^3}{[13][32]}. \quad (\text{B.60})$$

While considering momenta as complex, it can be fruitfully used to construct amplitudes involving more than three gluons through the BCFW recursion relations. Only at the end of the computation the limit of real momenta will be performed to give the final physical result.

B.6.2 BCFW recursion relations

The use of complex momenta is at the base of a powerful tool, the BCFW (Britto-Cachazo-Feng-Witten) recursion relations [13, 33, 34]. In fact, suppose to have a tree-level n -gluon scattering amplitude. The idea is to choose two external gluons, labeled as i and j , and shift them as:

$$|\hat{i}\rangle \longrightarrow |i\rangle + z|j\rangle, \quad |\hat{i}\rangle \longrightarrow |i\rangle - z|j\rangle, \quad |\hat{i}\rangle = |i\rangle, \quad |\hat{j}\rangle = |j\rangle. \quad (\text{B.61})$$

It is obvious to notice that such a shifting is possible since the spinors are complex, while z is an arbitrary complex number. The corresponding momenta are then shifted as:

$$\hat{p}_i = |i\rangle[i + z|j], \quad \hat{p}_j = |j\rangle[j - z|i]. \quad (\text{B.62})$$

They preserve the masslessness condition, as well as momentum conservation. As a consequence of this shifting, we can think of the original amplitude as an holomorphic function of z . Our purpose is to get an expression for the physical amplitude $\mathcal{A}(0)$. Consider the function on the complex z -plane:

while in formulas, using (B.64), we get:

$$-\frac{1}{z_{ab}^*} \text{Res}_{z \rightarrow z_{ab}^*} \left[\frac{\mathcal{A}_1(z) \mathcal{A}_2(z)}{(p_a + \dots + p_b)^2 - z \sum_k \langle ik \rangle [kj]} \right] = \frac{\mathcal{A}_1(z_{ab}^*) \mathcal{A}_2(z_{ab}^*)}{(p_a + \dots + p_b)^2}, \quad (\text{B.68})$$

and finally the BCFW relation:

$$\mathcal{A}(0) = \mathcal{A}(1, 2, \dots, n) = \sum_{ab\lambda} \frac{\mathcal{A}_1(a, \dots, b \rightarrow \hat{P}^\lambda) \mathcal{A}_2(\hat{P}^{-\lambda} \rightarrow 1, \dots, a-1, b+1, \dots, n)}{(p_a + \dots + p_b)^2}, \quad (\text{B.69})$$

where λ is the helicity of the internal on-shell propagator. Notice that the helicities are opposite at the endpoints of this propagator since the momentum $\hat{P}^\mu(z_{ab}^*)$ flows from the left to the right. This relation allows us to construct any tree-level amplitude recursively, using amplitudes with a lower number of external gluons as bricks. However, are we sure we can guarantee that $\mathcal{A}(z) \rightarrow 0$ as $|z| \rightarrow +\infty$? It turns out that this fear is groundless, since for Yang-Mills theories we can always find a pair of external helicities $(+, -)$ such that this essential requirement is satisfied. Thus Yang-Mills theories are on-shell constructible through BCFW recursion [35]. As a nice application of this powerful tool, we can use it to prove the reflection identity for color-ordered partial amplitudes (3.29) by induction. For $n = 3$ this relation trivially holds. Suppose indeed that the reflection identity holds even for $(n-1)$ external gluons. Hence we choose to shift:

$$\hat{p}_1 = |1\rangle[1] + z|1\rangle[n], \quad \hat{p}_n = |n\rangle[n] - z|1\rangle[n]. \quad (\text{B.70})$$

Thus we can write:

$$\begin{aligned} A(1, 2, \dots, n) &= \sum_{i=2}^{n-2} \sum_{\lambda=\pm} A(\hat{1}, 2, \dots, i, \hat{P}_{1,\dots,i}^\lambda | \hat{P}_{1,\dots,i}^{-\lambda}, i+1, \dots, \hat{n}) = \\ &= \sum_{i=2}^{n-2} \sum_{\lambda=\pm} (-1)^{i+1} (-1)^{n-i+1} A(\hat{n}, n-1, \dots, i+1, \hat{P}_{i,\dots,2,1}^{-\lambda} | \hat{P}_{i,\dots,2,1}^\lambda, i, \dots, \hat{1}) = \\ &= (-1)^n A(n, n-1, \dots, 2, 1), \end{aligned}$$

where the inductive step is used to get the second equality. We also used a shorthand notation for the amplitude splitting (see [30]), for example:

$$A(\hat{1}, 2, \hat{P}_{12}^+ | \hat{P}_{12}^-, 3, \dots, \hat{n}) = \frac{A_1(\hat{1}, 2 \rightarrow \hat{P}_{12}^+) A_2(\hat{P}_{12}^- \rightarrow 3, \dots, \hat{n})}{\hat{P}_{12}^2}. \quad (\text{B.71})$$

In addition, we can use the recursive power of this tool to prove the $U(1)$ decoupling identity. The path of the proof can be shown considering the $n = 5$ case. In fact, suppose that it holds for $n = 3, 4$ (the proof is straightforward using reflection identity). We want to show that:

$$\sum_{\sigma \in \text{cyclic}} A(1, \sigma(2, 3, 4, 5)) = 0. \quad (\text{B.72})$$

We choose to shift p_1 and p_2 and expand each term in this sum using the BCWF relations, namely:

$$\begin{aligned} A(\hat{1}, \hat{2}, 3, 4, 5) &= A(\hat{1}, P_{\hat{2}3}, 4, 5) + A(\hat{1}, P_{\hat{2}34}, 5), \\ A(\hat{1}, 5, 2, 3, 4) &= A(\hat{1}, 5, P_{\hat{2}3}, 4) + A(\hat{1}, 5, P_{\hat{2}34}) + A(\hat{1}, P_{5\hat{2}}, 3, 4) + A(\hat{1}, P_{5\hat{2}3}, 4), \\ A(\hat{1}, 4, 5, \hat{2}, 3) &= A(\hat{1}, 4, 5, P_{\hat{2}3}) + A(\hat{1}, 4, P_{5\hat{2}}, 3) + A(\hat{1}, 4, P_{5\hat{2}3}) + A(\hat{1}, P_{45\hat{2}}, 3), \\ A(\hat{1}, 3, 4, 5, \hat{2}) &= A(\hat{1}, 3, 4, P_{5\hat{2}}) + A(\hat{1}, 3, P_{45\hat{2}}). \end{aligned}$$

A new shorthand notation was used to further lighten the expansions and to make the color ordering manifest [30]. At this point, we can sum all these equations. Collecting all the terms containing the same momentum for the on-shell internal line, we see that they are proportional to the decoupling identities for $n = 3, 4$, hence they identically vanish, implying that (B.72) holds. For example, considering those splittings with momentum $P_{\hat{2}3}$ and fixed helicity λ of the on-shell internal gluon, we get:

$$\begin{aligned} &\frac{\mathcal{A}_3(\hat{2}, 3, P^\lambda)}{P_{\hat{2}3}^2} \left[\mathcal{A}_4(P^{-\lambda}, 4, 5, \hat{1}) + \mathcal{A}_4(P^{-\lambda}, 4, \hat{1}, 5) + \mathcal{A}_4(P^{-\lambda}, \hat{1}, 4, 5) \right] = \\ &= \frac{\mathcal{A}_3(\hat{2}, 3, P^\lambda)}{P_{\hat{2}3}^2} \left[\mathcal{A}_4(P^{-\lambda}, 5, \hat{1}, 4) + \mathcal{A}_4(P^{-\lambda}, 4, \hat{1}, 5) + \mathcal{A}_4(P^{-\lambda}, \hat{1}, 4, 5) \right] = 0. \quad (\text{B.73}) \end{aligned}$$

In the last step we used reflection identity. This method can be generalized to an arbitrary n and can be used to prove the decoupling identity by induction. BCFW relations can be even used to prove the Kleiss-Kuijf and BCJ relations presented in the third chapter.

Bibliography

- [1] D. J. Gross F. A. Wilczek, Asymptotically Free Gauge Theories, Phys. Rev. D8, 3633-3652 (1973).
- [2] H. D. Politzer, Reliable Perturbative Results for Strong Interactions?, Phys. Rev. Lett. 30, 1346-1349 (1973).
- [3] H. E. Stanley, Spherical Model as the Limit of Infinite Spin Dimensionality, Phys. Rev. 176 (1968).
- [4] K. Wilson, Quantum Field-Theory Models in Less Than 4 Dimensions , Phys. Rev. D7, 2911 (1973).
- [5] G. 't Hooft, A Planar Diagram Theory for Strong Interactions, Nucl. Phys. B72 (1974) 461.
- [6] G. 't Hooft, A Two-Dimensional Model for Mesons, Nucl. Phys. B75 (1974) 461.
- [7] A. V. Manohar, Large N QCD, arXiv:hep-ph/9802419.
- [8] S. Coleman, $1/N$, in Aspects of Symmetry, Cambridge University Press, Cambridge, 1985.
- [9] J.D. Gross and A. Neveu, Phys. Rev. D10 (1974) 3235.
- [10] C. Patrignani *et al.* (Particle Data Group), Chin. Phys. C, 40, 100001 (2016).
- [11] P. Nason, Lectures Delivered at the 1997 CERN School.
- [12] M. L. Mangano, Introduction to QCD, <http://cern.ch/mlm/talks/cern98.ps.gz>.
- [13] M. D. Schwartz, Quantum Field Theory and the Standard Model, Cambridge University Press.
- [14] H. Elvang, Y. Huang, Scattering Amplitudes, arXiv:1308.1697v2 [hep-th].
- [15] M. L. Mangano, S. Parke and Z. Xu, Nucl. Phys. B298, 653 (1988).

- [16] F.A. Berends and W.T. Giele, Nucl. Phys. B294, 700 (1987);
M. Mangano, S. Parke and Z. Xu, Nucl. Phys. B298, 653 (1988).
- [17] R. Kleiss and H. Kuijf, Nucl. Phys. B312, 616 (1989).
- [18] V. Del Duca, L. Dixon and F. Maltoni, New Color Decompositions for Gauge Amplitudes at Tree and Loop Level, arXiv:hep-ph/9910563v1.
- [19] M. L. Mangano and S. J. Parke, Multiparton Amplitudes in Gauge Theories, Phys. Rept. 200, 301 (1991) [hep-th/0509223].
- [20] Z. Bern, J. J. M. Carrasco and H. Johansson, New Relations for Gauge-Theory Amplitudes, Phys. Rev. D 78, 085011 (2008) [arXiv:0805.3993 [hep-ph]].
- [21] M. Srednicki, Quantum Field Theory, Cambridge University Press.
- [22] D. Tong, Lectures on Gauge Theory, chapter 6: Large N.
<http://www.damtp.cam.ac.uk/user/tong/gaugetheory/6n.pdf>.
- [23] F. Tellander, The 't Hooft Model as a Testing Ground for Quantum Chromodynamics,
<http://lup.lub.lu.se/luur/download?func=downloadFilerecordOId=8882816fileOId=8882817>.
- [24] S. J. Parke and T. R. Taylor, An Amplitude for n Gluon Scattering, Phys. Rev. Lett. 56 (1986) 2459.
- [25] W. Greiner and J. Reinhardt, Quantum Electrodynamics, fourth edition, Springer.
- [26] J. Schwinger, Gauge Invariance and Mass. II. Physical Review, Volume 128, p. 2425 (1962).
- [27] S. Weinberg, The Quantum Theory of Fields, Volume 1, Cambridge University Press.
- [28] D. Vaman and Y.P. Yao, Constraints and Generalized Gauge Transformations on TreeLevel Gluon and Graviton Amplitudes, JHEP 1011, 028 (2010) [arXiv:1007.3475 [hep-th]].
- [29] Y. Chen, Y. Du and B. Feng, A Proof of the Explicit Minimal-basis Expansion of Tree Amplitudes in Gauge Field Theory, 2010, arXiv:arXiv:1101.0009v1 [hep-th].
- [30] B. Feng, R. Huang and Y. Jia, Gauge Amplitude Identities by On-shell Recursion Relations in S-matrix Program, 2010, arXiv:1004.3417v3 [hep-th].
- [31] N. E. J. Bjerrum-Bohr, P. H. Damgaard and P. Vanhove, Minimal Basis for Gauge Theory Amplitudes, Phys. Rev. Lett. 103, 161602 (2009) [arXiv:0907.1425 [hep-th]].

- [32] S. Stieberger, Open and Closed vs. Pure Open String Disk Amplitudes, arXiv:0907.2211 [hep-th].
- [33] R. Britto, F. Cachazo and B. Feng, New Recursion Relations for Tree Amplitudes of Gluons, Nucl.Phys. B715 (2005) 499522, [hep-th/0412308].
- [34] R. Britto, F. Cachazo, B. Feng and E. Witten, Direct Proof of Tree-level Recursion Relation in Yang-Mills theory, Phys. Rev. Lett. 94 (2005) 181602, [hep-th/0501052].
- [35] N. Arkani-Hamed and J. Kaplan, On Tree Amplitudes in Gauge Theory and Gravity, JHEP 0804 (2008) 076, arXiv:0801.2385 [hep-th].
- [36] B. Truijen, Britto-Cachazo-Feng-Witten Recursion, an Introduction, Master Thesis, Utrecht University.
- [37] L. Dixon, J. Henn, J. Plefka and T. Schuster, All tree-level Amplitudes in Massless QCD, arXiv:1010.3991v4 [hep-ph] (2011).
- [38] D. Maitre and P. Mastrolia, S@M, a Mathematica Implementation of the Spinor-Helicity Formalism, arXiv:0710.5559v2 [hep-ph] (2007).
- [39] M. Sjödahl, ColorMath - A Package for Color Summed Calculations in SU(N), arXiv:1211.2099v2 [hep-ph].
- [40] F. Maltoni, K. Paul, T. Stelzer, S. Willenbrock, Color-flow decomposition of QCD amplitudes, arXiv:hep-ph/0209271v2 [hep-ph].